



Rahel Beuchel BSc

# New Fluorescent Materials for the Detection of Carbon Dioxide and Ammonia

## **MASTERARBEIT**

zur Erlangung des akademischen Grades

Diplom-Ingenieurin

in

Technische Chemie

[gemeinsames Studium im Rahmen von NAWI Graz]

eingereicht an der

**Technischen Universität Graz**

### **Betreuer**

Ass. Prof. kand. Sergey Borisov

Institut für Analytische Chemie und Lebensmittelchemie  
Technische Universität Graz

Graz, September 2015



---

## Abstract

Optical sensors offer new possibilities for CO<sub>2</sub> and ammonia sensing applications, since they show many advantages over other sensing systems. They do not consume the analyte, are quite cheap, easily miniaturized and easy to use.

In this thesis, aza-BODIPY dyes were used for preparation of CO<sub>2</sub> and ammonia sensors. Aza-BODIPY dyes show emissions in the NIR region, are highly photostable, show high quantum yields and tuning of the pKa values is easily achieved due to a straightforward synthesis of the dyes. These properties make them excellent candidates for applications in CO<sub>2</sub> and ammonia sensing systems.

CO<sub>2</sub> detection is important for many fields such as the industry, oceanography or medicine. This leads to the need of a broad dynamic range of CO<sub>2</sub> sensors for different applications. Two aza-BODIPY dyes were synthesized and characterized in this thesis for CO<sub>2</sub> sensing applications. Characterizations were done in solution as well as in thin film sensors.

The second part of this thesis focuses on the preparation of optical sensors for ammonia detection. Ammonia too is a very important gas, it is part of many industrial processes and present in the atmosphere, water and the soil. High ammonia concentrations pose a hazard to the environment as well as humans, therefore detection has been a major issue. So far, quantitative detection of ammonia has been very challenging.

In this thesis, two aza-BODIPY dyes were tested on their ammonia sensing abilities. Different materials for thin film sensor preparations were tested and promising candidates were characterized further using varying measurement set-ups.

Furthermore, two dye screenings for ammonia detection were done using different dyes such as coumarin or rhodamin dyes. Thin film sensors using cellulose acetate butyrate and Nafion® as matrices were prepared and characterized.



---

## Kurzfassung

Optische Sensoren sind vielversprechende Sensorkandidaten, da sie im Vergleich zu anderen Detektionsmethoden viele Vorteile bieten. Diese bestehen darin, dass sie den Analyten nicht verbrauchen, billig sind, einfach zu verkleinern und einfach zu handhaben.

Aza-BODIPY Farbstoffe wurden in dieser Arbeit verwendet um CO<sub>2</sub>- und Ammoniakensoren herzustellen. Aza-BODIPY Farbstoffe emittieren in der nahen infrarot Region, sind sehr Fotostabil, haben hohe Quantenausbeuten und der pKa Wert kann leicht verändert werden, da die Synthese sehr geradlinig ist. Aufgrund dieser Eigenschaften sind aza-BODIPYs eine exzellente Wahl für CO<sub>2</sub>- und Ammoniakensoren.

CO<sub>2</sub> Detektion findet in vielen Bereichen Anwendungen wie zum Beispiel, in der Industrie, Meeresforschung oder Medizin. Deshalb ist eine große Bandbreite von verschiedenen CO<sub>2</sub> Sensoren vonnöten.

In dieser Arbeit wurden zwei Aza-BODIPY Farbstoffe für die Anwendung als CO<sub>2</sub> Sensoren synthetisiert und charakterisiert. Die Charakterisierung wurde sowohl in Lösung als auch als Dünnschichtsensor durchgeführt.

Der zweite Teil dieser Arbeit bestand darin, optische Sensoren für Ammoniak herzustellen. Ammoniakdetektion ist sehr wichtig, da Ammoniak in vielen industriellen Prozessen Anwendung findet und außerdem in der Atmosphäre, im Wasser und im Erdboden präsent ist. Da hohe Ammoniakkonzentrationen zur Schädigung der Umwelt und auch des Menschen führen können, ist die Detektion sehr wichtig. Bis jetzt war die quantitative Bestimmung von Ammoniak sehr schwierig.

Es wurden zwei Aza-BODIPY Farbstoffe auf die mögliche Anwendung als Ammoniakensoren getestet. Dafür wurden verschiedene Materialien zur Sensorherstellung verwendet. Mögliche Kandidaten wurden mit verschiedenen Messmethoden genauer untersucht.

Außerdem wurden noch zwei Farbstoffuntersuchungen durchgeführt. Dafür wurden verschiedene Farbstoffe wie Coumarine und Rhodamine als Ammoniakensoren getestet. Dies geschah unter Verwendung von Cellulose acetat butyrat und Nafion® als Matrizen.



---

## Affidavit

I declare that I have authored this thesis independently, that I have not used other than the declared sources / resources, and that I have explicitly marked all material which has been quoted either literally or by content from the sources used. The text document uploaded to TUGRAZonline is identical to the present master's thesis dissertation.

## Eidesstattliche Erklärung

Ich erkläre an Eides statt, dass ich die vorliegende Arbeit selbstständig verfasst, andere als die angegebenen Quellen/Hilfsmittel nicht benutzt, und die den benutzten Quellen wörtlich und inhaltlich entnommenen Stellen als solche kenntlich gemacht habe. Das in TUGRAZonline hochgeladene Textdokument ist mit der vorliegenden Masterarbeit identisch.

Date

Signature





---

## Danksagung

Als Erstes möchte ich mich bei Prof. Ingo Klimant bedanken, der es mir ermöglicht hat, diese Arbeit zu schreiben und mir immer geholfen hat, wenn ich nicht mehr weiter wusste

Ein großes Danke geht auch an Sergey Borisov, der mir immer mit Rat und Tat zur Seite gestanden hat und selbst wenn ich geglaubt habe, das kann nicht mehr funktionieren, mit neuen Ideen und Anregung ausgeholfen hat. Außerdem würde es ohne ihn nie so viele tolle Kuchenpausen geben.

Ein weiteres Danke geht an Martin Strobl, der mich besonders in den ersten Monaten sehr unterstützt hat und auch später als Bürokollege eine Bereicherung meines Alltags war.

Ich möchte mich auch noch bei der ganzen Arbeitsgruppe für viele schöne Stunden bedanken. Sei es im Labor, in der Kaffeepause oder nach der Arbeit, der Zusammenhalt und die Freundlichkeit aller hat mich die Zeit hier noch mehr genießen lassen. Ich kann nur hoffen, dass ich auch in meinem restlichen Leben immer mit solchen tollen Menschen zusammenarbeiten kann.

Des Weiteren möchte ich mich noch bei meinen Freunden bedanken, ohne deren Unterstützung und Freundschaft ich dieses Studium wohl niemals zu Ende gebracht hätte.

Außerdem möchte ich mich noch bei meinem Freund bedanken, der mich in den Krisen der Masterarbeit wieder aufgebaut und zum Weitermachen ermutigt hat.

Als Letztes bedanke ich mich bei meinen Eltern, die es mir ermöglicht haben, zu tun was mir Freude bereitet.



---

# Contents

<b>1</b>	<b>Introduction</b>	<b>1</b>
<b>2</b>	<b>Theoretical Background</b>	<b>3</b>
2.1	Chemical Sensors . . . . .	3
2.1.1	Definition . . . . .	3
2.1.2	Components . . . . .	3
2.1.3	Important parameters of chemical sensors . . . . .	3
2.2	Optical chemical sensors . . . . .	6
2.2.1	Absorption . . . . .	6
2.2.2	Luminescence . . . . .	8
2.2.3	Internal conversion . . . . .	9
2.2.4	Fluorescence . . . . .	9
2.2.5	Intersystem crossing . . . . .	9
2.2.6	Phosphorescence . . . . .	10
2.2.7	Delayed Fluorescence . . . . .	10
2.2.8	Triplet-triplet transition . . . . .	10
2.2.9	Quenching . . . . .	10
2.2.10	Photoinduced electron transfer . . . . .	13
2.3	Fluorescence measurement principles . . . . .	14
2.3.1	Steady-state spectrofluorometry . . . . .	14
2.3.2	Time resolved fluorometry . . . . .	15
2.3.3	Dual lifetime referencing . . . . .	16
2.4	Carbon Dioxide . . . . .	17
2.4.1	Nondispersive infrared CO <sub>2</sub> sensors . . . . .	18
2.4.2	Severinghaus electrode . . . . .	18
2.4.3	Optical pH change based detections . . . . .	19
2.4.4	Materials . . . . .	21
2.4.5	Viscosity based CO <sub>2</sub> sensors . . . . .	27
2.4.6	Polarity based CO <sub>2</sub> sensors . . . . .	28
2.5	Ammonia . . . . .	29
2.5.1	Applications . . . . .	29

---

2.5.2	Sensing principles . . . . .	30
2.5.3	Materials . . . . .	31
<b>3</b>	<b>Experimental</b>	<b>35</b>
3.1	Methods . . . . .	35
3.2	Carbon Dioxide Sensors . . . . .	38
3.2.1	Synthesis of aza-BODIPY dyes . . . . .	38
3.2.2	pKa determination . . . . .	43
3.2.3	CO <sub>2</sub> sensor preparation . . . . .	44
3.2.4	Long-term stability test . . . . .	44
3.3	Ammonia Sensors . . . . .	45
3.3.1	Screening of 2 dyes for possible ammonia sensitivity . . . . .	45
3.3.2	Investigation of potential suitability of different dyes for ammonia sensors <b>1</b>	48
3.3.3	Investigation of potential suitability of different dyes for ammonia sensors <b>2</b>	48
<b>4</b>	<b>Results and Discussion</b>	<b>51</b>
4.1	Carbon Dioxide Sensors . . . . .	51
4.1.1	Synthesis . . . . .	51
4.1.2	pKa determination . . . . .	52
4.1.3	CO <sub>2</sub> sensor preparation . . . . .	54
4.1.4	CO <sub>2</sub> tests in solution . . . . .	55
4.1.5	Long term stability test . . . . .	63
4.1.6	Conclusion CO <sub>2</sub> . . . . .	65
4.2	Ammonia Sensors . . . . .	66
4.2.1	Testing 2 dyes for their ammonia sensing abilities . . . . .	66
4.2.2	Investigation of potential suitability of different dyes for ammonia sensors <b>1</b>	70
4.2.3	Investigation of potential suitability of different dyes for ammonia sensors <b>2</b>	76
<b>5</b>	<b>Conclusion and Outlook</b>	<b>87</b>
<b>6</b>	<b>References</b>	<b>88</b>
<b>7</b>	<b>List of Figures</b>	<b>93</b>
<b>8</b>	<b>List of Tables</b>	<b>97</b>
<b>9</b>	<b>Appendix</b>	<b>98</b>
9.1	List of Chemicals . . . . .	98
9.2	Abbreviations . . . . .	100
9.3	Carbon dioxide sensors . . . . .	101
9.3.1	NMR Spectra . . . . .	101

---

9.3.2	Extracted dyes in solution . . . . .	105
-------	--------------------------------------	-----



---

# 1 Introduction

Optical chemical sensors have been applied for sensing of various analytes including carbon dioxide and ammonia.

Sensing applications for quantitative determination of carbon dioxide are widespread. They are used in biotechnology for the control of fermentation processes [1] in industries such as food packaging [2], emission monitoring [3], wastewater control and treatment [4] and CO<sub>2</sub> control in the working environment, to minimize health risks [5]. Another large application field is medicine, especially breath analysis [6][7].

Recently environmental CO<sub>2</sub> monitoring has become increasingly important due to ocean acidification [1] and the global climate change [5].

So far the Severinghaus electrode and IR spectroscopy have been used for carbon dioxide detection.[8] However, the IR method can only be applied in the gaseous phase and has shown strong interferences with water[1]. The Severinghaus electrode is mostly used for the detection of dissolved CO<sub>2</sub> [9] but detection of low concentrations is not possible [1].

Therefore quite a few optical chemical sensors have been developed, HPTS [2] being one of the most commonly used materials. In recent years new indicator dyes were developed for example dihydroxy-aza-BODIPY [1]. Most of them work by detecting an absorption or fluorescence change of the indicator dye due to a pH change caused by CO<sub>2</sub> [10].

Since aza-BODIPY dyes show many advantageous properties for applications as optical sensors, such as high quantum yields, intense absorption, high photostability and emission and absorption bands in the NIR region [11] they have been investigated in this thesis as CO<sub>2</sub> sensors as well as ammonia sensors.

Ammonia is present all over the earth [12]. It can be found in water, soil and the atmosphere [13]. Nowadays, most of the ammonia emissions are caused by human activity [12]. Ammonia is toxic to the environment as well as to humans [14] and therefore detection, especially at low ammonia concentrations, is very important, for example in fish farming [15].

Traditionally the Berthelot reaction or the Nessler's method have been used for detection of ammonia but they exhibit drawbacks such as consumption of chemicals and the analyte [16][13].

Furthermore, electrochemical methods have been applied for ammonia sensing but they often require expensive instrumentation [13].

Optical sensors do not suffer from these drawbacks and are therefore a good alternative.

In this thesis, aza-BODIPY dyes were tested as ammonia sensors, because of the major advantages explained earlier. Furthermore, two dye screenings were performed to test different dyes on their ammonia sensing abilities.



---

## 2 Theoretical Background

### 2.1 Chemical Sensors

#### 2.1.1 Definition

There are several definitions for chemical sensors, the two most common ones are stated below.

“A chemical sensor is a device that transforms chemical information, ranging from the concentration of a specific sample component to total composition analysis, into an analytically useful signal. The chemical information, mentioned above, may originate from a chemical reaction of the analyte or from a physical property of the system investigated” [17]

“Chemical sensors are miniaturised devices that can deliver real time and on-line information on the presence of specific compounds or ions in even complex samples.”[18]

#### 2.1.2 Components

A chemical sensor generally contains two components, a receptor and a transducer.

The receptor is the recognition element of the sensing system, it interacts with the analyte to give chemical information which is then transformed by the transducer into a useful signal

The signal is generally read out by an extra device for example a computer. All components together are parts of an analyzer. The analyzer itself may also be able to perform other tasks such as sampling or sample processing. [17]

#### 2.1.3 Important parameters of chemical sensors

All information was obtained from [19] and [20] unless stated otherwise.

### **Reversibility**

Defines whether a sensor shows the same value at the same concentration, after concentrations have been decreased or increased. This means the sensor can easily return to its original state. This is in contrast to regeneration, where a sensor can be reused, by treating it for example with a chemical or using high pressures or high temperatures to remove the analyte.

### **Sensitivity**

The sensitivity describes a change of signal which is directly proportional to the change of the analyte in the sample. It is also equivalent to the slope of a calibration curve.

### **Limit of detection**

The limit of detection of a sensor describes the lowest concentration still possible to detect at defined conditions. At the limit of detection the amount of analyte cannot necessarily be quantified.

### **Dynamic range**

The dynamic range describes the concentrations between the limit of detection and the highest concentration that can be detected. This is the concentration range in which the sensor can be used.

### **Selectivity**

The selectivity describes the response of a sensor to a certain analyte. This could be a group of analytes or just one specific analyte.

### **Linearity**

The linearity defines the deviation of the calibration curve, experimentally detected, from a straight line. The linearity is generally given only for a certain concentration range. Linearity is a very important parameter, since sensor use and quantification are difficult if linearity is not given.

## Resolution

The resolution describes the minimum concentration difference that can still be detected by the sensor, when the composition is changed continuously. This is especially important in dynamic processes.

## Stability

Stability or long term stability defines how long a sensor can be used without a change in performance. The quantification is generally done by using drift values. This is not equivalent with the lifetime that is described in the next section.

## Lifetime

The lifetime describes how long a sensor is usable. The lifetime can be divided into shelf-life, which is the maximum storage time, and the operating life, which describes the maximum operating time.

## Response time

The response time describes how much time a sensor needs to respond to a sudden concentration change. Response times are usually given by percentages of the final value. The most commonly used value is  $t_{90}$ .

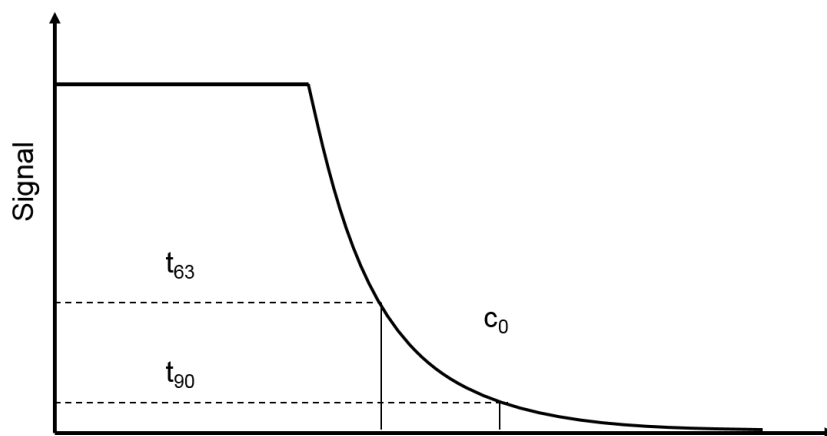


**Figure 2.1:** Exemplary homogenous response time [19]

## 2.2 Optical chemical sensors

“Optical devices transform changes of optical phenomena, which are the result of an interaction of the analyte with the receptor part.”[17]. There are two main categories for optical sensors, direct sensors and reagent-mediated sensors. The direct sensor responds to some intrinsic optical property, for example luminescence or absorption of the analyte. The reagent mediated sensors have an intermediate agent, for example a sensitive dye molecule, which then responds optically to the analyte. The latter is used when the analyte has no useful intrinsic optical properties, that could be detected by a sensor.[18]

Optical sensors can also be divided into 7 categories [17]:

1. Absorption
2. Reflection
3. Luminescence
4. Fluorescence
5. Refractive index
6. Optothermal effects
7. Light scattering

Sensors based on absorption and luminescence are the most commonly used optical sensors and will be described more thoroughly at another point. All information for the next chapters was taken from [21] and [22] unless stated otherwise.

### 2.2.1 Absorption

Absorption is a type of electronic transition, where an electron is moved from an orbital in the ground state (HOMO, highest occupied molecular orbital) to a higher unoccupied orbital (generally, LUMO, lowest unoccupied molecular orbital).

There are different kinds of bonding orbitals, the  $\sigma$  orbital can be formed from s and p orbitals with a collinear relationship, whereas the  $\pi$  orbital can only be formed from p orbitals that overlap laterally. The absorption of a photon raises an electron into the anti-binding  $\sigma$  or  $\pi$  orbital (written as  $\sigma^*$  or  $\pi^*$ , respectively). Also non-bonding electrons, which are usually present on heteroatoms such as oxygen or nitrogen, can be promoted from their corresponding orbitals which are called n or p orbitals into an anti-bonding orbital.

All the orbitals have a certain energy level, and those levels are in the order shown below.

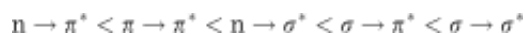


**Figure 2.2:** Order of energies of orbital transitions [21]

These transitions can also be seen in Figure 2.3 where formaldehyde is used as an example.

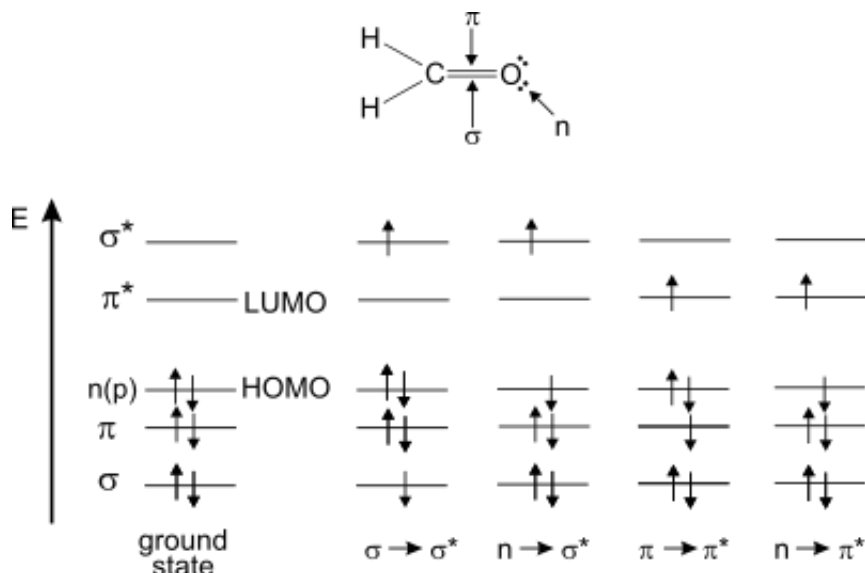


**Figure 2.3:** Orbital transition using formaldehyde as an example [21]

As can be seen in Figure 2.3 the spin of the electron remains unchanged when it is promoted to a higher orbital. This is then called a singlet state, or a singlet-singlet transition. If a singlet electron is in an excited state it can undergo a transition, which leads to a spin change and a so-called triplet state. This generally happens because the triplet state of the same configuration has a lower energy than the singlet state.

### The Lambert-Beer law

The Lambert-Beer law describes the efficiency of absorption of light at a certain wavelength.

$$A(\lambda) = \log \frac{I_0}{I} = \epsilon l c \quad (2.1)$$

In this equation  $A$  is the absorbance at a certain wavelength [nm],  $I_0$  is the intensity at the beginning (when entering the sample) and  $I$  is the intensity of light after the sample.  $\epsilon$  is the molar absorption coefficient [ $\text{L mol}^{-1} \text{ cm}^{-1}$ ],  $l$  (which is often also written as  $d$ ) is the length or thickness of the sample [cm] and  $c$  is the concentration [ $\text{mol L}^{-1}$ ].

## 2.2.2 Luminescence

Luminescence describes the emission of photons, ultraviolet, visible or infrared, from an electronically excited species.

This phenomenon is not induced by heat, which is in contrast to incandescence. Luminescence, (Latin; lumen = light) was first described by Eilhardt Wiedemann in 1888.

There are various types of luminescence which are differentiated by their mode of excitation.

Tab. 1.1. The various types of luminescence

Phenomenon	Mode of excitation
Photoluminescence (fluorescence, phosphorescence, delayed fluorescence)	Absorption of light (photons)
Radioluminescence	Ionizing radiation (X-rays, $\alpha$ , $\beta$ , $\gamma$ )
Cathodoluminescence	Cathode rays (electron beams)
Electroluminescence	Electric field
Thermoluminescence	Heating after prior storage of energy (e.g. radioactive irradiation)
Chemiluminescence	Chemical process (e.g. oxidation)
Bioluminescence	Biochemical process
Triboluminescence	Frictional and electrostatic forces
Sonoluminescence	Ultrasounds

**Figure 2.4:** Different types of luminescence [21]

In this thesis only photoluminescence (Figure 2.4) was applied as a sensing principle. The Jablonski Diagram (Figure 2.5) shows different de-excitation pathways after absorption of a photon.

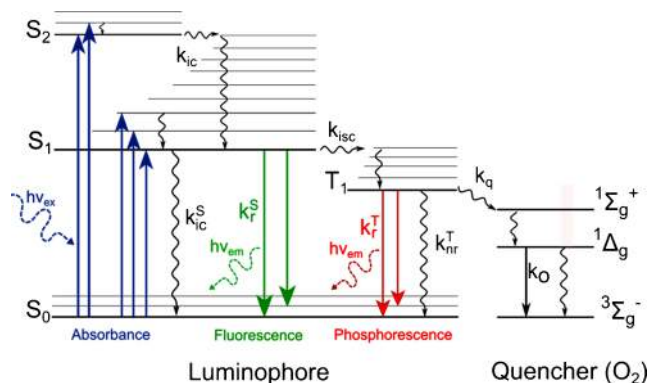


**Figure 2.5:** Jablonski Diagram[23]

As explained in subsection 2.2.1 the absorption of a photon leads to an excited state. From there different de-excitation processes are possible. Intersystem crossing, fluorescence, delayed fluorescence, phosphorescence, internal conversion, triplet-triplet transition and non radiative de-excitation.

### 2.2.3 Internal conversion

Internal conversion describes a non-radiative transition. The transition can occur between two electronic states, if they show the same multiplicity such as  $S_2$  and  $S_1$ , which describe two different excited singlet states. Internal conversion usually happens if excitation is higher than the  $S_1$  level, because internal conversion into the  $S_0$  state, which is the ground state, competes with other processes, for example fluorescence. Also the energy gap is much higher between the ground state and the first excited state, compared to, for example, the  $S_2$  and  $S_1$  state. In solution the excess energy caused by internal conversion can be transferred to solvent molecules.

### 2.2.4 Fluorescence

If de-excitation occurs from the  $S_1$  to the  $S_0$  state through emission of a photon, it is called fluorescence. It is usually a spontaneous process. Fluorescence usually happens from the  $S_1$  state and is therefore not dependent on the excitation wavelength. When comparing absorption and fluorescence spectra, the fluorescent spectra are always at higher wavelengths, which is due to the fact that in the excited state there is vibrational relaxation. However, often an overlap between the two spectra can be observed. This means that some part of the light is emitted at lower wavelengths than it is absorbed. This is due to the fact that at room temperature some molecules are at higher vibrational levels (over 0). The difference between the two maxima is called the Stokes shift.

Generally, absorption and emission of a photon happen at the same speed, but the molecule stays in an excited state for a certain time, which is called the lifetime. Lifetimes can be from picoseconds to nanoseconds and decrease exponentially.

### 2.2.5 Intersystem crossing

Intersystem crossing is a transition between two states that show different multiplicity but have the same vibrational energy, for example from  $S_1$  to a  $T_n$  state. Then, due to vibrational relaxation the molecule goes into the  $T_1$  state. The transition is non-radiative and generally a forbidden transition, but it can still occur if there is a large spin-orbit coupling. This is often favored if heavy atoms (e.g. Br or Pb) are present. Since intersystem crossing may be quite fast ( $10^{-7}$  -  $10^{-9}$  s) it can be in competition with other de-excitation processes.

### 2.2.6 Phosphorescence

Phosphorescence can only happen from the  $T_1$  level. The transition from that state to the  $S_0$  state is actually forbidden and the process is very slow. This means that non-radiative de-excitation is often favored over phosphorescence. Still, at low temperatures or in a rigid medium phosphorescence can often happen, since in these cases lifetimes may increase notably. Since the energy of the lowest vibrational level in  $T_1$  is lower than in  $S_1$  the spectra again shows a shift to higher wavelengths, compared to the fluorescent spectrum.

### 2.2.7 Delayed Fluorescence

There are 2 different types of delayed fluorescence.

#### Thermally activated

If  $T_1$  shows a long lifetime and the gap to the  $S_1$  state is very small, intersystem crossing back to the  $S_1$  level can occur (reverse intersystem crossing). It shows the same emission wavelengths as regular fluorescence, but with a much longer lifetime. Since it is thermally activated, this process is more likely at higher temperatures.

#### Triplet-triplet annihilation

This happens in highly concentrated solutions. If two molecules that are both in a  $T_1$  state collide, one of them can return to the  $S_1$  state. There de-excitation can occur through other processes such as fluorescence.

### 2.2.8 Triplet-triplet transition

If a molecule is already in the triplet state, it can take in another photon, since this is not forbidden, and be then raised into a higher energy level. This is only possible if the population in the triplet state is high enough.

### 2.2.9 Quenching

A quencher can have 2 different effects on a molecule in an excited state.

The quencher can either lead to faster decay times or to a decrease in quantum yields and therefore a decrease in fluorescent intensity. There are different cases in which quenching is possible:



- The quencher is present in a large excess. In an excited state, the possibility of Q (quencher) and M (molecule) being close to each other, and therefore able to interact, is very high.
- There is only a small amount of Q present but interaction between the two molecules can occur even at distances larger than the collision distance. In this case the excited state of the molecule is very short and therefore collision between Q and M is not possible.
- There is only a small amount of Q present but the existence of an excited state allows the two molecules to collide/interact within it. This process is diffusion-controlled and therefore time-dependent.

### Dynamic quenching

Dynamic quenching is also called collisional quenching, because here quenching can only occur upon collision of the quencher with the molecule [22]. It can affect the lifetime as well as the intensity of the fluorophore. In dynamic quenching the rate constant for the quenching process is assumed to be time independent and follows the given Stern-Volmer relation:

$$\frac{\Phi_0}{\Phi} = \frac{I_0}{I} = 1 + k_q\tau_0[Q] = 1 + K_{SV}[Q] \quad (2.2)$$

$\Phi$  is the quantum yield,  $I$  stands for the fluorescence intensity and  $I_0$  for the fluorescence intensity in absence of the analyte.  $k_q$  is the rate constant for the quenching process, and  $\tau$  is the fluorescence lifetime whereas  $\tau_0$  is the lifetime in absence of the analyte.  $k_q$  and  $\tau_0$  give  $K_{SV}$  which is the Stern-Volmer constant and  $[Q]$  is the concentration of the quencher. If  $I_0/I$  are plotted against the concentration of the quencher, a Stern-Volmer plot is obtained. If a linear relationship is given, the slope gives the Stern-Volmer constant and therefore  $k_q$  can be calculated. An exemplary Stern-Volmer plot can be seen in Figure 2.6.

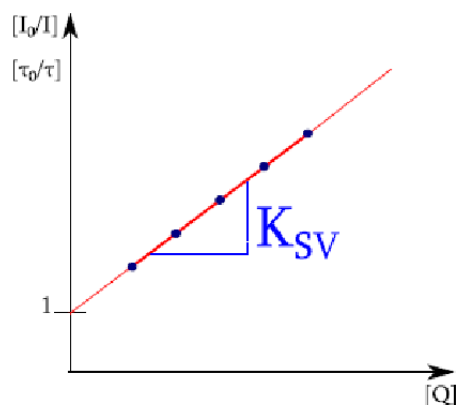


**Figure 2.6:** Stern-Volmer plot for dynamic quenching [24]

## Static quenching

There are 2 different types of static quenching. There has to be either a sphere of effective quenching or the formation of a ground state non fluorescent complex (Figure 2.7).

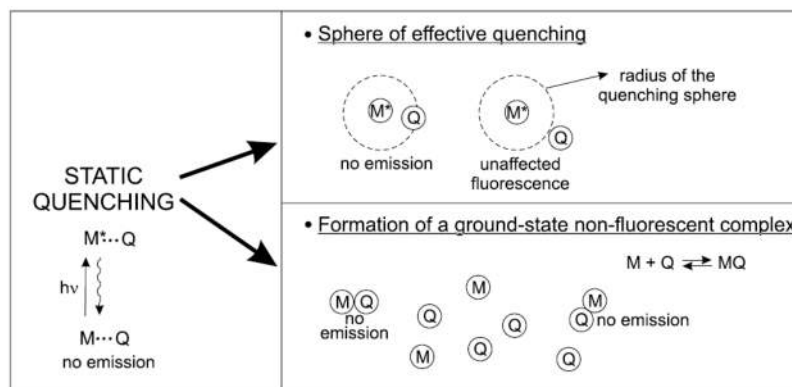
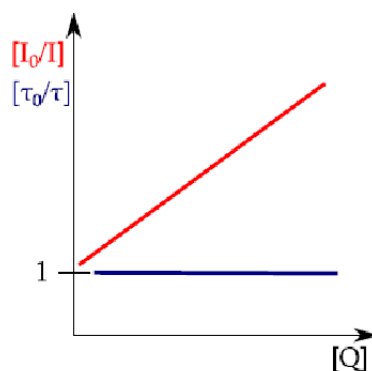


**Figure 2.7:** Illustration of possible static quenching processes [21]

The quencher has to be in a certain distance to the molecule in the excited state, which is called sphere of effective quenching process. If the quencher is further away, it has no influence on the molecule. Therefore addition of the quencher can decrease fluorescence intensity, but has no effect on the decay time. This often happens in a very viscous media or in rigid matrices.

The other possibility is the formation of a ground state non fluorescent complex, which also influences the intensity, but again lifetimes remain unchanged.

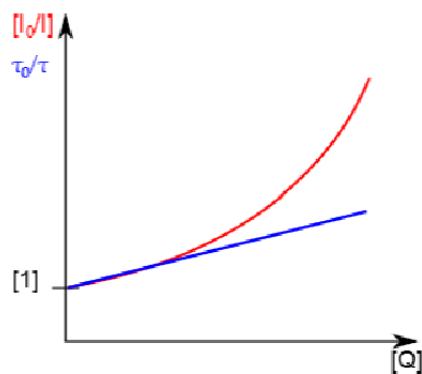
A linear Stern - Volmer plot for intensities vs. concentration of the quencher can be obtained (Figure 2.8).



**Figure 2.8:** Stern-Volmer plot for static quenching [24]

## Simultaneous static and dynamic quenching

For many molecules not one but both types of quenching can occur simultaneously. If this is the case, the Stern-Volmer plot does not show linearity anymore (Figure 2.9). The dynamic part of the quenching can be found through lifetime measurements [22].

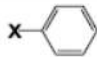
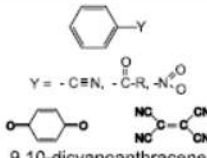


**Figure 2.9:** Stern-Volmer plot showing simultaneous quenching [24]

### 2.2.10 Photoinduced electron transfer

Fluorescence quenching is often induced through PET [25]. PET effects can be observed in different processes for example during photosynthesis.

Depending on the fluorophore, it can act as an electron donor, as well as an electron acceptor. Examples can be seen in Figure 2.10. Whether it is a donor or an acceptor can be determined through the reductive and oxidative potentials of the ground state and the excited state. This also makes this kind of quenching process more predictable compared to other quenching processes, since redox potentials are known, which describe the probability of an electron transfer [22].

electron donors $D^*$	electron acceptors $A^*$
 <p>X = H-, <math>(CH_3)_2N</math>-, <math>CH_3O</math>-, HS-</p> <p>naphthalene, anthracene, phenanthrene, pyrene, perylene</p>	 <p>Y = -C≡N, -C(=O)-R, -NO<sub>2</sub></p> <p>9,10-dicyanoanthracene</p>

**Figure 2.10:** Examples for electron donors and acceptors for PET [21]

PET effects are facilitated in an excited state because the oxidative or reductive abilities of the

molecules are much higher than in the ground state.

Electron donor [D] and acceptor [A] form a complex  $[D_p^+ A_p^-]$ . Due to quenching caused by this electron transfer, this complex then returns to the ground state without emission of a photon and subsequently the electron is returned to the electron donor.

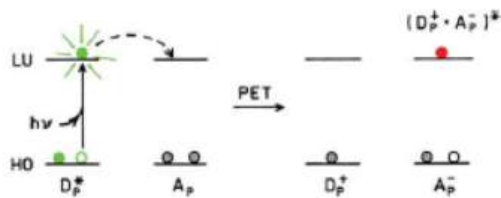


**Figure 2.11:** Scheme for PET [22]

In some cases, emission as an exciplex or excimer instead of quenching is possible. An exciplex is formed, when an excited molecule collides with a non-excited different molecule to form an excited complex. An excimer is formed when an excited molecule collides with the same molecule, but in a non-excited state. This then forms an excited dimer. Both formation processes are diffusion controlled.

## 2.3 Fluorescence measurement principles

### 2.3.1 Steady-state spectrofluorometry

A scheme of conventionally used spectrofluorometer can be seen in Figure 2.12.

It includes a light source, generally a xenon lamp and monochromators which are used to change the excitation and emission wavelengths. Fluorescence is detected in a  $90^\circ$  angle, to the incident beam, by a photomultiplier and data is read out with a computer. Additionally, various other parts such as polarizers or quantum counters can be included into the set-up.

The fluorescence intensity is dependent on the light source, the monochromators and the sensitivity of the detector. Light scattering, polarization and inner-filter effects can falsify the fluorescence spectra. Therefore, fluorescence intensity should always be stated on an arbitrary scale (a.u.) depending on experimental conditions.

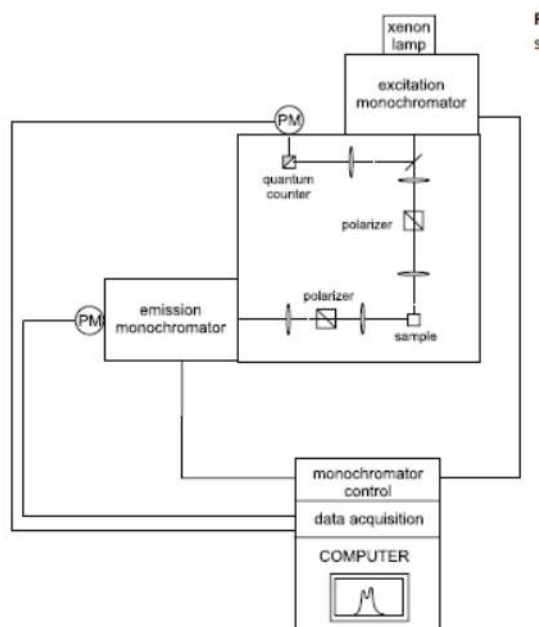


**Figure 2.12:** Schematic of a spectrofluorometer [21]

### Inner filter effects

There are 3 different types of inner filter effects.

- Excitation inner filter effect, if the sample concentration is too high a significant part of light is absorbed even before reaching the central part of the sample cell (e.g. cuvette). Therefore intensities go through a maximum and then decrease. This shows that only at a certain concentration range intensities are proportional to the concentration.
- Emission inner filter effect, also called self-absorption, can be observed when photons, emitted in the region of the absorption spectra, are re-absorbed. This leads to a distortion of the fluorescence spectra in this region.
- Inner filter effect due to other substances; they absorb light at the same wavelength as the sample emits it and can therefore act as filters.

### 2.3.2 Time resolved fluorometry

There are two general principles for time resolved measurements, pulse fluorometry and phase modulation fluorometry, both give the lifetime of the fluorescent sample. A schematic drawing of those can be found in Figure 2.13.

## Pulse fluorometry

The sample is excited by a short pulse of light. The pulse is kept as short as possible and has to be shorter than the decay time of the molecule. Then the response of the sample is detected as a function of time ( measurement in the time domain). Plotting intensity vs. time, gives an exponential slope which represents the lifetime or decay time.

## Phase modulation fluorometry

Excitation is performed at high frequencies through a sinusoidally modulated light. The sinusoidal response of the sample shows a shift compared to the excitation light. The shift is due to the lifetime of the molecule and therefore the response curve is used for determination of life- or decay times.

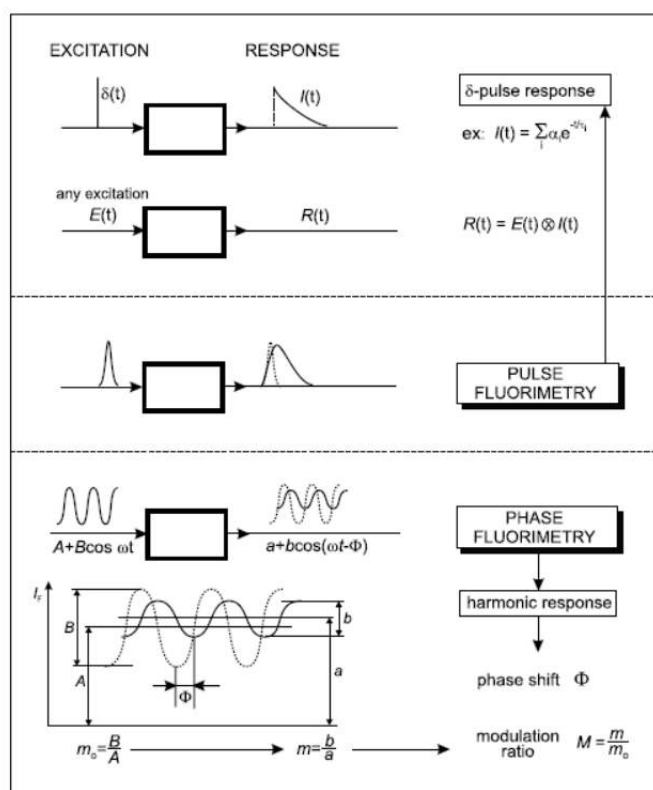


**Figure 2.13:** Schematic drawing of time resolved measurements [21]

### 2.3.3 Dual lifetime referencing

Dual lifetime referencing is often applied because of its many advantages over other measurement methods. Direct detection of lifetimes is expensive and the set-up is complicated. Unreferenced

intensity measurements do not give absolute values and are even dependent on the set-up, hence easily changeable.

To perform dual lifetime referencing a reference dye is needed. It should have a large decay time and show similar emission and excitation wavelengths as the indicator dye. It should not be sensitive to the analyte or other substances. The principle of this measurement is phase modulation fluorometry. The phase shift that is detected, depends on the intensities of both dyes (Figure 2.14). The reference dye should not change with changing analyte concentrations, whereas the indicator dye is influenced by the concentration of the analyte. This leads to a detectable change of the phase shift. [2][13][16]

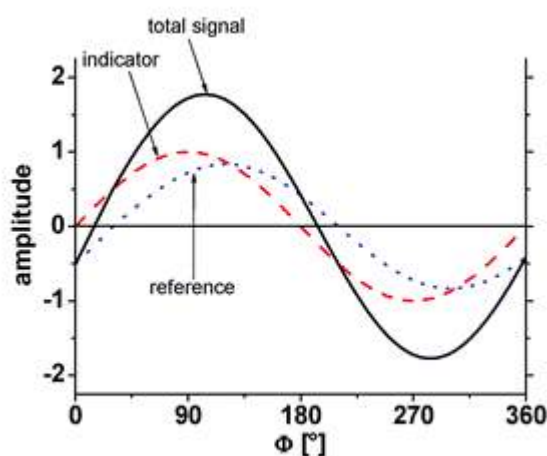


**Figure 2.14:** Principle of dual lifetime referencing measurement [26]

## 2.4 Carbon Dioxide

Carbon dioxide is a gas that is present everywhere in the atmosphere. Therefore detection of  $\text{CO}_2$  is very important.  $\text{CO}_2$  sensors are used in medicine, e.g. for clinical breath analysis. They also find application in environmental monitoring [7], since ocean acidification is a big problem, monitoring of  $\text{CO}_2$  in the oceans is important. They are also useful in industrial monitoring for food-packaging [2], wastewater treatment, bioreactor control [4] or other places where high  $\text{CO}_2$  concentrations may pose a risk and safety control is an issue [3] [5].

There are different approaches to measuring  $\text{CO}_2$ . The most common ones are infrared spectroscopy the Severinghaus electrode and measurements of pH changes through optical changes such as absorption or fluorescence [9].

### 2.4.1 Nondispersive infrared CO<sub>2</sub> sensors

This sensor is used to measure gaseous CO<sub>2</sub>. It works through detection of a characteristic absorption of the molecule. CO<sub>2</sub> absorbs in the near infrared region between about 4200 and 4400 cm<sup>-1</sup> [8]. The general set up can be seen in Figure 2.15.

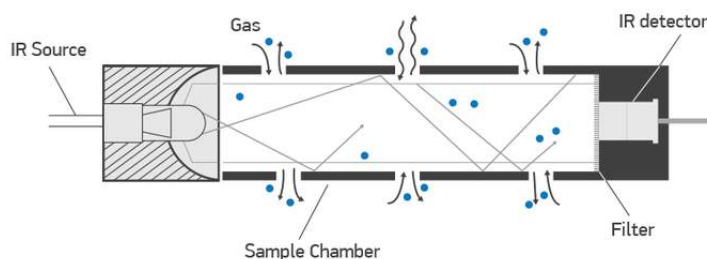


**Figure 2.15:** Infrared CO<sub>2</sub> detector [27]

The concentrations of the gases are measured by sensing how much of the infrared light is absorbed and since different gases absorb at different wavelengths, they can be easily distinguished. Detection can be done two ways.

The molecule can gain energy through absorption of infrared radiation. This leads to more vibrations, which can then result in a rise of temperature. The second possibility of detection is through detection of the decrease in the strength of radiation, which again is caused by the absorption of infrared radiation by the analyte.

Some problems associated with infrared detectors such as corrosion and contamination of the analyzer are caused by humidity. This and the IR absorption of water makes it unusable in aquatic environments. Another problem is that they are very expensive and difficult to miniaturize, though progress has been made in recent years.[28][29]

### 2.4.2 Severinghaus electrode

The Severinghaus electrode is an electrochemical sensor used for CO<sub>2</sub> measurements in solutions. The electrode is a pH electrode, that contains a bicarbonate buffer. The dissolved CO<sub>2</sub> can enter the electrode through a gas-permeable membrane thus leading to a change in partial pressure.[30] Interaction of CO<sub>2</sub> is shown in the scheme below:





This leads to the following pH dependence:

$$pH = pK_a + \log \frac{c\text{HCO}_3^-}{p\text{CO}_2 * a_{\text{CO}_2}} \quad (2.3)$$

Where  $c\text{HCO}_3^-$  is the concentration of  $\text{HCO}_3^-$ ,  $p\text{CO}_2$  the partial pressure of  $\text{CO}_2$  and  $a_{\text{CO}_2}$  is the activity of  $\text{CO}_2$ . Since detection is only due to the partial pressure of  $\text{CO}_2$ , measurements are very dependent on temperature and pressure. Another disadvantage is that it is very slow and drifts due to osmotic pressure can be observed.

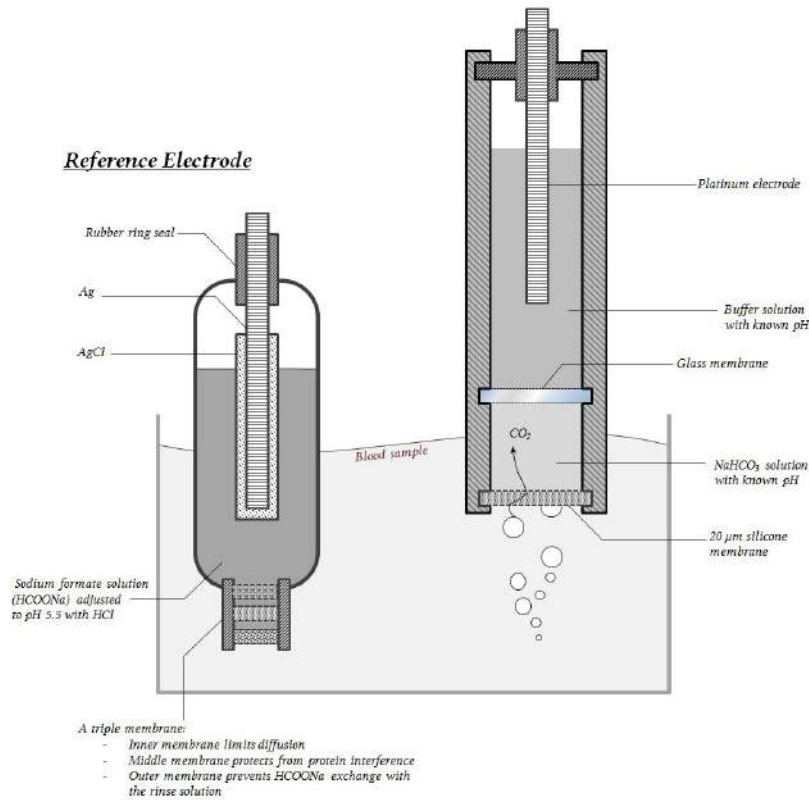
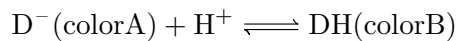


**Figure 2.16:** Schematic drawing of the Severinghaus electrode and a reference electrode [30]

### 2.4.3 Optical pH change based detections

There are 2 general systems that can be applied when preparing  $\text{CO}_2$  thin film sensors, the Severinghaus type and the Mills type.

The Severinghaus type sensors [10], need a trapped aqueous layer (can be part of the same layer as the indicator dye) to make sensing possible. The reaction it follows is the same as in the electrode described in subsection 2.4.2. It utilizes a dye that is also entrapped in the system, which can change the color or fluorescence upon change of the pH, induced through  $\text{CO}_2$ . The general reaction for this is:



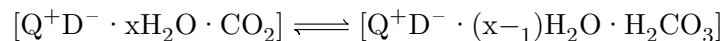
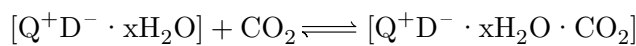
Color A describes the deprotonated form and color B the protonated form of the dye.

The water present in the system leads to several problems. On one hand, it makes the sensor sensitive to moisture, on the other hand evaporation of water decreases the shelf- and usage life of the sensor. Furthermore, it can enhance leaching of the dye. This can be prevented by addition of a hydrophobic membrane such as PTFE or silicone. However, this can lead to increased response and recovery times and it makes manufacturing the sensor more difficult. [9]

To overcome these problems a Mills type sensor was developed [10], which is a near solid state sensor. The dye is entrapped in a hydrophobic layer, such as a polymer or plastic film. Seeing that CO<sub>2</sub> sensing only works if water is present, and most dyes are rather hydrophilic, a lipophilic base has to be added. Water of solvation is usually associated with the lipophilic base, and therefore no extra water is needed in the sensing layer. The reaction is assumed to work in the following way:

The lipophilic base [Q<sup>+</sup>OH<sup>-</sup>] reacts with the dye [D<sup>-</sup>] to form the ion-pair [Q<sup>+</sup>D<sup>-</sup>]

This then reacts reversibly with CO<sub>2</sub>:



The protonated and deprotonated forms of the dye should show different absorption maxima (or fluorescence intensities) and can therefore be easily distinguished.

These thin films have the advantage of having a long shelf life, since evaporation of H<sub>2</sub>O poses no problem. They also show the advantage of being water insoluble and fabrication of these sensors is much easier due to the fact that no extra layer is needed when measuring in the gas phase. The layer cannot be omitted when measuring in the liquid phase due to other interactions such as H<sup>+</sup>. The problem with leaching of the dye is also greatly reduced by this type of sensor.

However, the use of a lipophilic base can lead to other problems, such as decomposition of the lipophilic base and therefore degradation of the sensor. Other problems that are often associated with this type of the sensor are that they are quite prone to drifts and often show cross-sensitivity to other acids or are poisoned by them, for example to SO<sub>2</sub> and NO<sub>x</sub> [8]

### 2.4.4 Materials

A CO<sub>2</sub> thin film sensor can contain the following components: indicator dye/ lipophilic base/ polymer/ plasticizer/ luminescent reference dye /protective layer and a solid support. Not every sensor contains all of those components.

#### Solid support

Thin film sensors are mounted on a solid support [31], this is often done by casting the sensor solution through a solid support or knife coating it [4]. There are not a lot of different materials used for solid supports. The most common ones are glass [31], a quartz plate [3] or, as used in this thesis, a polymeric support such as PET or other polyesters [4] [8] [32].

#### Matrix materials

Matrix materials are usually polymers. The dyes can be either entrapped physically, which can lead to leaching problems, or covalently bound to the matrix.[4]. Materials used are:

- Ethyl cellulose [3] [7] [8] [9] [31] [33]
- Poly(vinyl butyral) [3]
- Polystyrene [7] [31]
- Poly(methyl methacrylate) [31]
- Cellulose acetate butyrate [31]
- Poly(dimethylsiloxane) or other sol-gel matrices[4][18]
- Hydrogels D4, D7,.. [32]

Ethyl cellulose is the most commonly used material due to its high CO<sub>2</sub> permeability, whereas it is impermeable to protons. This reduces cross-sensitivity to pH changes.[8]

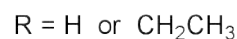
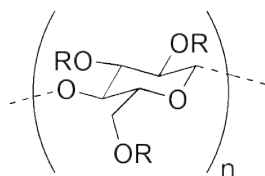


**Figure 2.17:** Structure of Ethyl cellulose

## Indicator dyes

There are 2 types of indicator dyes that are used for CO<sub>2</sub> sensing, either a colorimetric change is visible (change in absorption maxima) or a change in fluorescence can be observed. All of them respond to a change of pH induced by the CO<sub>2</sub> molecule.

The following materials are used as absorption based materials and the color change given has been observed for CO<sub>2</sub> sensors:

- Thymol blue (blue => yellow) [7] [10]; pKa<sub>1</sub> = 1,7, pKa<sub>2</sub> = 8,9 [34]; R<sub>1</sub>= -CH(CH<sub>3</sub>)<sub>2</sub>, R<sub>2</sub>= -CH<sub>3</sub>, R<sub>3</sub>= -CH<sub>3</sub>, R<sub>4</sub>= -CH(CH<sub>3</sub>)<sub>2</sub> (Figure 2.18)
- Phenol red (red => yellow) [7] [10] [31]; pKa<sub>1</sub> = 1,2, pKa<sub>2</sub> = 7,7 [35]; R<sub>x</sub> = -H (Figure 2.18)
- Cresol red (red => yellow) [3] [7] [10]; pKa<sub>1</sub> = 1, pKa<sub>2</sub> = 8,3 [36] [37]; R<sub>1</sub> = -CH<sub>3</sub> R<sub>3</sub>= -CH<sub>3</sub> (Figure 2.18)
- M-cresol purple (violet => yellow) [3] [10]; pKa<sub>1</sub> = 1,5, pKa<sub>2</sub> = 8,3 [38]; R<sub>2</sub> = -CH<sub>3</sub> R<sub>5</sub>= -CH<sub>3</sub> (Figure 2.18)
- Neutral red (red => orange/yellow) [10]; pKa = 5,9 [39] (Figure 2.19)
- Brilliant yellow (red => yellow) [10] (Figure 2.20)
- M-nitrophenol (yellow => colorless) [10]; pKa = 8,3 [38] (Figure 2.21)
- Dihydroxy aza-BODIPY (also fluorescence based measurements possible) (purple => green); pKa<sub>1</sub> = 8,2, pKa<sub>2</sub> = 10,3; [6] (Figure 2.22)

All of the dyes mentioned above shows absorptions in the UV-VIS range, except the aza-BODIPY dyes which absorbs in the NIR-region, where interferences are minimized. The triphenyl methane dyes show high pKa tunability and therefore high flexibility in sensitivity, but show low photostability, whereas the aza-BODIPY dye has very high photostability.

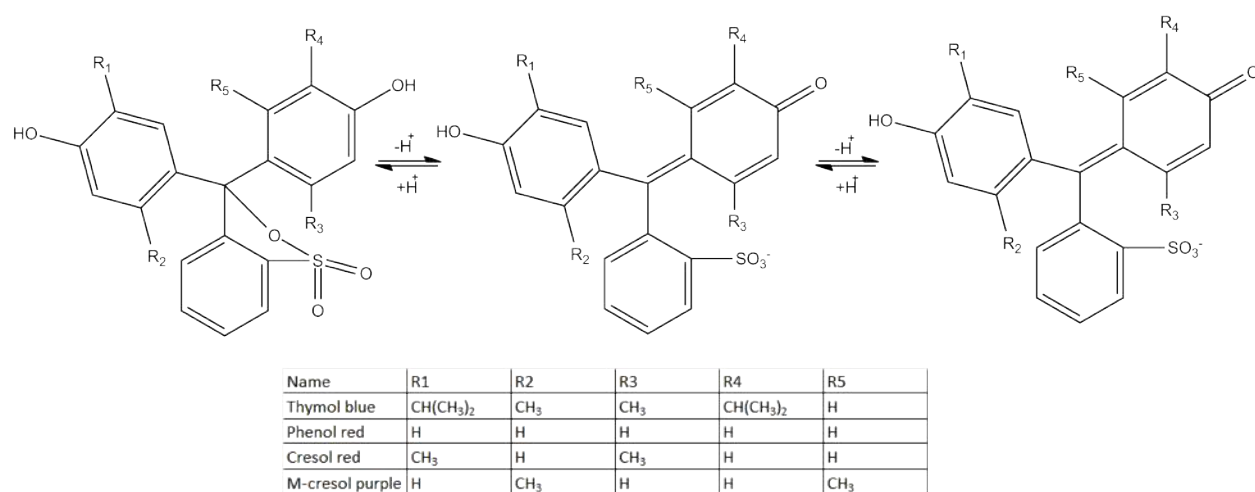


**Figure 2.18:** Structures of thymol blue, phenol red, cresol red, m-cresol purple in different protonated states

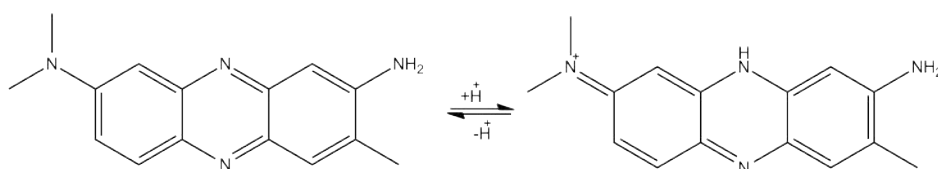


**Figure 2.19:** Structure of neutral red in neutral and protonated state

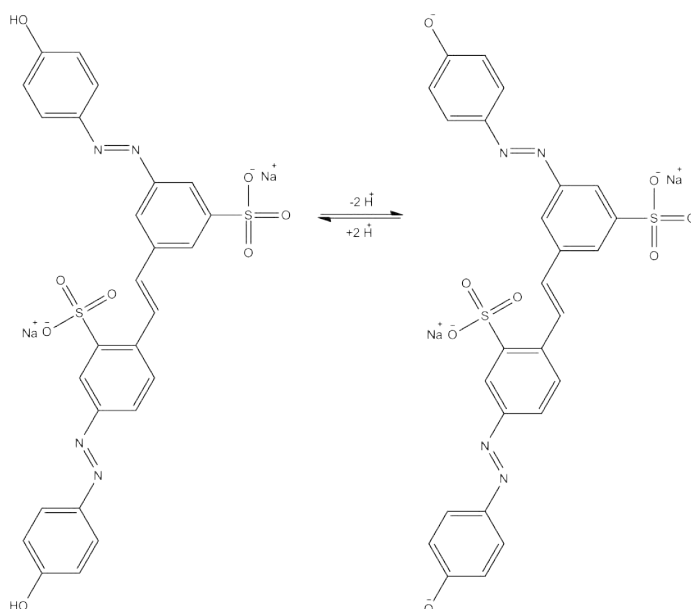


**Figure 2.20:** Structure of brilliant yellow in neutral and deprotonated state

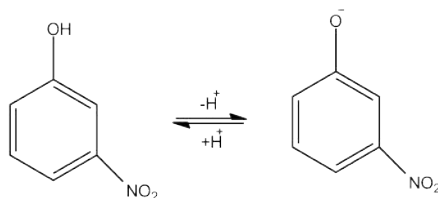


**Figure 2.21:** Structure of m-nitrophenol in neutral and deprotonated state

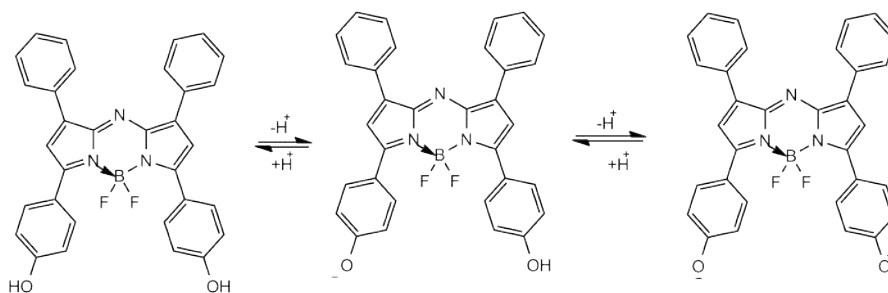


**Figure 2.22:** Structure of dihydroxy-aza-BODIPY dye in neutral and deprotonated states

The following materials are used as fluorescence based materials:

- Hydroxypyrene trisulfonate [1] [2] [4] [7] [9];  $pK_a = 7,3$  [40] (Figure 2.23)
- Diketo-Pyrrolo-Pyrrole dyes [1]  $pK_{a_{Ar1}} = 11,8$  (Figure 2.24)

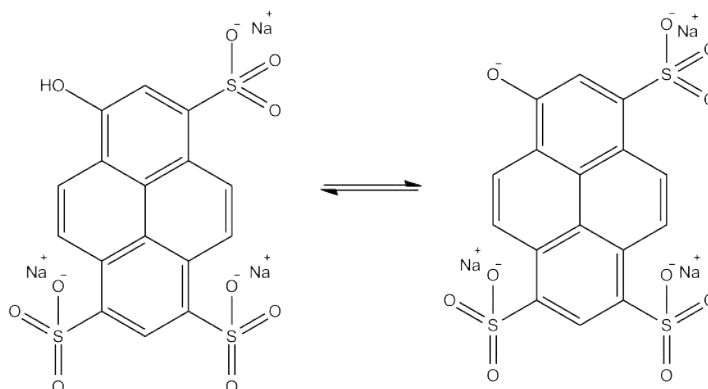


**Figure 2.23:** Structure of HPTS in neutral and deprotonated state

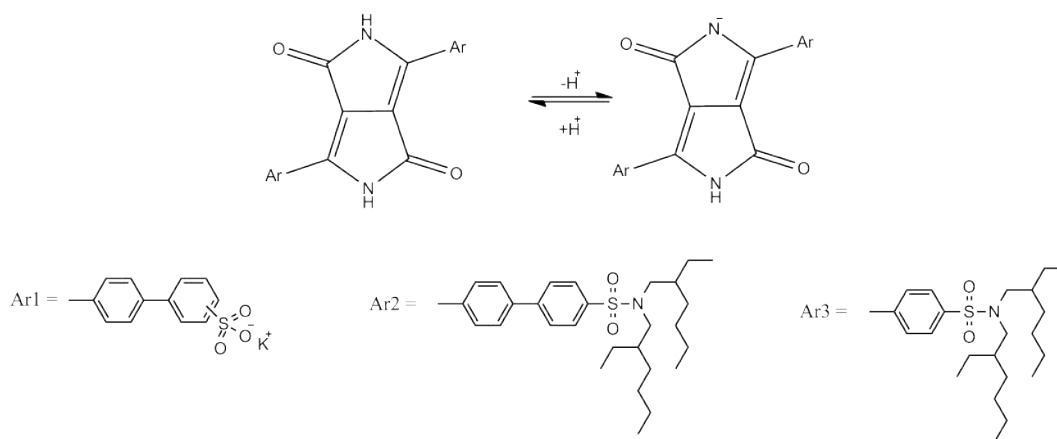


**Figure 2.24:** Structure of diketo-pyrrolo-pyrrole dyes in neutral and deprotonated state

HPTS is one of the most commonly used fluorescent indicator dyes for  $CO_2$ , it is commercially available, has relatively bright fluorescence but only moderate absorption coefficients. It is excited in the blue part of the spectrum, thus background fluorescence from the environment and optical components may be high.

Diketo-pyrrolo-pyrrole dyes are easy to prepare on a large scale from cheap pigments. Absorption and emission measurements are done ratiometric and may show bright fluorescence [41].

The sensitivity of the indicator dye to  $CO_2$  depends on various factors. Generally higher pKa values mean that the dye can be protonated more easily, which leads to an increase in  $CO_2$  sensitivity. The pKa values can be tuned, by changing other substituents [1]. This can be seen when comparing thymol blue with phenol red. Thymol blue shows more substituents, which are all donating groups and has therefore a higher pKa value.

The substituents can have another effect, steric hindrance. If the attached groups are too bulky, the deprotonable site is more difficult to access leading to a decrease in sensitivity. On the other hand, if competing groups are present, making them less accessible by bulky groups can be advantageous.

### Lipophilic Base

Lipophilic bases are used in the Mills type sensors. They are associated with water molecules and thus serve as a kind of buffer. They also help solubilize the indicator dye in the hydrophobic polymer. [33]

The most commonly used lipophilic bases are quaternary ammonium salts. [4] The following lipophilic bases have been used for  $CO_2$  sensing:

- Tetraoctyl ammonium hydroxide (TOAOH) [3] [4] [7] [9] [31]

- Cetyltrimethyl ammonium hydroxide (CTAOH) [2] [4]
- Cetyltrimethylammonium bromide (CTAB) [4]

### **Plasticizers**

The use of plasticizers enhances the mobility of the polymer chains and therefore improves gas permeability. Also, the glass transition temperature is lowered [3]. Mills et al. showed that the sensitivity to CO<sub>2</sub> and O<sub>2</sub> is mostly independent of the polymer matrix if a sufficient amount of plasticizer is added. [31]. The following plasticizers have been used:

- Dimethyl phthalate[31]
- Diethyl phthalate [31]
- Dipropyl phthalate[31]
- Diheptyl phthalate[31]
- Dioctyl phthalate[31]
- Diisodecyl phthalate[31]
- Tributyl phosphate [7] [9] [10]
- Tris (2-ethylhexyl) phosphate [3] [10]

### **Protective layer**

The protective layer is often used in Severinghaus type sensors, since in this case leaching of the dye poses a bigger problem. Most commonly used protective layers are PTFE and silicone layers since they are gas-permeable and hydrophobic. [9]. The extra layer can also be used to incorporate reference dyes or other particles, such as TiO<sub>2</sub>, which is added to increase signal intensities. A drawback of the extra layer is, that it often leads to increased response and recovery times.

### **Reference dyes**

CO<sub>2</sub> sensing is referenced by using reference dyes, which are often incorporated into an extra layer, which also gives extra protection. It is important that the luminescence of the reference dye is not influenced by the analyte. It should also show different spectral properties such as a different lifetime or a different emission spectra.

Reference dyes may increase photobleaching of the dye and therefore reduce the usage life of



the sensor.[6]

Reported reference dyes were a tris(thenoyltrifluoroacetato) europium(III) dihydrate complex [7] and ruthenium complexes such as  $[\text{Ru}(\text{dpp})_3^{2+}]$  [4] [7] [31] .

Also several phosphor complexes such as CrGAB [42] and Egyptian blue [43] have shown promising criteria to be used as reference dyes. They offer high photostability, they are inert to oxygen and therefore do not produce reactive singlet oxygen.

### 2.4.5 Viscosity based $\text{CO}_2$ sensors

A viscosity sensor works by change of viscosity due to the presence or absence of  $\text{CO}_2$ . Su et al. [44] reported a viscosity sensor based on a four-armed star-like polymer. The polymer contains polyacrylamide as a core, which is water soluble and poly(N,N-diethylaminoethyl methacrylate) on the ends (Figure 2.26).

The chain ends are at first hydrophobic leading to a high viscosity. This is due to the fact, that the hydrophobicity leads to a formation of a network structure. Upon addition of  $\text{CO}_2$  the chain ends become charged, making the polymer more hydrophilic and therefore viscosity decreases (Figure 2.25).

A major drawback is that these sensors are prone to interferences of NaCl. High concentrations of NaCl can enhance the viscosity of the solution.

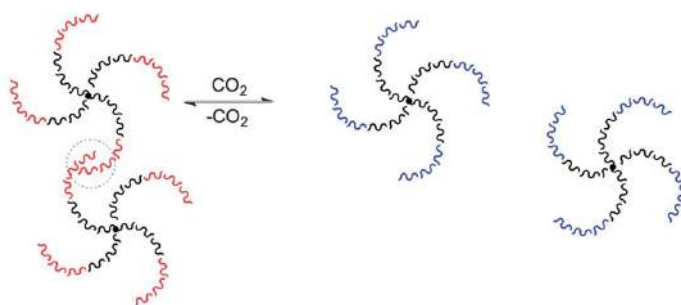


**Figure 2.25:** The polymer changes its viscosity upon exposure to  $\text{CO}_2$  [44]

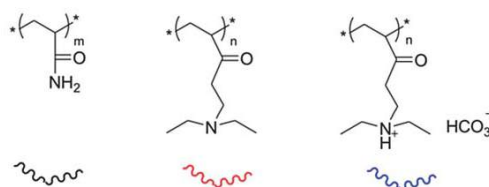


**Figure 2.26:** Structures of the polymers [44]

Another viscosity sensor was reported by Liu et al. [45]. Here a dye that is non-emissive, can be turned strongly fluorescent. This is achieved when the dye, here HPS (Figure 2.28), is dissolved

in a carbamate ionic liquid and then CO<sub>2</sub> is bubbled through. The addition of CO<sub>2</sub> leads to an increase in polarity and viscosity and thus activates the molecule.

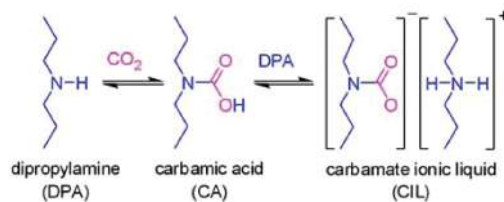


**Figure 2.27:** Reaction of a secondary amine with CO<sub>2</sub> to form a carbamate [5]

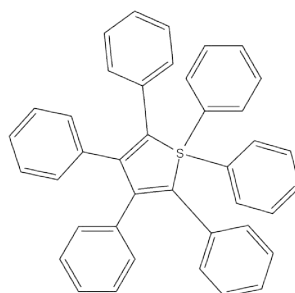


**Figure 2.28:** Structure of 1,1,2,3,4,5-Hexaphenylsilole (HPS)

#### 2.4.6 Polarity based CO<sub>2</sub> sensors

Here a solvatochromic dye is used, which is affected by the polarity of the surrounding environment. An additive, usually a hydrophobic amidine that can reversibly bind CO<sub>2</sub>, has to be used in this sensor system [8]. Ali et al. [8] used Nile red as an indicator dye. Upon exposure to CO<sub>2</sub> a change in color as well as fluorescence of the dye can be observed due to a change in the polarity of the environment. A major drawback is that response times were between 3-25 min, which is very slow.

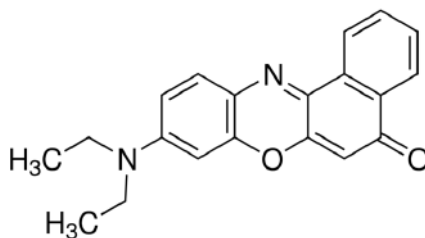


**Figure 2.29:** Nile red

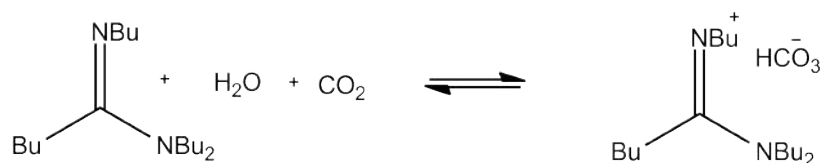


**Figure 2.30:** Reversible reaction of the amidine with  $\text{CO}_2$

## 2.5 Ammonia

Ammonia is present all over earth's atmosphere. It can originate from natural sources such as degradation of amino acids in animal cells [13] or bacterial oxidation of organic carbon [46]. Recently, human activities have been the biggest source of ammonia [12]. This includes the chemical industry, production of house hold cleaners, food industry and especially waste or waste water. Also agriculture, through the use of fertilizers and the excretion of animals, held in farm houses, contributes to a significant increase of ammonia on earth [14].

Ammonia has a bad effect on humans as well as animals. For gaseous ammonia long term exposure is set at 20 ppm and at about 500 ppm severe irritation of the nose and throat occur.[12] In water ammonia concentrations above 25  $\mu\text{g}/\text{l}$  are harmful for organisms [15].

### 2.5.1 Applications

Ammonia sensors find applications in various fields such as:

1. Environmental analysis: Since high ammonia concentrations are toxic, measurements are very important. High concentrations can often be found in stables or other intensive farming areas and can reach up to or even exceed 10 ppm [12]. Other sources are fertilizers, [14] and waste water from different industries which can reduce water quality also near habitats, making controls of drinking and surface water necessary [47].
2. Automotive industry: Here gaseous ammonia is measured, usually exhaust gases, which are a big pollution source in cities or areas with a significant number of human habitants. Another important controlling parameter is air control in the car itself, made necessary by the new development of air conditioning [12].
3. Chemical industry: Ammonia is used in quite a few production processes and these have to be closely monitored, since a leakage could cause serious damage. Processes include the production of explosives, fertilizers, chemicals, cleaning products, textiles or refrigerants. [14] [12]

4. Medical applications: For some health issues it is known that ammonia concentration in the breath is increased. Therefore, ammonia sensors for breath analysis are a potential field of application [12].

## 2.5.2 Sensing principles

### Gaseous ammonia

1. Metal-oxides: These are commercially available sensors, which have been produced in high numbers over the past years. Most of them are based on  $\text{SnO}_2$ . The advantage of these sensors is that they are inexpensive and robust, but they suffer from bad selectivity to a particular gas.

The sensor works due to a conductance change, that is caused by the chemisorption of gas molecules onto the sensing layer [12].

2. Catalytic ammonia sensors: Certain metals can react specifically and catalytically with gases such as ammonia. There are two generally applied principles.

The first one operates through change of the charge carrier concentration due to the gas analyte. The gas is quantified done by using a capacitor or a transistor.

The second principle is the use of a chemical cell, usually a modified electrode. The metal layer is used together with a solid-state ion conductor. Ammonia concentrations are measured by analyzing the potential difference between a counter or reference electrode and the ammonia sensitive electrode[12][16]

3. Conducting polymers: The principle of this is a change of conductivity in the polymer due to the presence of gaseous ammonia. Detection is done either resistometric or amperometric. Mainly two different materials have been commercially used for ammonia sensing, polypyrrole and polyaniline

The change in conductivity is given by deprotonation of the molecule by ammonia. [12]

4. Optical analysis: The system reported in [12] uses a laser and a spectrograph. The light beam goes through the sample and is then detected giving a spectrum which is influenced either by the gas composition or by changes of the material due to the gases present. These analyzers are commercially available but are very expensive and therefore not very interesting candidates.

Other optical sensors that have been described, function by detecting ammonia due to absorption or fluorescence change of an indicator dye. [47] [48]

## Dissolved ammonia

Several measurement methods for dissolved ammonia have been applied. The first two are irreversible, whereas the latter two present a reversible detection option.

1. The Nessler reaction was one of the first detection principles of dissolved ammonia. For this reaction the Nessler reagent is used, which is a dilute alkaline solution (usually sodium hydroxide) containing dipotassium tetraiodomercurate(II). The reagent is added to the water sample and change in color is detected. This method suffers from major drawbacks, first of all the reagent is quite toxic, the formed reaction product is insoluble in water and quantification of the color change is challenging. Also the reagents are consumed and therefore the reaction is irreversible [12].
2. A second method using a color change due to a reaction is the Berthelot reaction. Here ammonia reacts with phenol and hypochlorite to show a blue color. The reagents are not as harmful as in the Nessler reaction, the product formed is water soluble, but still quantification poses a problem. Other drawbacks are the slow kinetics and the consumption of reagents, which makes the reaction irreversible. [12] [15]
3. The above described modified pH electrode can also be used for dissolved ammonia and detection is quite fast, but the effect of salinity on the measurement and a drift due to osmotic pressure are considerable problems.[15]
4. Recently, optochemical methods have been proposed which work mainly with dyes that show fluorescence or absorption changes when exposed to ammonia. They are incorporated into a matrix and often a protective layer is used to reduce cross-sensitivity.[14] [16] [15].

### 2.5.3 Materials

In this thesis, detection of ammonia concentrations based on fluorescence or absorption changes of an indicator dye have been investigated.

Materials commonly used for detection of ammonia will be described. Generally a thin film optical ammonia sensor consists of an analyte sensitive dye which is fixed in a matrix either by covalent binding, adsorption or embedding of the dye [15]. This combination is then deposited on a solid support, usually glass or a polymer, such as PET, and a protective layer is added on top. [13]

### Indicator dyes

Most indicator dyes are chosen by their pKa value, a low pKa value is promising for ammonia detection.[13] The dyes can be either absorption or emission based. Most of these developed

sensors respond to a pH change caused by ammonia[13].

The dye described in [47] works by a different principle, the used rhodamine dye is converted into a lactone, which shows no fluorescence, upon exposure to ammonia.

Also metalloporphyrins have been described as ammonia probes, they work by coordination of the ammonia gas molecule to the metal of the corresponding metalloporphyrin.[48]

The following dyes have been applied for ammonia sensing:

- Bromophenol blue (Absorption) [13] [16] [49]; yellow =>blue; R = -H Figure 2.32
- Bromocresol green (Absorption) [46], yellow =>blue, R = -CH<sub>3</sub> Figure 2.32
- Meso-tetrakis(4-nitrophenyl)porphyrin (Absorption) [14]; blue shift due to ammonia,  $\lambda_{\max}$  changed from 447 nm to 424 nm (in Nafion film) (Figure 2.31)
- Meso-tetrakis(4-pyridyl)porphyrin (Absorption) [14], blue shift due to ammonia, (Figure 2.31)
- 5,15-bis(ferrocenyl)-10,20-bis(4-nitrophenyl)porphyrin (Absorption) [14], blue shift due to ammonia, (Figure 2.31)
- 5,15-bis(4-nitrophenyl)-10,20-bis(3,5-dimethoxy-phenyl)porphyrin (Absorption) [14], blue shift due to ammonia, (Figure 2.31)
- 5,10,15,20-tetra(phenyl)porphyrin complexated with different metals such as Mn(II) (Absorption)[48] blue shift due to ammonia, (Figure 2.31)
- Coumarin 545T with Macrolex Fluorescent Red G (Fluorescence) [13];  $\lambda_{\max,abs} = 480$  nm,  $\lambda_{\max,em} = 505$  nm in chloroform [50]
- Eosin (Fluorescence) [16] [46];  $\lambda_{\max,abs} = 525$  nm,  $\lambda_{\max,em} = 546$  nm in pH = 8 solution [50]
- 2',7'-dichlorofluorescein methylester (Fluorescence) [15];  $\lambda_{\max,abs} = 522$  nm,  $\lambda_{\max,em} = 538$  nm in sodium phosphate buffer
- Rhodamin B or tetramethylrhodamine ethyl ester with bromophenol blue (Fluorescence) [47];  $\lambda_{\max,abs} = 540$  nm,  $\lambda_{\max,em} = 565$  nm in EtOH (??)

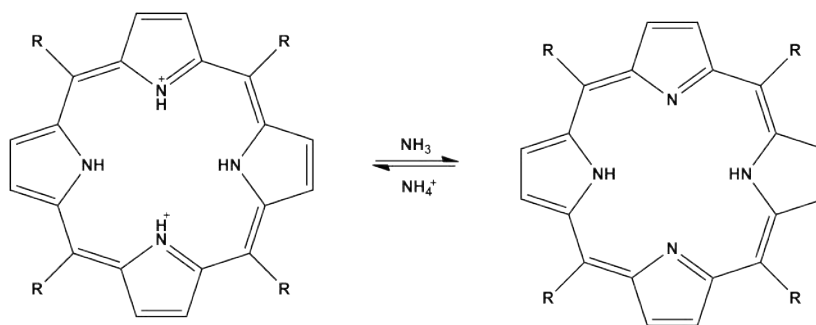


**Figure 2.31:** Reaction of porphyrin dyes with ammonia

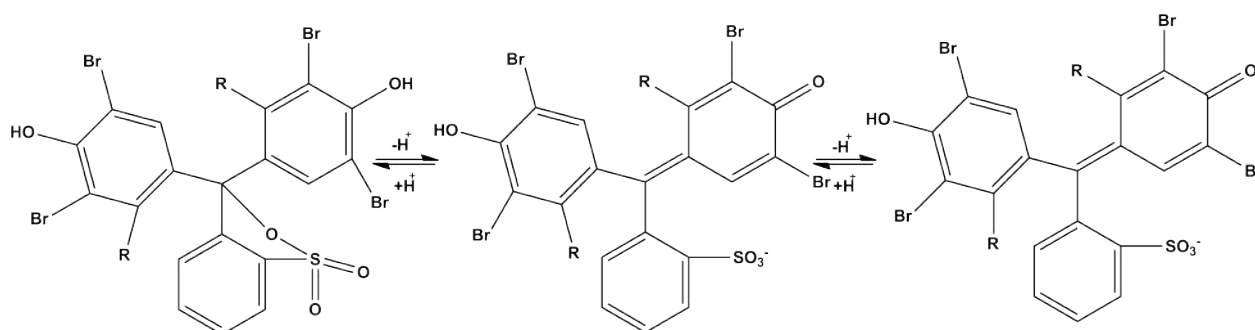


**Figure 2.32:** Mechanism for protonation and deprotonation of bromophenol blue ( $R = -H$ ) and bromocresol green ( $R = -CH_3$ )

## Matrices

The polymer that is chosen for the matrix, has to show certain properties, such as stabilization of the dye and the ammonium ion and no alkaline behavior [13]. Several different polymers have been used as matrices for ammonia sensing.

- Cellulose esters such as cellulose acetate, cellulose acetate butyrate or propionate [13] [15] [16]
- Hydrogels have been used, due to their high water uptake [13]
- Silicone [14] [46] [49]
- Nitrocellulose [14] [48]
- Porous silica gel [14]
- PVC [14][47]
- Nafion [14]

- Sol-gel matrices can show good properties. Depending on the silan that was used, those features are chemical and mechanical stability and good response times. [47]

### **Proton barrier**

Since most of the ammonia sensors work through pH changes caused by ammonia, a proton barrier is needed, especially in solution. The two most commonly used proton barriers are silicone rubber [13] and PTFE [13][46].

### **Interferences**

Ammonia sensors are not influenced by changes of salinity and the influence of pH changes can be eliminated by using a proton barrier [13]

The temperature dependency of optical ammonia sensors is probably due to the pKa dependency on the temperature and a general increase of fluorescence at lower temperatures. This can be easily compensated by simultaneous temperature measurements [13].

A big problem is the cross-sensitivity of ammonia sensors with other amines and can even lead to irreversible damage of the sensor[47][49].

Also a dependence on humidity has been reported, this is due to the fact that water molecules can interact with the sensor.[48]



---

## 3 Experimental

### 3.1 Methods

Absorption measurements were performed on a Cary 50 UV-VIS Spectrometer from Varian ([www.varian.com](http://www.varian.com)). Samples were placed in a OS Type 100 precision cuvette, made of special optical glass from Hellma Analytics ([www.hellma-analytics.com](http://www.hellma-analytics.com)).

Fluorescence measurements were done on a F-7000 Fluorescence spectrometer from Hitachi ([www.hitachi-hta.com](http://www.hitachi-hta.com)) with a red-sensitive PMT R9876 from Hamamatsu. Again samples were placed in a OS Type 100 precision cuvette, made of special optical glass ([www.hamamatsu.com](http://www.hamamatsu.com)). Alternatively more sensitive measurements were performed on a Fluorolog 3 from Horiba ([www.horiba.com](http://www.horiba.com)) equipped with a NIR-sensitive photomultiplier R2658 from Hamamatsu ([www.hamamatsu.com](http://www.hamamatsu.com)). CO<sub>2</sub> and N<sub>2</sub> were obtained from Linde ([www.linde-gas.at](http://www.linde-gas.at)) and were pumped through a Red-y smart series gas mixer from Vögtlin ([www.voegtlin.com](http://www.voegtlin.com)). The gas was then pumped through a humidifier unit containing silica gel that was kept at specific temperatures by a F12 thermostat from Julabo ([www.julabo.com](http://www.julabo.com)). The sample was placed in a flow cell (Figure 3.2) and mounted into the Fluorolog. Measurements on the Fluorolog were done at 15°C, 25°C and 35°C with an excitation wavelength of 650 nm and an emission wavelength of 720 nm.

NMR measurements were recorded on an Avance III spectrometer(300MHz) from Bruker ([www.bruker.com](http://www.bruker.com)).

Ammonia measurements were carried out with a Firesting O<sub>2</sub> from Pyroscience ([www-pyro-science.com](http://www-pyro-science.com)) and POF simplex fibers with PE coating from Ratioplast (diameter 2mm) ([www.ratioplast.com](http://www.ratioplast.com)).The sensor was prepared for measurements by attaching a piece with PTFE filter to a home-made plastic cap (Figure 3.1) with a hole for fiber insertion using E4 silicone from Wacker (<http://www.wacker.com/cms/de/home/index.jsp>). Dual-life time measurements were done at a frequency of 2500 Hz, 40% intensity and 800x amplification.

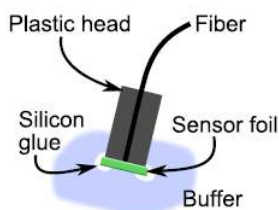


**Figure 3.1:** Measurement set up including the home made plastic cap

Additionally measurements were done on a SR830 DSP Lock-In Amplifier from Stanford ([www.thinksrs.com](http://www.thinksrs.com)) including a home-built LED/Photomultiplier unit. The sensor film was either directly attached to the fiber or mounted in a flow-cell (Figure 3.2). If the sensor was attached directly to the fiber, the fiber and the sensor were put into a 50 ml glass flask with screw top. Small amounts of ammonia were added and the signal change due to the ammonia vapor was measured. When maximal response was reached, the sensor was regenerated by flooding the flask with gaseous  $N_2$ .

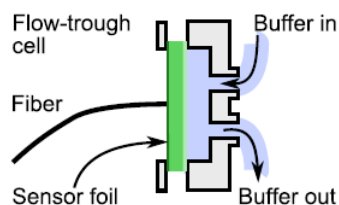


**Figure 3.2:** Flow cell set up

The following settings were used for measurements:

- Sensitivity:  $1 \text{ V}/\mu\text{A}$
- Time constant: 30 ms
- Low pass filter: 18 dB/oct
- Time between measurements between: 15-60 s
- Exposure to light before measurement: 1 s
- Amplitude: between 4-5 V
- Modulation frequency: 1500 Hz

- LED: 450 nm for the porpyhrin and 470 nm for rhodamin dyes
- Filter 1: BG12 for excitation
- Filter 2: for emission, OG570 for the porphyrin and OG530 for the rhodamin dyes
- PMT voltage: 250

For the preparation of the dyes and thin film sensors the following methods were used:

Solvent removal was done on a Laborota 4000 rotary evaporator from Heidolph ([www.heidolph-instruments.com](http://www.heidolph-instruments.com)).

Drying and regeneration of sensor films was done with a B-585 Büchi glass oven ([www.büchi.com](http://www.büchi.com)).

pH determination was done with a SevenEasy pH-meter from Mettler Toledo ([www.mettler-toledo.com](http://www.mettler-toledo.com)).

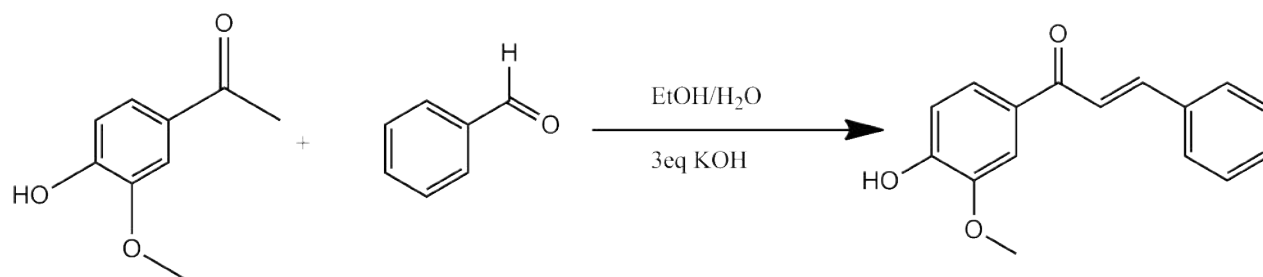
The CO<sub>2</sub> sensor film was prepared by stirring at high speed with a Eurostar digital from IKA ([www.ika.de](http://www.ika.de)) with an attached spatula.

Sensor thin films were knife coated with 1 mil and 3 mil knives from BYK Gardner ([www.byk.com](http://www.byk.com)).

## 3.2 Carbon Dioxide Sensors

### 3.2.1 Synthesis of aza-BODIPY dyes

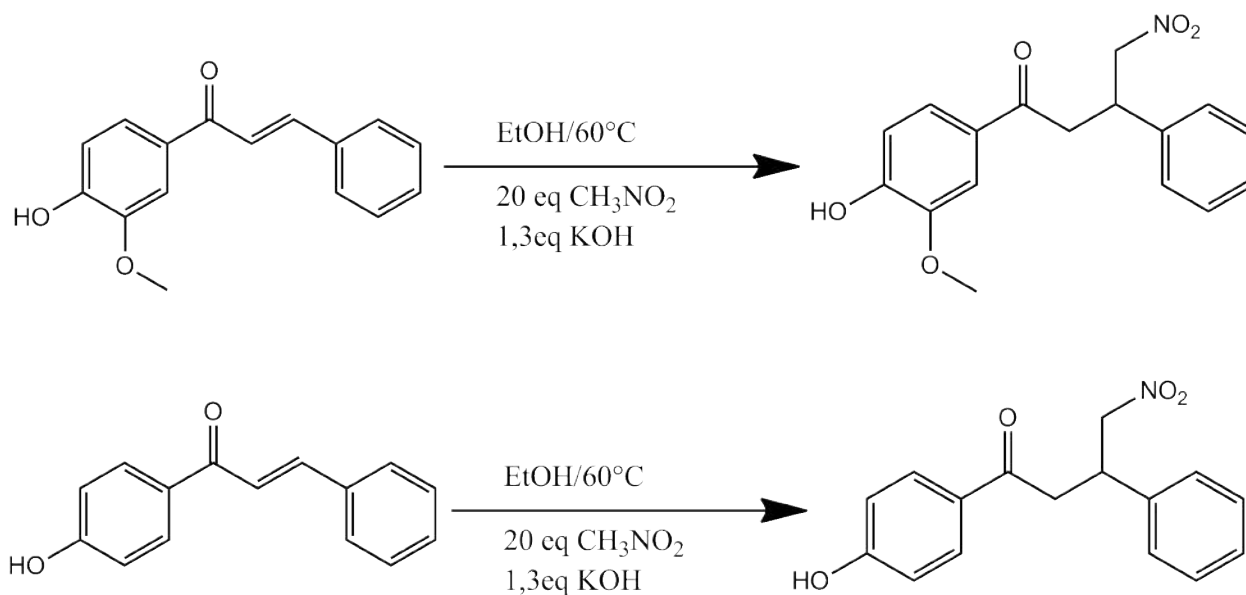
#### Synthesis of 1-(4-hydroxy-3-methoxyphenyl)-3-phenylprop-2-en-1-one



**Figure 3.3:** Reaction scheme for 1-(4-hydroxy-3-methoxyphenyl)-3-phenylprop-2-en-1-one

4-Hydroxy-3-methoxy acetophenone (1 eq, 4,00 g, 24,22 mmol) was dissolved in EtOH (50 ml) and benzaldehyde (1,01 eq, 2,48 ml, 24,45 mmol) was added. Then KOH (3 eq, 4,07 g, 72,65 mmol) was dissolved in H<sub>2</sub>O (5 ml) and added to the mixture. The solution was stirred overnight at room temperature. Then the solution was acidified with 1 M HCl. Since no precipitate was formed, the solvent was removed under reduced pressure and the product was extracted with CH<sub>2</sub>Cl<sub>2</sub> and washed twice with H<sub>2</sub>O. The CH<sub>2</sub>Cl<sub>2</sub> solution was dried over sodium sulfate, filtrated and the solvent was removed under reduced pressure to give a dark brown oily product, that was dried in an oven overnight and used for the next step without further purification (4,88 g, 79%)

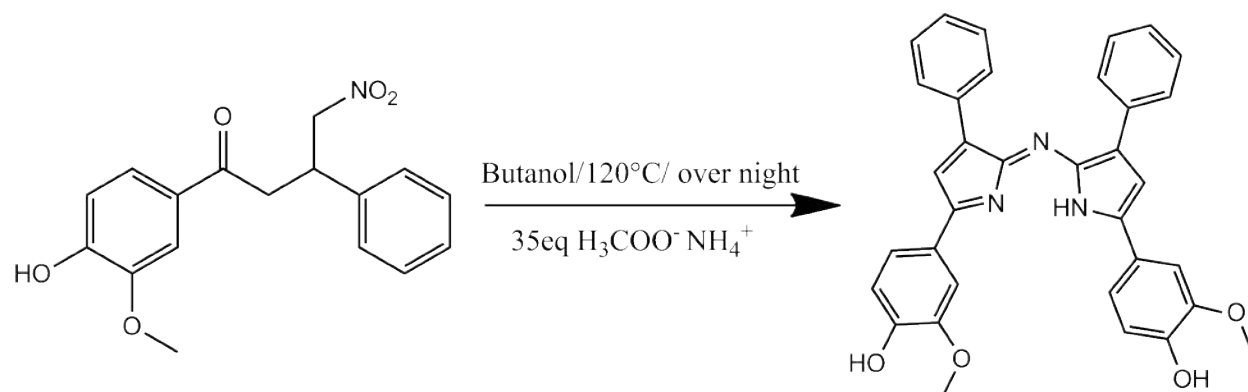
**Synthesis of 1-(4-hydroxy-3-methoxyphenyl)-4-nitro-3-phenylbutan-1-one [2a]  
and 1-(4-hydroxyphenyl)-4-nitro-3-phenylbutan-1-one**



**Figure 3.4:** Reaction scheme for chalcones

The chalcones (1 eq, 4,88 g, 19,19 mmol / 1 eq, 4,00 g, 17,84 mmol) were dissolved in EtOH (50 ml) and nitromethane (20 eq, 20,7 ml, 383,8 mmol / 20 eq, 19,27 ml, 356,7 mmol) was added to the solution. KOH (1,3 eq, 1,40 g, 24,95 mmol / 1,3 eq, 1,30 g, 23,19 mmol) was dissolved in EtOH (5 ml) and then added to the solution. The solution was heated to 60°C and stirred for 4 hours.

The solvent was removed under reduced pressure, then acidified with 1 M HCl and extracted with H<sub>2</sub>O and ethylacetate three times. The organic phase was dried over sodium sulfate, filtrated and then the solvent was removed under reduced pressure. The product was a brown oily substance which was for the next step used without further purification (4,8 g , 79% / 4,9 g, 96%)

**Synthesis of 4-(2-((5-(4-hydroxy-3-methoxyphenyl)-3-phenyl-1H-pyrrol-2-yl)imino)-3-phenyl-2H-pyrrol-5-yl)-2-methoxyphenol**

**Figure 3.5:** Reaction scheme for 4-(2-((5-(4-hydroxy-3-methoxyphenyl)-3-phenyl-1H-pyrrol-2-yl)imino)-3-phenyl-2H-pyrrol-5-yl)-2-methoxyphenol

1-(4-hydroxy-3-methoxyphenyl)-4-nitro-3-phenylbutan-1-one (1 eq, 5,00 g, 15,86 mmol) was dissolved in 1-butanol (100 ml). Ammonium acetate (17,5 eq, 21,40 g, 277,6 mmol) was added and the solution was heated to 120°C and stirred overnight. The product was extracted in  $\text{CH}_2\text{Cl}_2$  and  $\text{H}_2\text{O}$  three times. The organic phase was dried over sodium sulfate, filtrated and the solvent was removed. The product was redissolved in acetone and dried over silica gel.

The product was purified by column chromatography and eluted with cyclohexane and ethylacetate (1:1/v:v). The solvent was removed under reduced pressure and the obtained product showed a blue color. It was used for the next step without further purification (1,71 g, 40 %).

$^1\text{H}$  NMR (300 MHz,  $\text{DMSO-d}_6$ )  $\delta$  8.18 – 8.07 (m, 4H), 7.70 – 7.59 (m, 4H), 7.56 (dd,  $J = 8.4, 1.9$  Hz, 2H), 7.47 (dd,  $J = 8.3, 6.6$  Hz, 4H), 7.42 – 7.32 (m, 2H), 6.93 (d,  $J = 8.2$  Hz, 2H), 3.98 (s, 6H)

**Synthesis of BF<sub>2</sub>-chelate of 4-(2-((5-(4-hydroxy-3-methoxyphenyl)-3-phenyl-1H-pyrrol-2-yl)imino)-3-phenyl-2H-pyrrol-5-yl)-2-methoxyphenol [A] and 4-(5-((5-(4-hydroxyphenyl)-3-phenyl-2H-pyrrol-2-ylidene)amino)-4-phenyl-1H-pyrrol-2-yl)-2-methoxyphenol [B]**

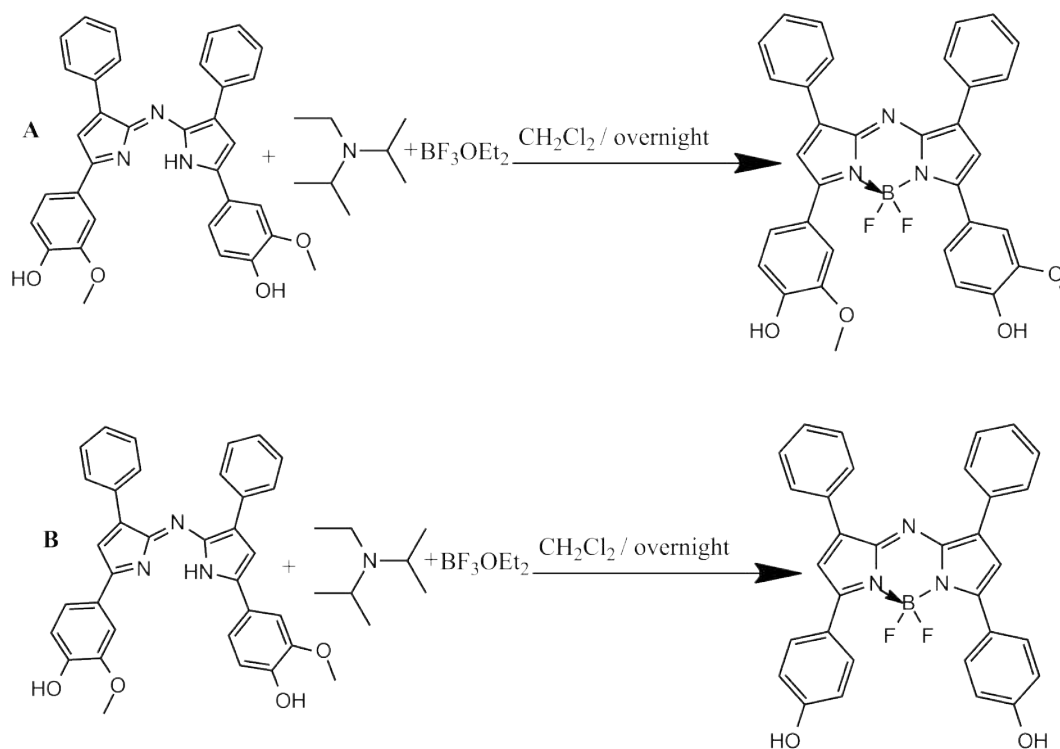


**Figure 3.6:** Reaction scheme for the synthesis of the BF<sub>2</sub>-chelate

A (1 eq, 0,233 g, 0,43 mmol)/ B (1 eq, 0,411 g, 0,85 mmol) was dissolved in anhydrous CH<sub>2</sub>Cl<sub>2</sub> (40ml). Diisopropylethylamine (10 eq, 0,732 ml, 4,3 mmol/ 10 eq, 1,45 ml, 8,5 mmol) was added. When everything was dissolved BF<sub>3</sub> diethyletherate (15 eq, 0,387 ml, 6,45 mmol/ 15e q, 0,768 ml, 12,80 mmol) was added and the solution was stirred overnight under inert conditions (N<sub>2</sub>). The next day the solution was extracted with H<sub>2</sub>O, the organic phase dried over sodium sulfate, filtrated and dried over silica gel. The product was purified by column chromatography, eluting with 2% MeOH/CH<sub>2</sub>Cl<sub>2</sub>.

The solvent was removed under reduced pressure and the product was dissolved in THF and some n-hexane was added for recrystallization. Metallic red crystals were obtained and used for further reactions (0,192 g, 76% / 0,250 g, 55% ).

**A** <sup>1</sup>H NMR (300 MHz, DMSO-d<sub>6</sub>) δ 8.22 – 8.14 (m, 4H), 7.88 (d, J = 2.2 Hz, 2H), 7.79 (dd, J = 8.5, 2.1 Hz, 2H), 7.65 (s, 2H), 7.59 – 7.42 (m, 6H), 6.96 (d, J = 8.4 Hz, 2H), 3.89 (s, 6H)

B  $^1\text{H}$  NMR (300 MHz, DMSO- $d_6$ )  $\delta$  8.29 – 7.96 (m, 8H), 7.67 – 7.29 (m, 8H), 6.95 (d,  $J = 8.6$  Hz, 4H)

**Sulfonation of the 4-(2-((5-(4-hydroxy-3-methoxyphenyl)-3-phenyl-1H-pyrrol-2-yl)imino)-3-phenyl-2H-pyrrol-5-yl)-2-methoxyphenol- and the 4-(5-((5-(4-hydroxyphenyl)-3-phenyl-2H-pyrrol-2-ylidene)amino)-4-phenyl-1H-pyrrol-2-yl)-2-methoxyphenol-  $\text{BF}_2$ -complex**

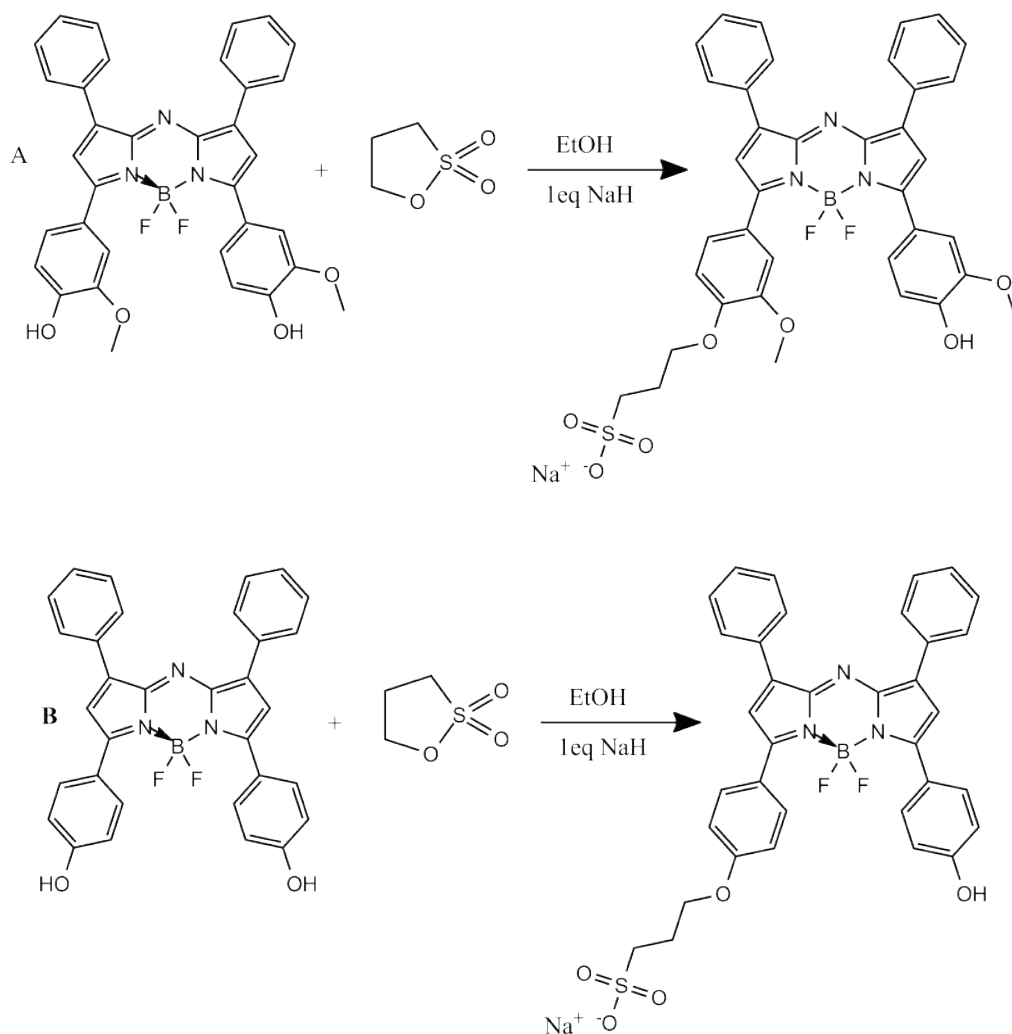


**Figure 3.7:** Sulfonation reaction of  $\text{BF}_2$ -complex

The reaction was performed under inert atmosphere. First the  $\text{BF}_2$ -complex (1 eq, 0,085 g, 0,14 mmol/ 1 eq, 0,043 g, 0,081 mmol) was dissolved in EtOH. Then sodium hydride (60% in mineral oil) (1 eq, 0,006 g, 0,14 mmol/ 1 eq, 0,003 g, 0,081 mmol) was added and gas formation



was observed. After there was no more gas formation propane sultone (1 eq, 0,0176 g, 0,14 mmol/ 1 eq, 0,01 g, 0,081 mmol) was added. The reaction was stirred overnight and then dried over silica gel.

Then the product was purified by column chromatography eluting with 15% MeOH/CH<sub>2</sub>Cl<sub>2</sub>. The solvent was removed under reduced pressure and the product was dissolved in THF, then n-hexane was added for recrystallization. The product obtained showed a blue color (0,030 g, 28%/ 0,014 g, 26%).

**A** <sup>1</sup>H NMR (300 MHz, DMSO-d<sub>6</sub>) δ 8.19 (dd, J = 8.0, 6.0 Hz, 4H), 7.93 – 7.71 (m, 5H), 7.63 – 7.41 (m, 7H), 7.14 (d, J = 8.8 Hz, 1H), 6.96 (d, J = 8.5 Hz, 1H), 4.27 – 4.10 (m, 2H), 3.88 (s, 6H), 2.62 (t, J = 7.5 Hz, 2H), 1.77 (p, J = 6.7 Hz, 2H)

**B** <sup>1</sup>H NMR (300 MHz, DMSO-d<sub>6</sub>) δ 8.28 – 8.02 (m, 8H), 7.74 – 7.35 (m, 8H), 7.13 (d, J = 8.5 Hz, 2H), 6.95 (d, J = 8.5 Hz, 2H), 4.21 (q, J = 7.9, 7.2 Hz, 2H), 2.62 (dd, J = 8.5, 6.3 Hz, 2H), 2.06 (td, J = 13.8, 6.8 Hz, 2H)

### 3.2.2 pKa determination

For pKa determination, buffer solutions of certain pH-values were prepared. Buffer preparation was done using MES, MOPS, CHES and CAPS in a pH range between 6 and 11,4. The dyes were dissolved in an EtOH/ buffer mixture (1:1) and the ionic strength was adjusted to 0.15 M using sodium chloride. The pH electrode was calibrated with pH = 4 and pH = 7 buffers.

### 3.2.3 CO<sub>2</sub> sensor preparation

A “cocktail” containing ethylcellulose (5 w%, 50 mg), dye (0,1 w%, 1 mg) and TOAOH (100  $\mu$ l) was prepared with DMF/toluene/EtOH; 2/4/4 as a solvent mixture. Before addition of the TOAOH, the solution had to be saturated with 100% CO<sub>2</sub>. Finally, the cocktail was knife coated with a 3 mil knife on Mylar®

Unfortunately, in this matrix none of the dyes showed CO<sub>2</sub> sensitivity.

After extraction of the dye in toluene with TOAOH and washing it with H<sub>2</sub>O three times, sensitivity was restored. The sensors only showed sensitivity in solution, therefore a thin film with a non-evaporating polar solvent was produced.

A suspension was prepared containing 13% Hyflon in perfluorodecalin and a solution of 100 $\mu$ l tetraethylenglycol, 20  $\mu$ l Na<sub>3</sub>PO<sub>4</sub> as a base (TOAOH was too strong) and 0,5 mg of the dye. This was stirred vigorously until a homogenous suspension was obtained and a thin film could be prepared (1 mil). An extra Hyflon layer containing TiO<sub>2</sub> was added on top.

Furthermore, a new concept was developed using tributylphosphate as a plasticizer. A “cocktail” (100 mg) was prepared containing ethylcellulose (5%, 50 mg), dye (0.05% 0,5 mg) and 25 mg plasticizer in an EtOH/toluene mixture. This sensor too brought no results in respect to CO<sub>2</sub> sensitivity.

### 3.2.4 Long-term stability test

The CO<sub>2</sub> sensors were stored under CO<sub>2</sub> atmosphere at 4°C. Additionally, some samples were stored in the laboratory at room temperature and exposed to light. Fluorescence measurements were taken right after sensor preparation and after one month of storage. Obtained results will be discussed in subsection 4.1.5

### 3.3 Ammonia Sensors

#### 3.3.1 Screening of 7-(4-butoxyphenyl)-3-(4-((4-(dimethylamino)benzyl)carbamoyl)phenyl)-5,5-difluoro-1,9-diphenyl-5,9a-dihydro-1H-dipyrrolo[1,2-c:2',1'-f][1,3,5,2]triazaborinin-6-ium-5-uide (Amino-dye) and 7-(3,5-dichloro-4-hydroxyphenyl)-3-(4-(dodecylcarbamoyl)phenyl)-5,5-difluoro-5,9a-dihydro-1H-dipyrrolo[1,2-c:2',1'-f][1,3,5,2]triazaborinin-6-ium-5-uide (DiCl-dye) for ammonia sensitivity

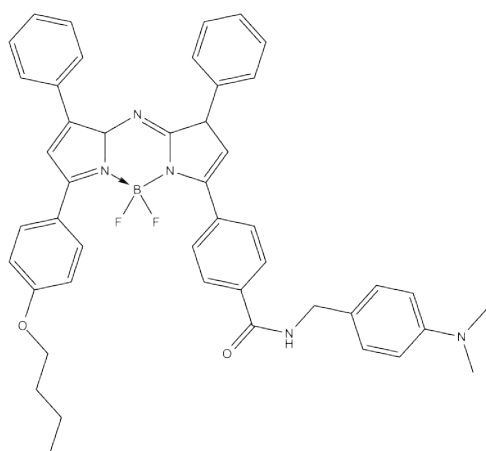


**Figure 3.8:** Amino-dye used for ammonia sensor preparation

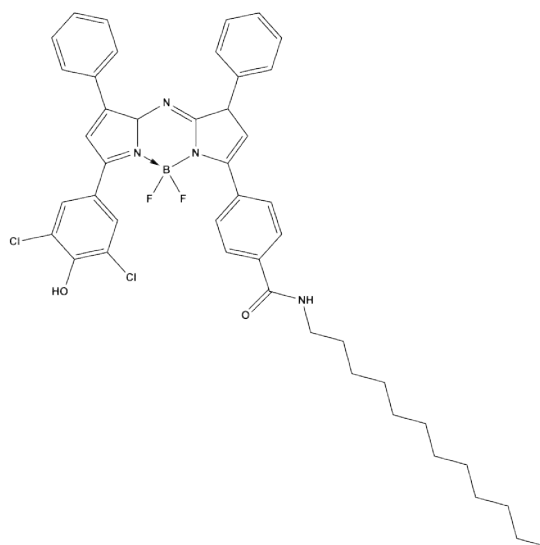


**Figure 3.9:** DiCl-dye used for ammonia sensor preparation

The two dyes presented in Figure 4.30 and Figure 4.31 were tested for their possible application as ammonia sensors. Table 3.1 summarizes the screening of the two dyes using different matrices, acids and concentrations.

**Table 3.1:** Compositions for preliminary ammonia sensor tests

Sample Name	Dye	Amount [mg]	Matrix	Amount[w%]	Acid	Amount[mg]	Solvent
AF1	Amino-dye	0,7	D4	15	DBSA	25	THF
AF2	Amino-dye	0,6	EC	10	DBSA	25	Toluene/EtOH
AF3	Amino-dye	0,9	CAP	20	DBSA	25	Acetone
AF4	Amino-dye	0,4	CAP	15	MSA	0,054	Acetone
AF5	Amino-dye	0,4	CAP	15	MSA	0,18	Acetone
AF6	Amino-dye	0,3	CAP	15	MSA	1,17	Acetone
AF7	Amino-dye	0,3	CAP	16	MSA	1	Acetone
AF8	Amino-dye	0,25	D4	15	MSA	25	THF
AF9	Amino-dye	0,2	CAP	15	MSA	2	Acetone
AF10	DiCl-dye	0,1	D4	15	MSA	1,6	THF
AF11	DiCl-dye	0,1	EC	5	MSA	1,6	Toluol/EtOH
AF12	DiCl-dye	0,1	CAB	15	MSA	1,6	Acetone
AF13	DiCl-dye	0,1	D7	15	MSA	0,38	THF
AF14	Amino-dye	0,2	D7	15	MSA	0,75	THF

Only sample number AF10 showed promising results such as response at acceptably low concentrations and reversibility.

Therefore, a new thin film sensor containing a reference dye was produced. It contained 15% D4, 0,2 mg of the DiCl-dye, 3 mg MSA and 50 mg of Egyptian blue silanized with TMS groups in a 500 mg cocktail with THF. The thin film was knife coated with a 1 mil knife on Mylar®. On one part of the thin film sensor a PTFE membrane was attached.

For sensor characterization in the liquid phase buffer solutions with a fixed ammonia concentration were prepared.

A stock solution of a buffer containing  $\text{NaH}_2\text{PO}_4$  at  $\text{pH} = 7$  was prepared. The buffer system and ammonium chloride were then used to prepare ammonia solutions with defined concentrations.

**Table 3.2:** Concentrations of prepared ammonia solutions

$\mu\text{g/l NH}_3$	$1 \mu\text{mol/l NH}_3$	$1\mu\text{mol/l TAC}$	$\text{mmol/l TAC}$	$\text{mg/flask}$
1	0,06	12,1	0,01	0,06
3	0,18	36,4	0,04	0,19
10	0,59	121	0,12	0,65
30	1,76	363	0,36	1,94
100	5,87	1212	1,21	6,48
300	17,6	3635	3,63	19,4
1000	58,7	12115	12,1	64,8
3000	176,2	36345	36,4	194

Then measurements were performed on the Firesting as described in section 3.1. For comparison, several measurements were done. For further measurements on the Lock-In a new sensor thin film was prepared:

The sensor consisted of 3 layers:

1. Sensor layer with 0,15 mg DiCl-dye in 15w% D4 with 10 mg MSA dissolved in THF (250 mg)
2. Reference silicon layer with 15w% E4 and 30 mg Egyptian blue silanized dissolved in cyclohexane (500 mg)
3. Amplification silicon layer with 15w% E4 and 50 mg  $\text{TiO}_2$  dissolved in cyclohexane (500 mg)

The sensor was tested by measuring the signal in the gas phase, first the prepared sensor without further treatment, then exposing the sensor to gaseous ammonia. Since functionality was given, measurement in a flow cell was done. The set-up for this can be seen in section 3.1. Ammonia solutions were changed at set intervals to higher concentrations and the signal change was measured.

### **3.3.2 Investigation of potential suitability of different dyes for ammonia sensors 1**

10 dyes were screened for their potential application in ammonia detection. All films were prepared as follows:

0,5 mg of the dye were dissolved in acetone or dichloromethane, then 15w% cellulose acetate propionate and about 5 mg of MSA were added. The “cocktail” was stirred until all was dissolved and then knife coated with a 3 mil knife onto Mylar®.

The sensors were placed in a cuvette and responses in absence and presence of gaseous ammonia were measured.

Furthermore, the thin films were tested on their regeneration abilities. Regeneration was done at 60°C and under reduced pressure in a Büchi glass oven. Promising dyes were tested more thoroughly.

Since none of the dyes was reversible after exposure to ammonia no further experiments were done.

### **3.3.3 Investigation of potential suitability of different dyes for ammonia sensors 2**

18 dyes were screened for their potential application in ammonia detection. The first preliminary test was done by dissolving about 1 mg of each dye in 2 ml of EtOH or THF depending on their solubility. Then small pieces of a Nafion 117® membrane were put into the solution for about 2 hours. Most of the samples showed a high dye concentration in the membrane. The pieces were then exposed to gaseous ammonia and change in color (absorption) or fluorescence was detected. Then the samples were put into a Büchi® glass oven under reduced pressure and at high temperatures to test regeneration.

Promising candidates were tested further. For this about 200  $\mu$ l of the solution were taken and mixed with 2 ml of the respective solvent to obtain less intensively colored samples. Larger pieces of Nafion 117® were used for this preparation to facilitate absorption and fluorescence detection. The promising sensor films were dipped into a 20% E4 silicon mixture in cyclohexane to obtain a protective layer and were dried overnight. A little piece was cut out and put into a saturated solution of sodium phosphate to test whether the silicone layer works as a protective layer.

Since the Nafion 117® membrane was too thick a sensor film was prepared using a Nafion 117® solution. About 0,1 mg of the dye were added to 500 mg of the Nafion 117® solution. The sensor was knife coated on to Mylar® with a 1 mil knife.

The dyes were tested in solution using a flow cell and the Lock-In (section 3.1). No working

results could be obtained, therefore measurements in the gas phase under humid conditions were done.

Furthermore, it was tried to increase the sensitivity of a rhodamine dye by adding TOACl. For this 2, 6,5 and 9 mg were added to about 500 mg of a 5% Nafion 117® solution and then 0,07 mg of a rhodamin dye were added. The 3 solutions were knife coated with a 3 mil knife and then measured on the Lock-In.





---

## 4 Results and Discussion

### 4.1 Carbon Dioxide Sensors

#### 4.1.1 Synthesis

Preliminary experiments showed that aza-BODIPY dyes with only one hydroxy group are not CO<sub>2</sub> sensitive. This was probably due to an ionic pair formation of the phenoxide with TOAOH that was too strong to be deprotonated by CO<sub>2</sub>. This effect was observed independently of the pKa value of the used aza-BODIPY dye.

Tests with several different aza-BODIPY dyes showed, that only symmetrical dyes possess CO<sub>2</sub> sensitivity.

Schutting et al [6] showed that a dihydroxy-aza-BODIPY dye exhibits CO<sub>2</sub> sensitivity. To achieve this effect, a high pKa and more importantly, a quaternary ammonium base such as TOAOH are necessary. It was shown, that the base plays a major role for CO<sub>2</sub> sensitivity, since it is very bulky and therefore, offers sterical hindrance on one of the hydroxy groups. This leads to the fact that the second ionic pair that is formed, is more easily protonated or deprotonated. The dihydroxy-aza-BODIPY dye presented by Schutting et al. showed a major drawback, the first ionic pair formation of the phenoxide quenches fluorescence, so only absorption based detection based on a modulated inner filter effect could be performed (section 2.4).

The aim of this thesis was to develop an NIR-emitting, fluorescent, CO<sub>2</sub> sensitive aza-BODIPY dye. The new strategy was to introduce a sulfonate group to one of the hydroxy groups and therefore eliminate the quenching effect of the ionic pair formation. This strategy was inspired by the sensing mechanism of HPTS. HPTS is a commonly used fluorescent indicator for CO<sub>2</sub> and exhibits 3 sulfonate groups. The sulfonate group is quite bulky and therefore offers the steric hindrance that is needed to achieve CO<sub>2</sub> sensitivity.

Synthesis of the symmetrical aza-BODIPY dye was done as described by Jokic et al [51]. The pKa values of the dyes can be tuned by changes of substituents, generally introducing electron donating or withdrawing groups. This could be easily achieved by changing the acetophenone or chalcone precursor used for the synthesis. This was attempted in this thesis by using a 4-hydroxy-3 methoxy acetophenone precursor to give an extra methoxy group. It was

hoped, that the introduction of the methoxy group would lead to an increased pKa value. The sulfonation of the dye was performed at the end using the conditions described by Chen et al [52].

#### 4.1.2 pKa determination

First the pKa values of the dyes were determined in EtOH/buffer (1:1/vv).

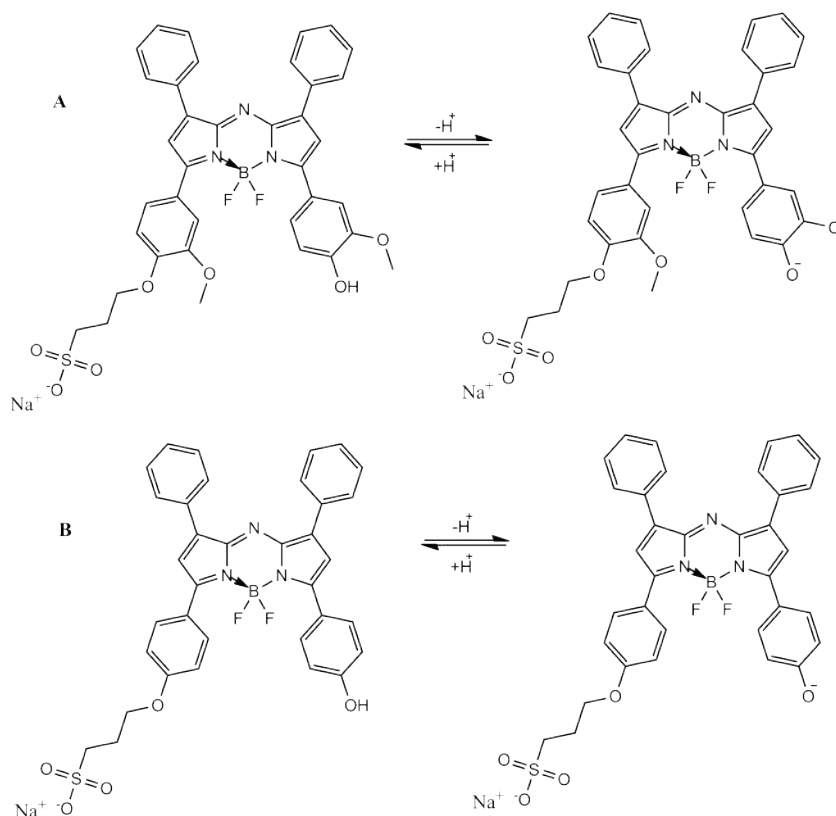


**Figure 4.1:** Structures of DiMeOH (A) aza-BODIPY dye and DiOH (B) aza-BODIPY dye in protonated and deprotonated forms

As can be seen in Figure 4.2 and Figure 4.4, both dyes exhibit good response to pH changes. The maxima for the protonated and deprotonated forms could be easily identified. The determination of the pKa values of the dyes gave 8,81 and 8,18 for the DiOH and the DiMeOH dye, respectively.

This result is in contrast with the hoped effect of the dimethoxy substituents. It was assumed that because of the lone-pair of oxygen, the methoxy-group acts as an electron donor and therefore a decrease in acidity should be detected. This should generally lead to a higher pKa value. In this case the negative inductive effect of the oxygen is so strong that it leads to a decrease in pKa value.

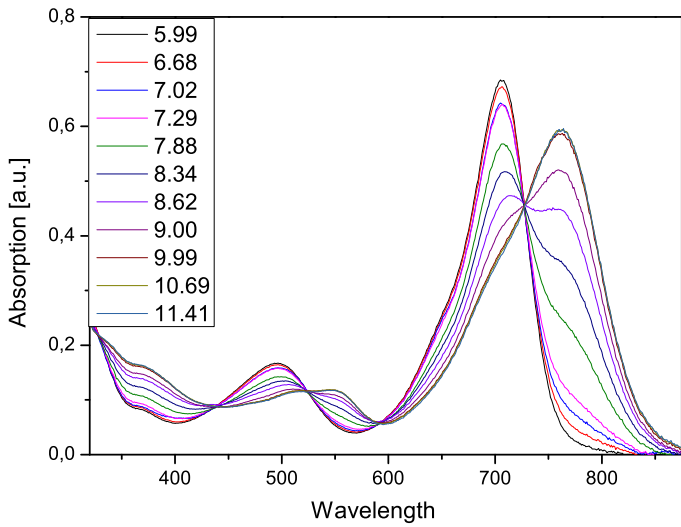


**Figure 4.2:** pH dependence of absorption in EtOH/aq. buffer solution (1:1) IS = 150 (DiMeOH)

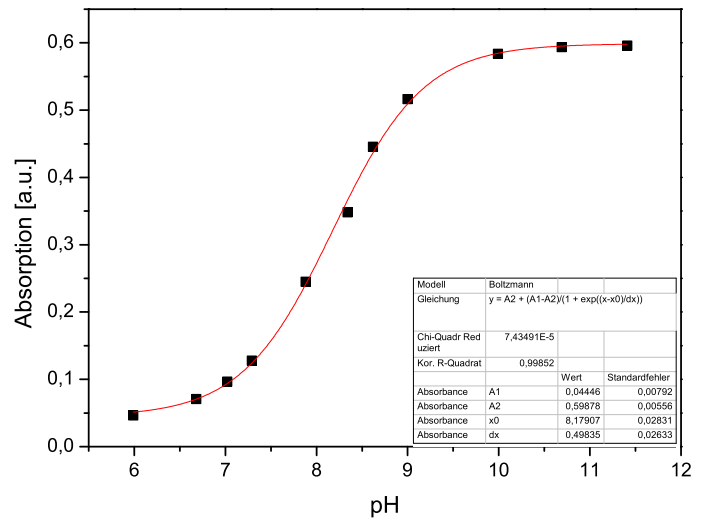


**Figure 4.3:** Corresponding calibration curve of DiMeOH

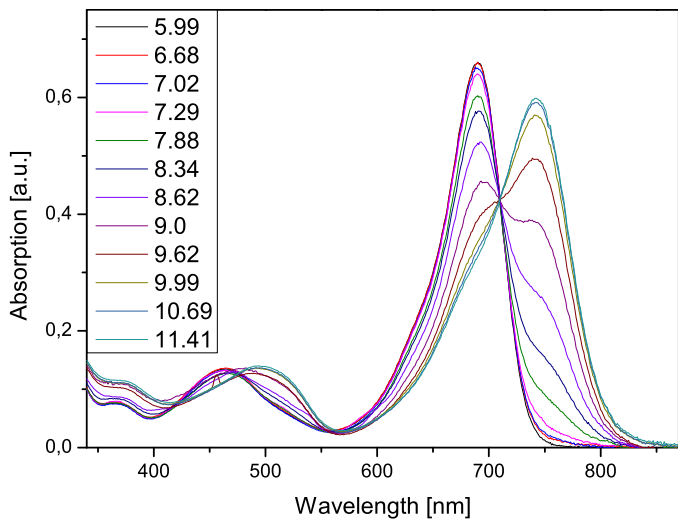


**Figure 4.4:** pH dependence of absorption in EtOH/aq. buffer solution (1:1) IS = 150 (DiOH)

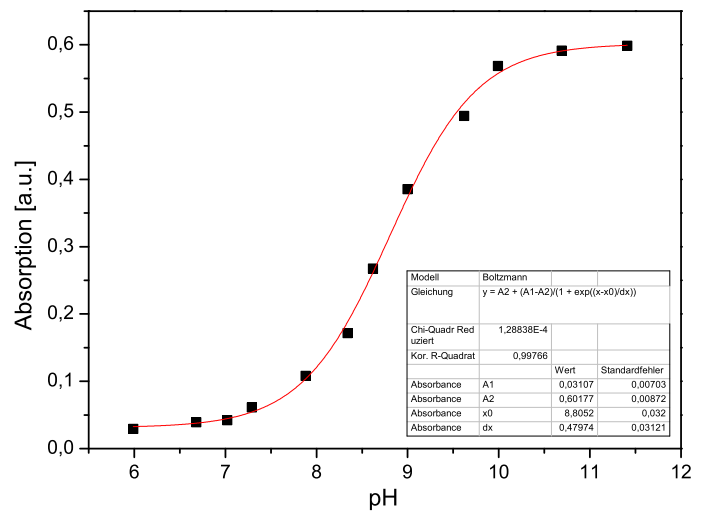


**Figure 4.5:** Corresponding calibration curve of DiOH

### 4.1.3 CO<sub>2</sub> sensor preparation

#### Primary sensor tests

Preliminary experiments indicated that the DiOH dye shows CO<sub>2</sub> sensitivity in solution and was therefore directly used for sensor film preparation.

Unexpectedly, the dyes were only soluble in DMF (bad solubility) and DMSO, which challenges thin film sensor preparation.

Ethylcellulose is the most commonly used sensor material, and is generally dissolved in a toluene/EtOH mixture but adding DMSO or DMF to this mixture results in a precipitation of EC during the drying process. This was even a problem when the drying process was done under reduced pressure and at elevated temperatures (about 60-80°C) (Figure 4.6).



**Figure 4.6:** Thin film with EC and DMSO/Toluene/EtOH; 1/4/5

Eventually a possible mixture was found which consisted of DMF/toluene/EtOH; 2/4/4. It only worked if, immediately after the sensor film was knife coated, the thin film was put into a glass oven at elevated temperatures and reduced pressure and all solvents were removed at the same time.

The prepared sensor film was measured in the presence and absence of 100% CO<sub>2</sub> but no response could be observed.

Further tests in other matrices and in solution were performed but either solubility of the polymer was a problem or there was no response to CO<sub>2</sub>.

Tested possibilities can be seen in Table 4.1.

**Table 4.1:** Matrix and solvents used for primary test

Polymer	Solvent	Dissolved Polymer
EC	DMF /Toluene/EtOH	yes
D4	DMF	yes
D7	DMF	yes
Polystyrol	DMF	no
Hydrothane	DMF	no
Solution	DMF/EtOH	-

Preliminary tests showed, that the DiOH dye possesses CO<sub>2</sub> sensitivity in solution with EtOH. For this reason it was assumed that the extensive purification and drying process caused aggregation of the dye, leading to a strong bond of the Na<sup>+</sup> to the sulfonate group. Therefore it could not be removed anymore and ionic pair formation with TOAOH was inhibited. In order to remove the Na<sup>+</sup>, the dye was dissolved in a small amount of DMSO and then extracted with toluene and TOAOH. Then the solution was washed with H<sub>2</sub>O three times.

Thus, the dye showed CO<sub>2</sub> sensitivity, which could be detected through a change in absorption, where the deprotonated form showed a purple color and the protonated form appeared light green.

Further absorption measurements were done in different solvents in order to find maximum CO<sub>2</sub> sensitivity. The best results were obtained in 1-butanol.

#### 4.1.4 CO<sub>2</sub> tests in solution

Consequently, tests in solution with the extracted dye showed CO<sub>2</sub> sensitivity. Tests were done in different solvents and best results could be achieved using 1-butanol. Emission and absorption spectra of both dyes in 1-butanol can be seen in Figures 4.7 - 4.10.

The absorption spectra showed a shift to lower wavelengths in the protonated form and a shift to higher wavelengths in the deprotonated form. The recorded spectra were reversible and identical at different cycles

The intensity of the emission spectra is higher in the protonated form, i.e. in the presence of CO<sub>2</sub>, and much lower if exposed long enough to N<sub>2</sub>. This can be explained due to the PET effect. Fluorescence is quenched by the photoinduced electron transfer from a hydroxyl group (which would be the receptor group for H<sup>+</sup>) to the aromatic backbone of the dye.[24]

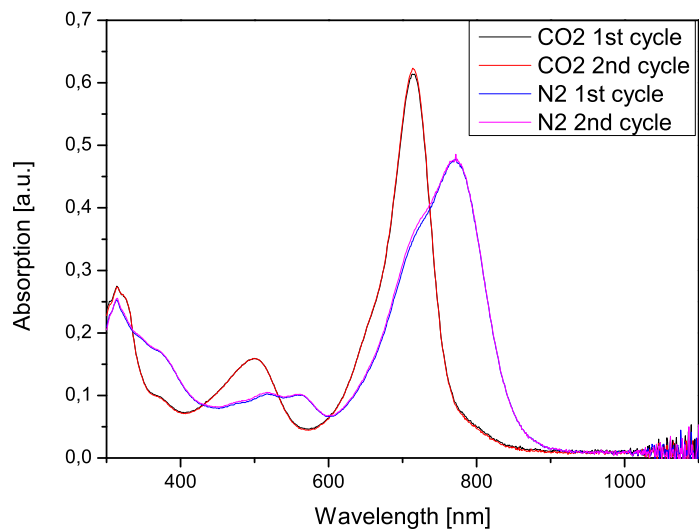


**Figure 4.7:** Absorption changes of the DiOH dye in 1-butanol

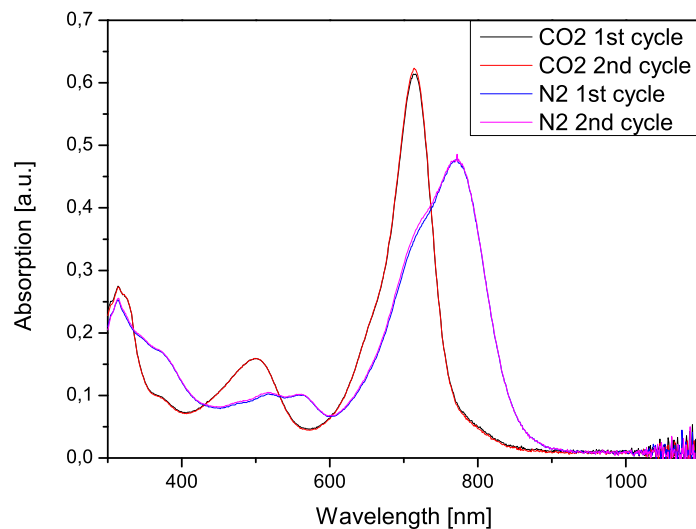


**Figure 4.8:** Absorption changes of the DiMeOH dye in 1-butanol

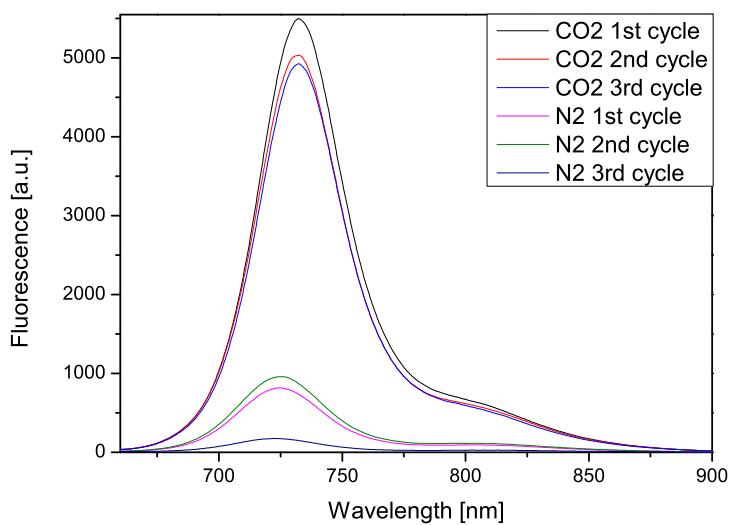


**Figure 4.9:** Emission spectra of DiOH dye in 1-butanol

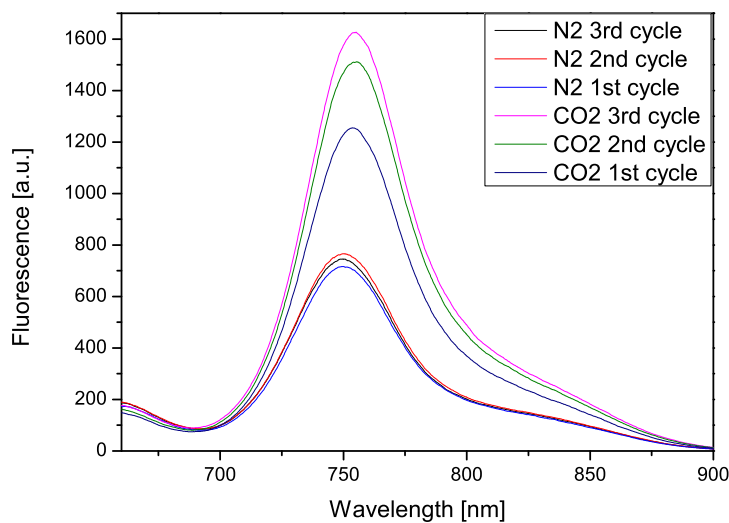


**Figure 4.10:** Emission spectra of DiMeOH dye in 1-butanol

For the preparation of a thin film sensor, a polar solvent was needed in the mixture. 1-butanol was promising in solution, but evaporated when used for sensor preparation. Therefore a polar solvent with a high boiling point, which would not evaporate was chosen to be used for further

sensor preparations. Tetraethyleneglycol (TEG) was chosen because of its polarity and high boiling point. Absorption and emission spectra are presented in Figure 4.11 and Figure 4.12.

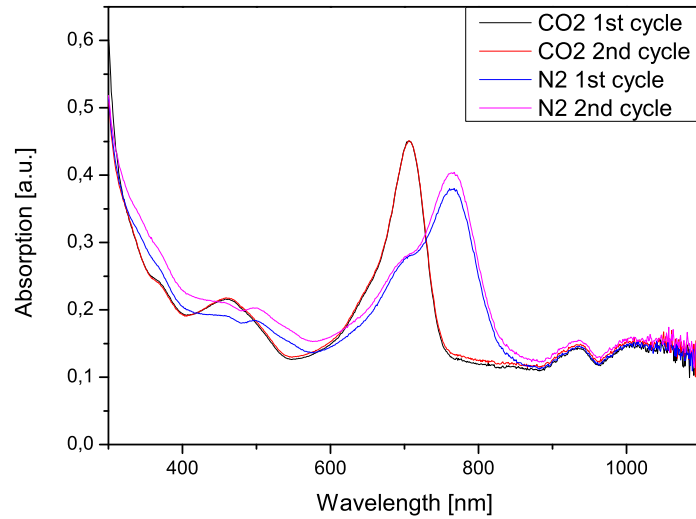


**Figure 4.11:** Absorption changes of DiOH dye in TEG

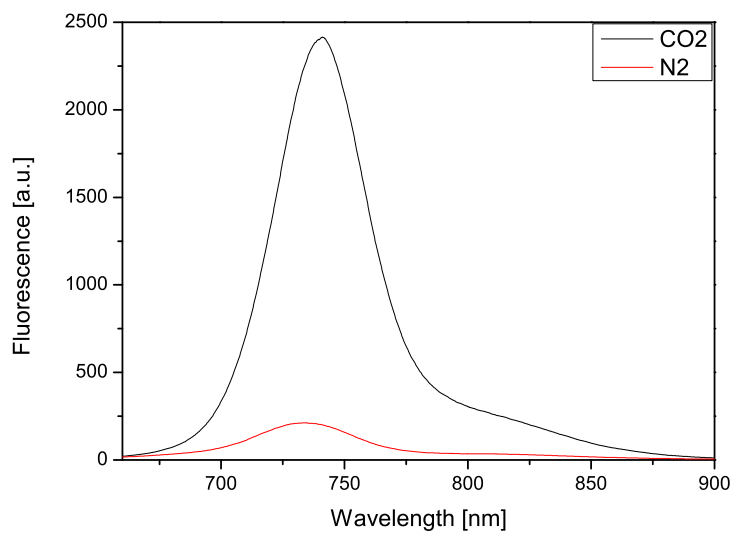


**Figure 4.12:** Emission spectra of DiOH dye in TEG

## Preparation and characterization of optical thin film sensors

There are 2 general types of thin film sensors that were tried to be applied to our sensing systems. The Severinghaus type sensor and the Mills type sensor.

The Severinghaus type sensor needs the presence of  $\text{H}_2\text{O}$  and therefore leaching of the dye is often a problem, so a hydrophobic second layer such as PTFE is needed [9]. The Mills type sensor is a near-solid state sensor, which employs a lipophilic base, in our case TOAOH. Generally, some molecules of  $\text{H}_2\text{O}$  are associated with the ion pair of the lipophilic base. Hence, application as a  $\text{CO}_2$  sensor is possible in those “dry” sensors. [10]

At first different matrices were tested on their solubility in polar solvents. Only EC could be dissolved in a mixture containing butanol, which was so far the most promising solvent for the dyes. A thin film sensor was prepared using the DiOH dye and 5% EC in butanol/toluene (4:1/vv). A short test showed that no reaction to  $\text{CO}_2$  could be detected.

Based on these results, it was assumed, that the sensor only worked in a system containing a polar solvent, since the butanol evaporated due to its low boiling point, it was not present anymore when the sensor was tested.

This led to the preparation of a thin film with a solution containing microcapsules. Sensor preparation was done using TEG as a solvent and mixing everything with Hyflon (Figure 4.13). Hyflon was chosen as a matrix material because of its high stability, high  $\text{CO}_2$  sensitivity and none of the used components is soluble in it, therefore the components are not extracted. TEG was chosen as the solvent because the sensor worked in this solvent and it has a very high boiling point. This means it does not evaporate during drying of the thin film sensor.

First tests with TOAOH as a base did not work because the ion-pair was too stable and the dye could not be protonated anymore after deprotonation with TOAOH. Therefore a weaker base was chosen which was  $\text{Na}_3\text{PO}_4$ . When preparing the cocktails, before and after addition of the base, the solution was exposed to 100%  $\text{CO}_2$ . Detection of the color change, gave an indication whether the thin film may work.

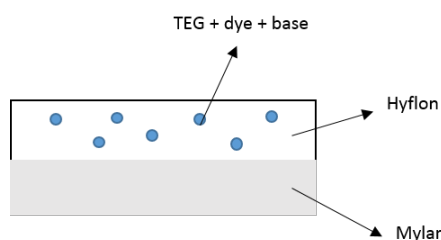


**Figure 4.13:** Schematic drawing of a sensor containing TEG and Hyflon as a matrix

Sensor films were prepared with both dyes and tested on the Fluorimeter. The emission spectra



of the DiMeOH dye indicated low fluorescence even at 100% CO<sub>2</sub> and it was concluded that this dye is not suitable for CO<sub>2</sub> sensors. (Figure 4.14).

The DiOH dye showed better results. The first functioning sample can be seen in Figure 4.15.

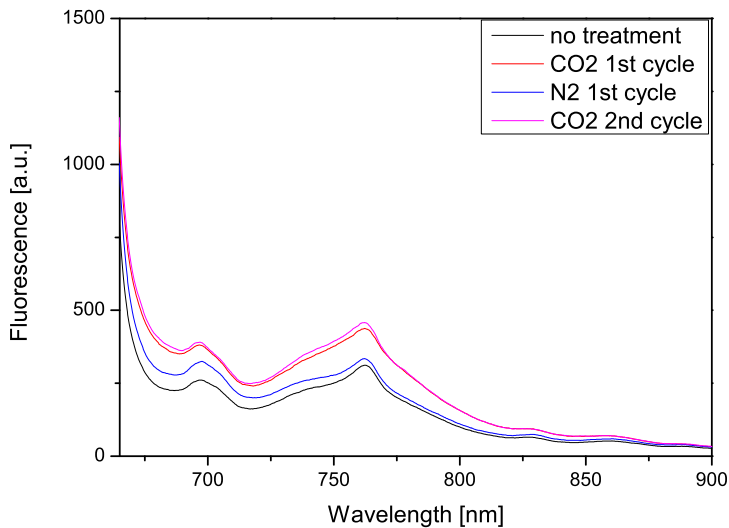


**Figure 4.14:** DiMeOH in TEG/Hyflon shows only minimal changes when exposed to CO<sub>2</sub>

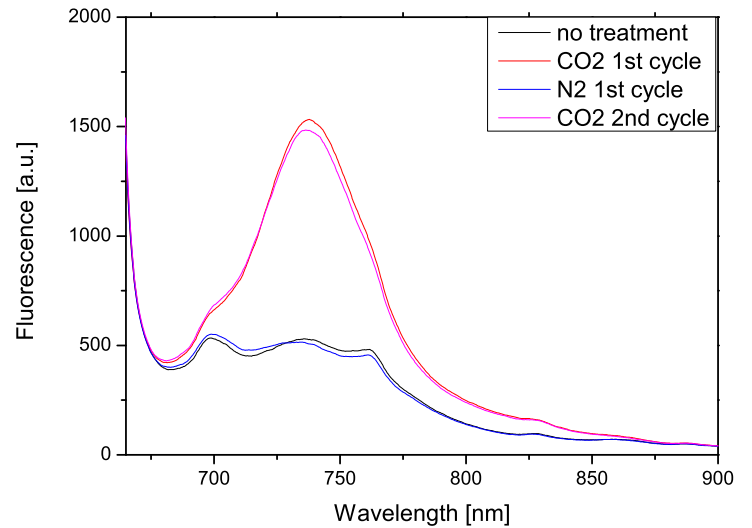


**Figure 4.15:** Preliminary test showed acceptable sensitivity for DiOH in TEG/Hyflon

For characterization of the CO<sub>2</sub> sensor kinetic measurements were done on the Fluorolog at 15°C, 25°C and 35°C and emission spectra at 25°C (Figure 4.16). The gas mixtures were set between 0%, and 100% CO<sub>2</sub>. At least 3 cycles were done at each temperature to confirm reproducibility.

As can be seen in Figure 4.17 - Figure 4.19 the first cycle was generally needed for conditioning then cycles of similar responses were achieved, showing reproducibility. Regeneration of the sensor posed no problem and was done within about 15 min.

Figure 4.20 and ?? show the normalized intensity vs pCO<sub>2</sub> [kPa] of the DiOH dye at all three temperatures. It is important to note, that even at 100% CO<sub>2</sub> the dye is not completely switched on. It can be easily seen, that the sensor worked best at 35°C. The slope is much steeper than for the other two. This is also reflected in Figure 4.19 where the steps are much easier distinguishable compared to the other temperatures. A general temperature trend cannot be observed, since sensitivity seems to be slightly better at 15°C compared to 25°C.

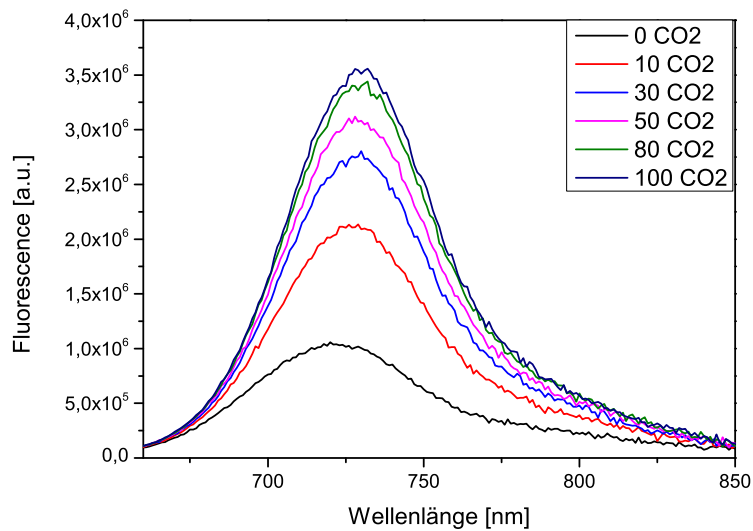


**Figure 4.16:** Emission spectra of DiOH dye in TEG/Hyflon; Fluorolog

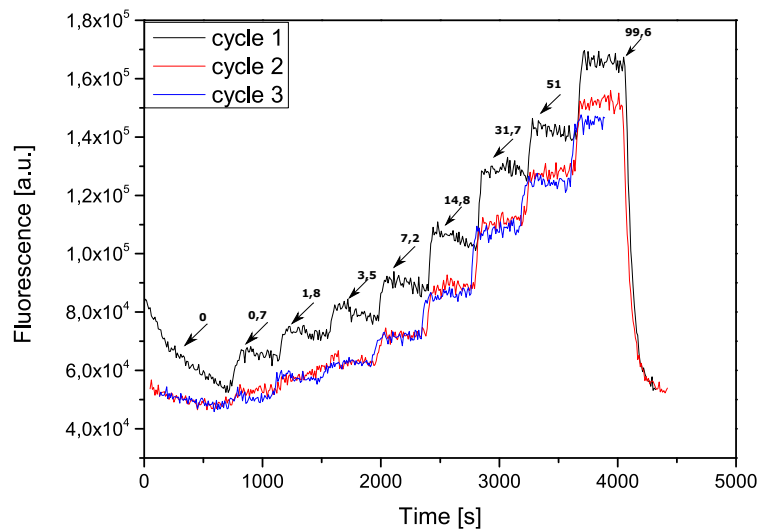


**Figure 4.17:** Gas cycles at 15°C for DiOH in TEG/Hyflon; steps are kPa CO<sub>2</sub>

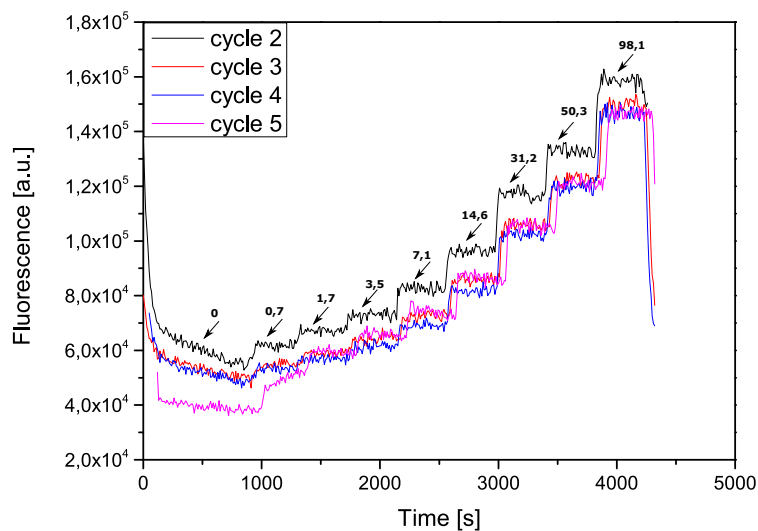


**Figure 4.18:** Gas cycles at 25°C for DiOH in TEG/Hyflon; steps are kPa CO<sub>2</sub>

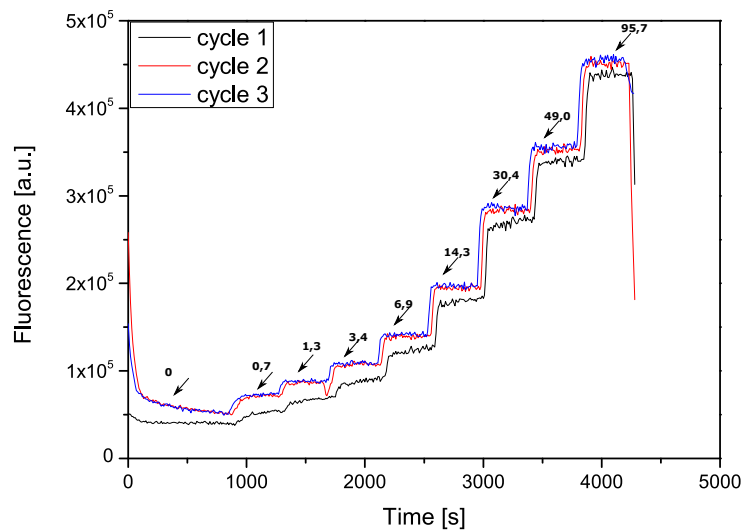


**Figure 4.19:** Gas cycles at 35°C for DiOH in TEG/Hyflon; steps are kPa CO<sub>2</sub>

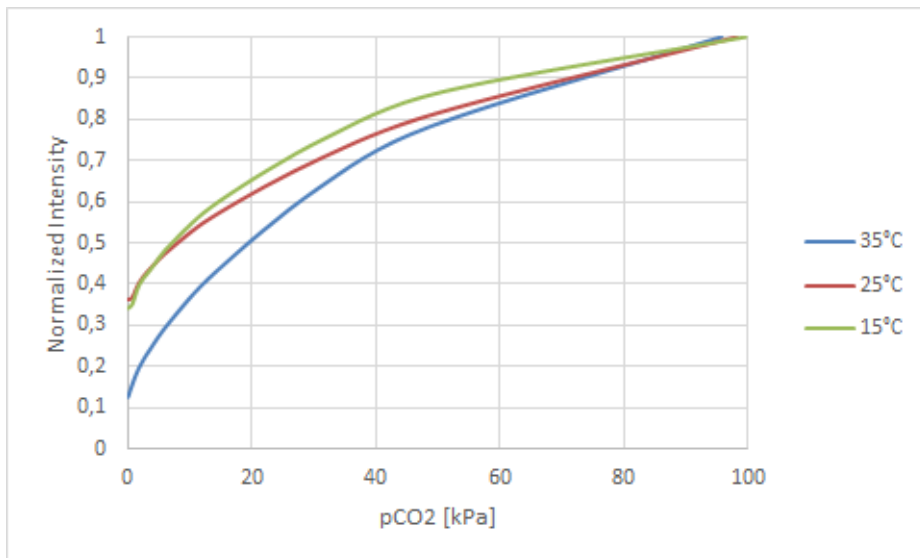


**Figure 4.20:** Normalized intensities for DiOH dye in TEG/Hyflon at different temperatures

During sensor characterization, it was found that reproducible preparation of a CO<sub>2</sub> sensor in TEG/Hyflon was not possible. This can be seen in Figure 4.21 and Figure 4.22 where two thin films are presented, which were prepared exactly the same way but only one of them reacts with CO<sub>2</sub>.

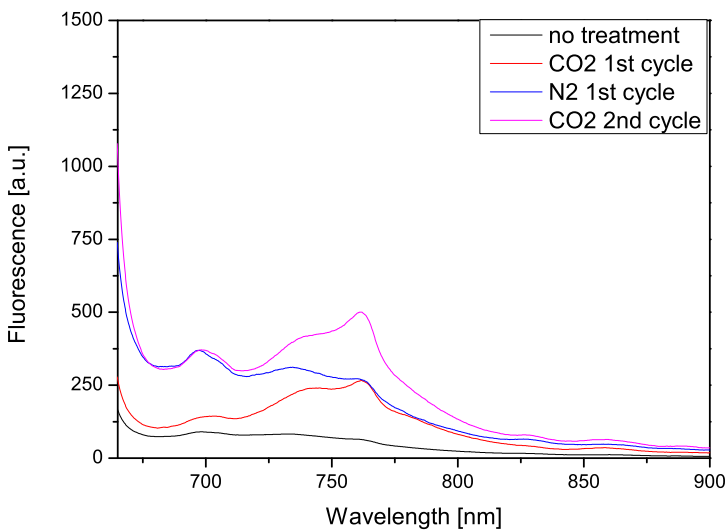


**Figure 4.21:** DiOH in TEG/Hyflon that did not show acceptable CO<sub>2</sub> response

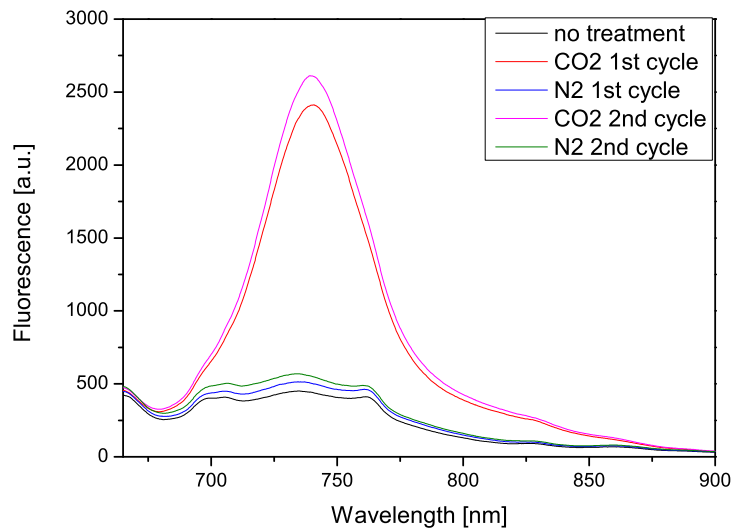


**Figure 4.22:** DiOH in TEG/Hyflon that showed acceptable CO<sub>2</sub> response

Finally, another variation of a thin film sensor was tested. Again EC was used as a matrix and a plasticizer was added to the mixture. This thin film did not show any response to CO<sub>2</sub>, in Figure 4.23 only artefacts are visible, and was therefore not investigated further.

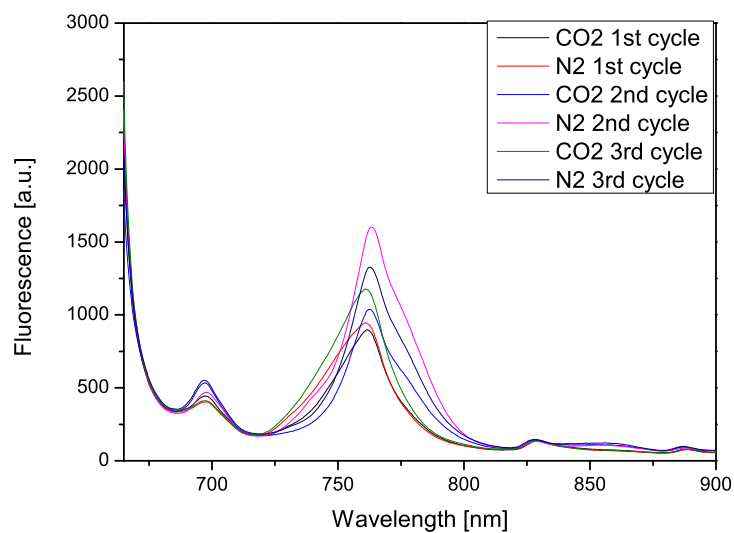


**Figure 4.23:** DiOH in EC including tributylphosphate as a plasticizer

### 4.1.5 Long term stability test

During characterization of the DiOH dye in the TEG/Hyflon matrix, several samples were used for long term stability tests. This included samples number 5, 7 and 14. Sample number 5 was first stored under CO<sub>2</sub> atmosphere and at low temperatures and still showed acceptable sensitivity to CO<sub>2</sub> after one month, though some degradation could be observed (Figure 4.24 and Figure 4.25). Then the sample was stored at room temperature in the laboratory with light exposure. After one month CO<sub>2</sub> sensitivity had strongly decreased (Figure 4.26).

Also sample number 7, which showed good responses, was strongly degraded after 1 month storage in the laboratory (Figure 4.27).

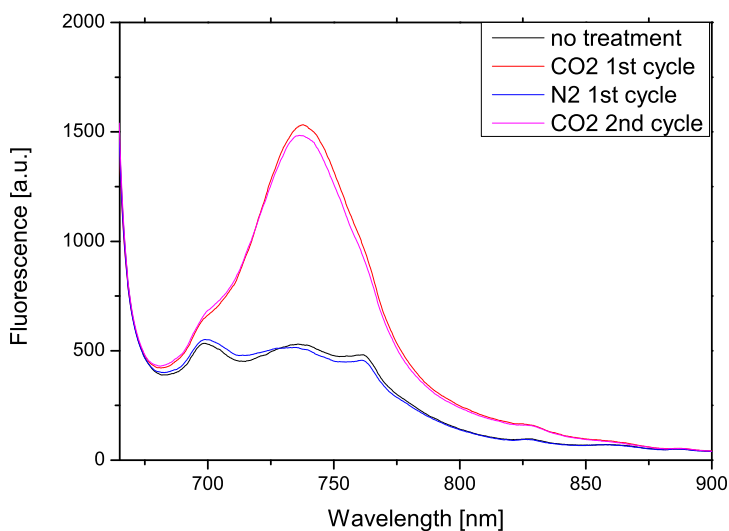


**Figure 4.24:** Sample number 5 after preparation

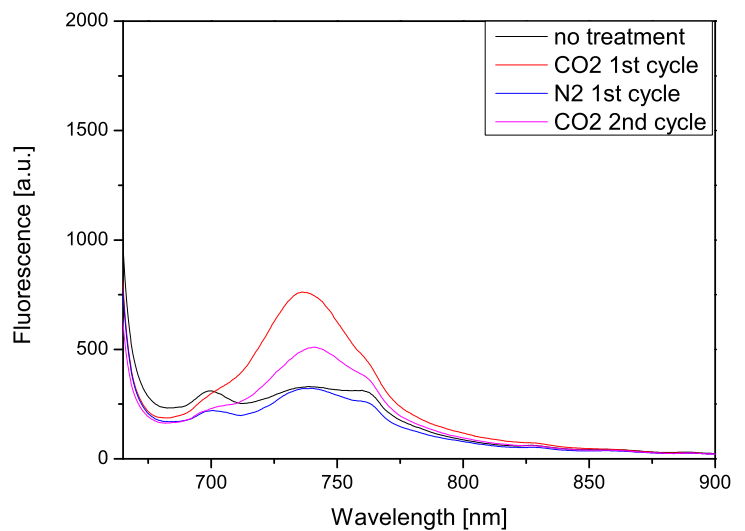


**Figure 4.25:** Sample number 5 after 1 month ideal storage

Sample number 14, which was the last functioning thin film sensor, showed similar results. Differences between N<sub>2</sub> and CO<sub>2</sub> could be detected but intensities were much lower and the curve looked very different (Figure 4.36 / Figure 4.37). Degradation of the sensor due to poisoning (neutralization of the base) would lead to constant high intensities but here a decrease in intensity is observed. Therefore, it is assumed that the dye aggregated leading to a loss in signal.

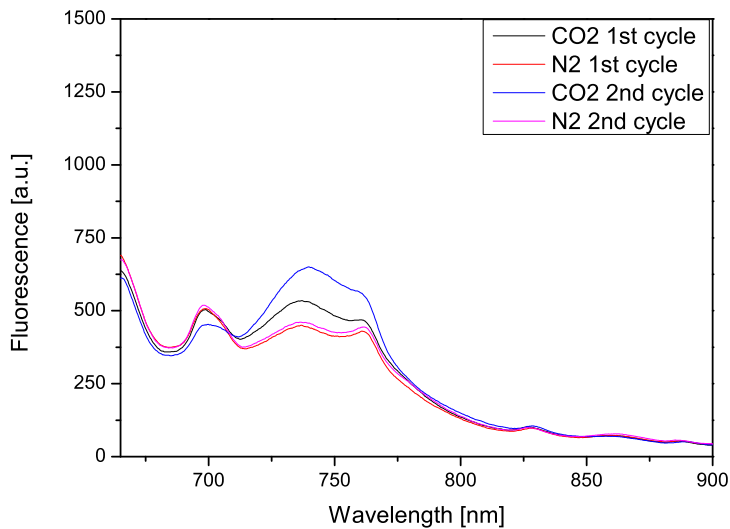


**Figure 4.26:** Sample number 5 after 1 month storage in the laboratory

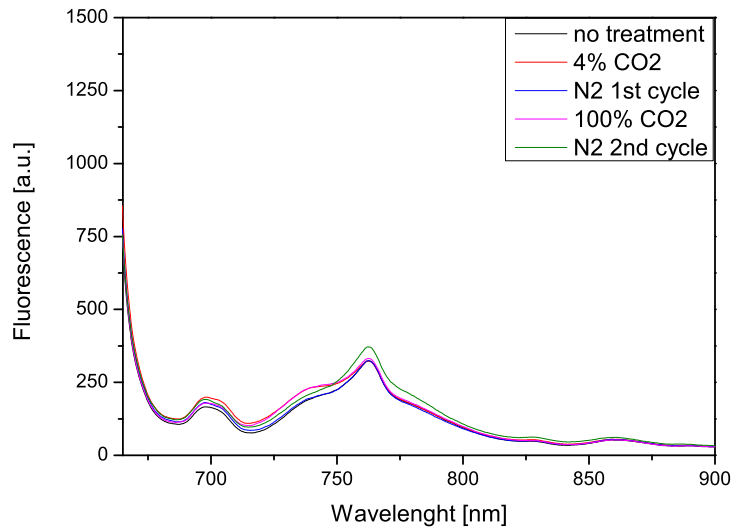


**Figure 4.27:** Sample number 7 after 1 month storage in the laboratory

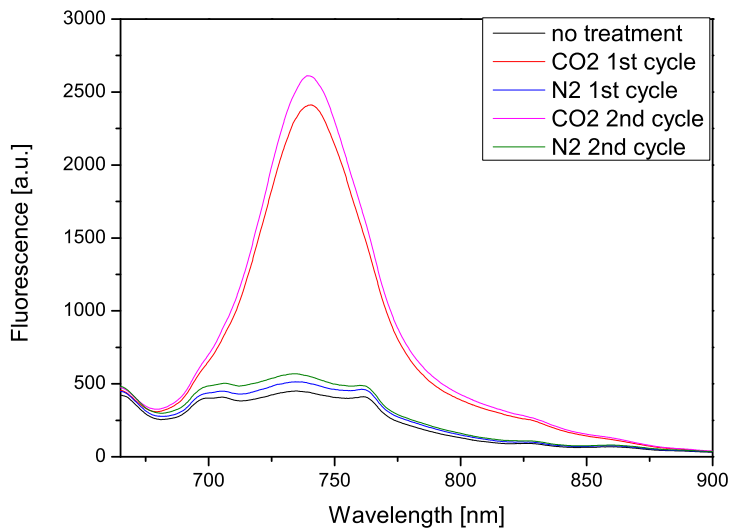


**Figure 4.28:** Sample number 14 after sensor preparation

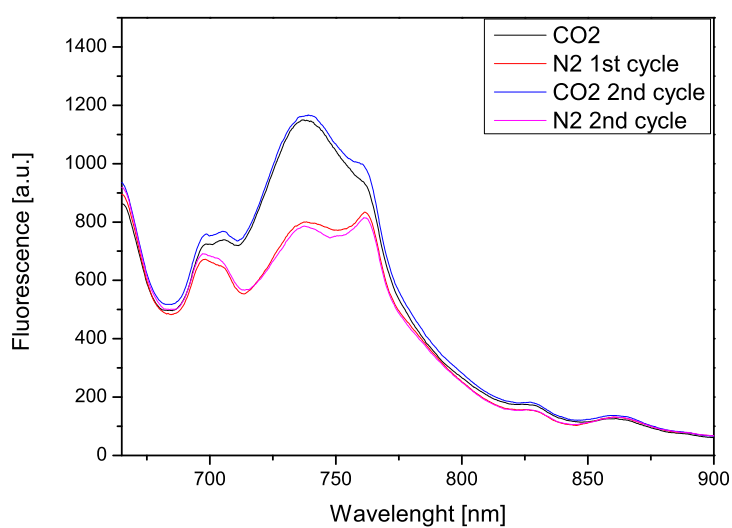


**Figure 4.29:** Sample number 14 after 1 month storage in the laboratory

#### 4.1.6 Conclusion CO<sub>2</sub>

The tests showed that only the DiOH dye was a suitable candidate for CO<sub>2</sub> sensors. It worked well in solution, but preparation of a thin film sensor was challenging. Even after a working system could be achieved, reproducibility was a problem. Also degradation of the sensor after storage, even at ideal conditions could be observed.

## 4.2 Ammonia Sensors

### 4.2.1 Testing 2 dyes for their ammonia sensing abilities

Two aza-BODIPY dyes (Figure 4.30 and Figure 4.31) were tested on their application as ammonia sensors.

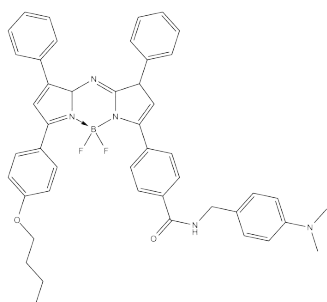


**Figure 4.30:** Amino-dye

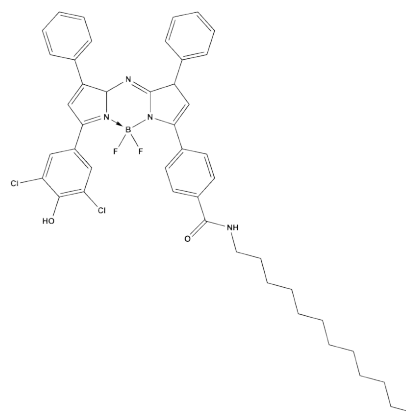


**Figure 4.31:** DiCl-dye

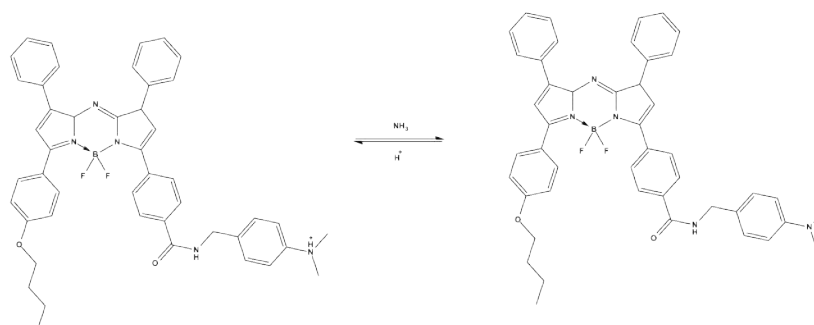


**Figure 4.32:** Reaction of amino dye with ammonia

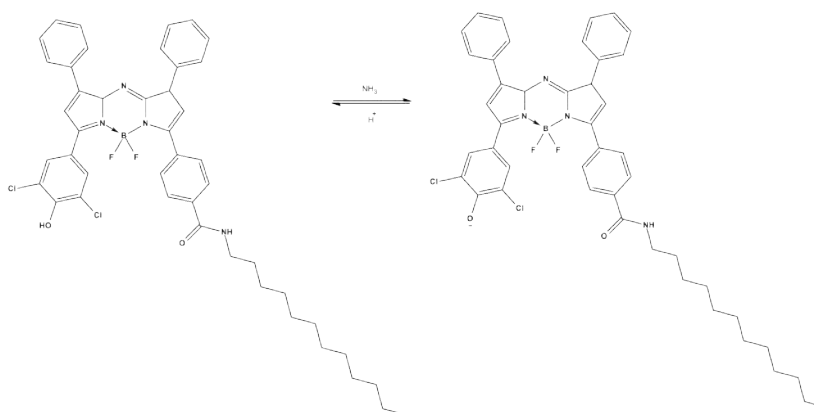


**Figure 4.33:** Reaction of DiCl dye with ammonia



The amino-dye was hoped to apply a new principle, where the dye is first in the protonated form, due to the acid present in the thin film sensor. Upon exposure to ammonia, the amino group was expected to go back to its neutral state (Figure 4.32). As described in section 3.3 different sensor thin films were prepared. For the amino-dye no functioning sensor could be prepared and the concept was aborted, as the dye did not seem to respond to ammonia in any way.

The DiCl-dye showed acceptable behavior in D4 and was therefore investigated further. A drawback was that the film was only reversible if the ammonia was removed under vacuum and at elevated temperatures. This is rather inconvenient because no continuous sensor use was possible. Even long exposure to N<sub>2</sub> showed only minimal recovery.

In Figure 4.34 a test of the DiCl sensors in the gaseous phase is shown, amounts of added ammonia are only approximate.

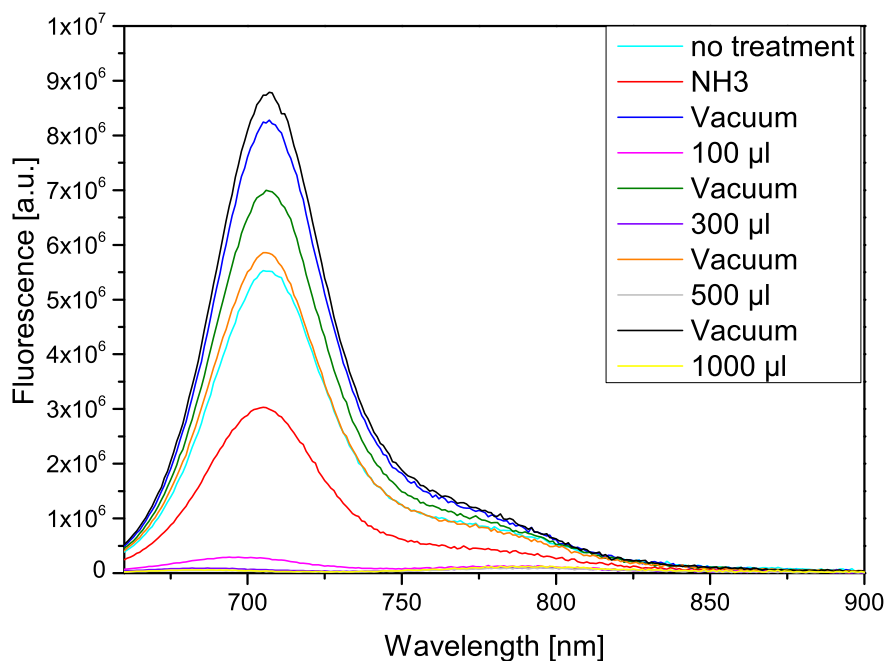


**Figure 4.34:** Measurement of the DiCl sensor in the gas phase

These results were quite acceptable and therefore measurements in solution were performed. For these measurements a sensor containing a reference dye and a PTFE membrane was prepared as well as solutions with defined ammonia concentrations.

Parts of the sensor were cut out and attached with silicone to a home-made plastic device (Figure 3.1). The measurement was done applying the DLR principle with a Firesting by dipping the plastic devices in buffer solutions with different ammonia concentrations.

First results seemed quite promising, since reactions to changing ammonia concentrations could be detected. The regeneration of the sensor was still a big challenge since sensors could only be reversed under vacuum and at elevated temperatures.

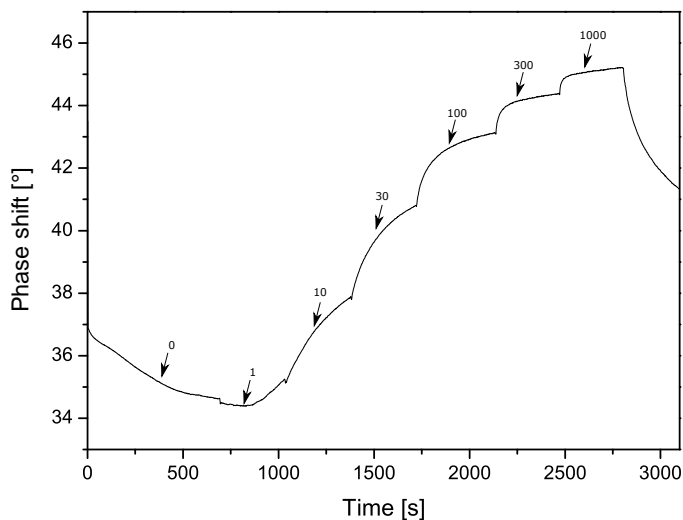


**Figure 4.35:** DiCl sensor A liquid phase measurements 2<sup>nd</sup> cycle steps are in  $\mu\text{g/l}$

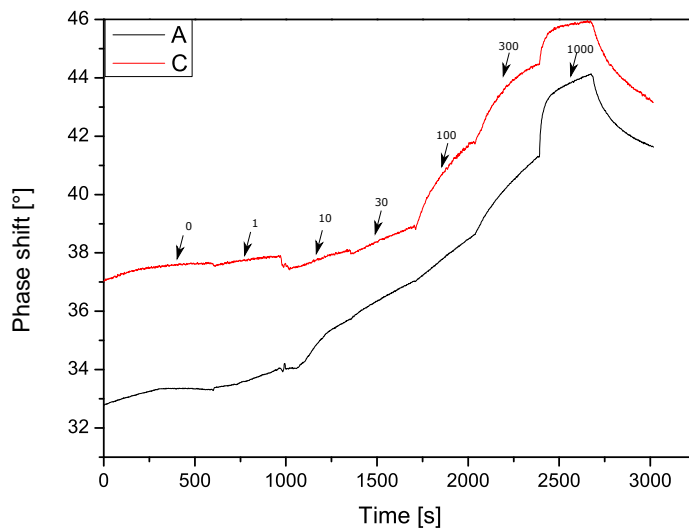


**Figure 4.36:** DiCl sensors A and C liquid phase measurements 1<sup>st</sup> cycle steps are in  $\mu\text{g/l}$

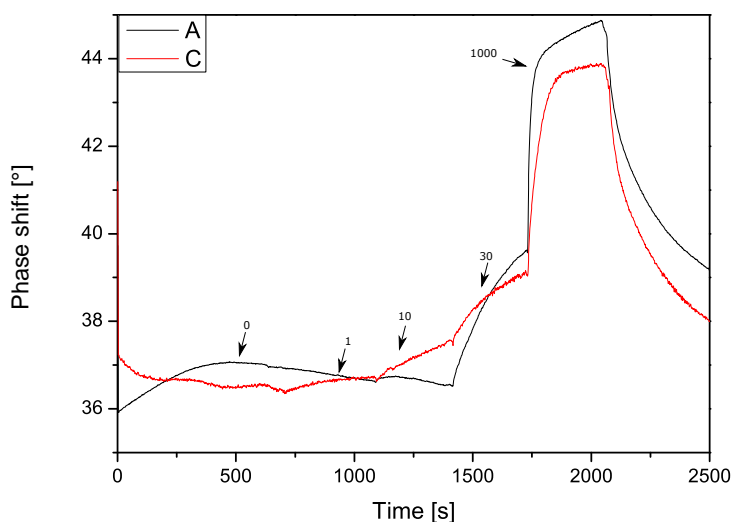


**Figure 4.37:** DiCl sensors A and C liquid phase measurements 2<sup>nd</sup> cycle steps are in  $\mu\text{g/l}$

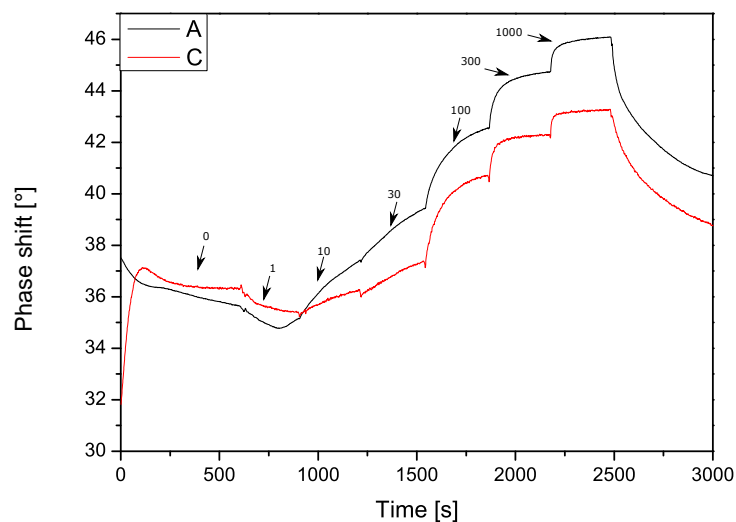


**Figure 4.38:** DiCl sensors A and C liquid phase measurements 3<sup>rd</sup> cycle steps are in  $\mu\text{g/l}$

Several samples were tested and reproducibility of the results proved to be impossible. Problems included irreversibility of some of the samples, extremely low signals and different phase shifts even within the same sample.

Some samples showed a bubble between the PTFE membrane and the sensor support after measurements. This could mean that water might have entered the sensor, which could have lead to a degradation or even complete damage of the sensor and made it unusable. Another explanation could be that the bubble is an accumulation of gas leading to a very slow response of the sensor.

As shown in Figure 4.35 - Figure 4.38 samples A and C first showed good responses to ammonia. Steps are visible and maxima seemed reproducible at about 45 (phase shift) for sample A and about 44 (phase shift) for C, respectively

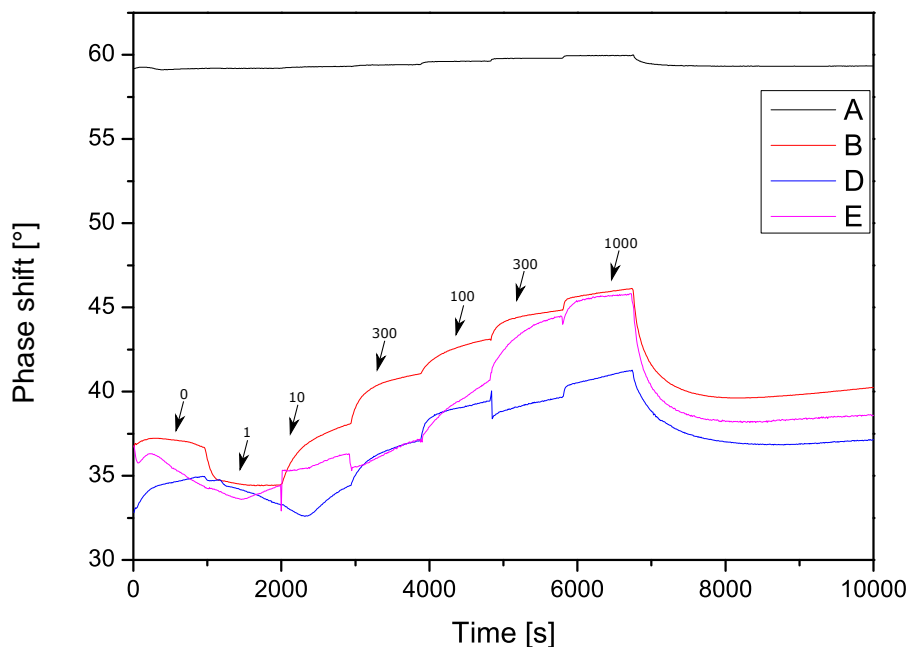


**Figure 4.39:** DiCl sensors A,B,D,E measured together after 2 weeks of storage

Two weeks later further measurements showed a strong degradation in sample A (Figure 4.39). Samples D and E showed extremely low signals so their values cannot be taken into account. Only sample B showed somewhat acceptable behavior. It was also the only sample that showed no bubble beneath the PTFE membrane after the measurement, which could be the reason for its better response.

These measurements showed that for this sensor or set-up no reproducible results can be obtained. Therefore, a new measurement method was applied.

For this, a sensor was prepared using silicone instead of PTFE. The sensor was prepared with three layers to rule out interaction of the reference dye with the indicator dye. The layers are described in section 3.3.

The sensor was first tested in the gas phase, then the sensor was mounted into a flow cell (Figure 3.2). Ammonia concentrations were changed at set intervals.

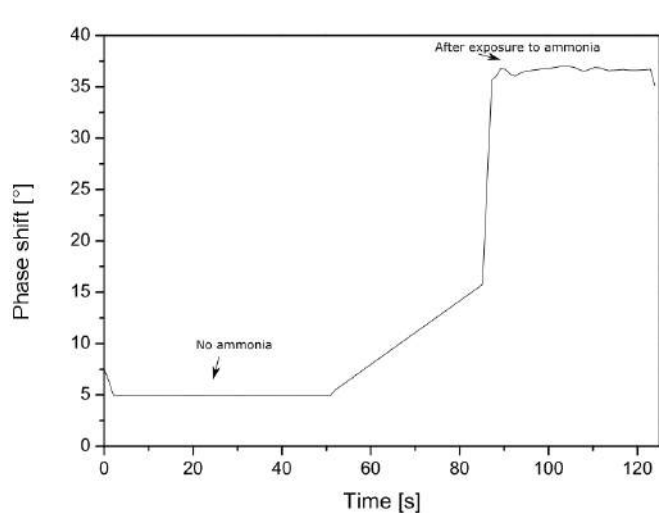


**Figure 4.40:** Test of the DiCl sensor in the gas phase

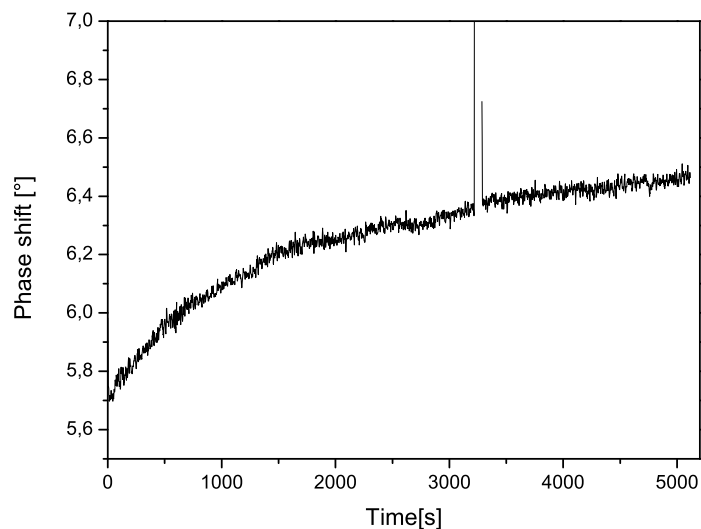


**Figure 4.41:** Measurement of DiCl sensor in the flow cell with buffers

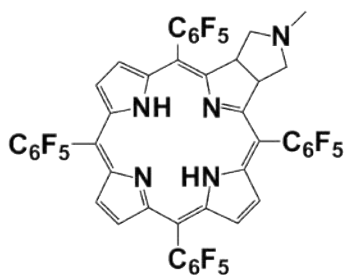
Figure 4.40 shows that a significant change in phase shift could be observed after exposure to gaseous ammonia.

Nevertheless, no signal changes could be detected when measuring in the flow cell.

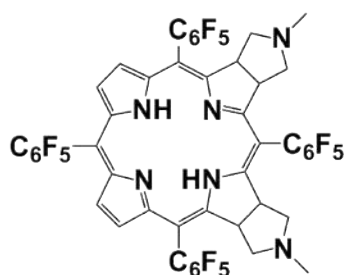
These results led to the conclusion that the sensor is not suitable for ammonia detection. It is possible that it only works in the gas phase and only responds to high concentrations of ammonia. Another possibility is that the sensors were destroyed upon long exposure to ammonia.

#### 4.2.2 Investigation of potential suitability of different dyes for ammonia sensors 1

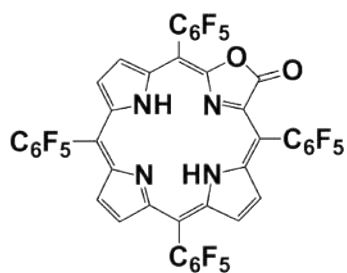
The dyes used in the screenings were chosen based on the existence of one or more deprotonable groups. The following dyes were used (some only for one of two screenings):



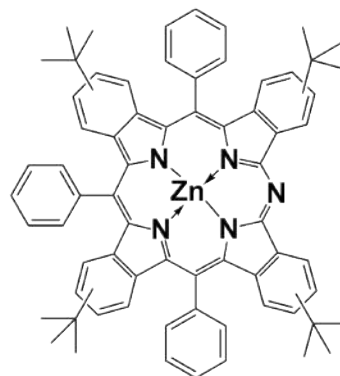
H2TFPP chlorin



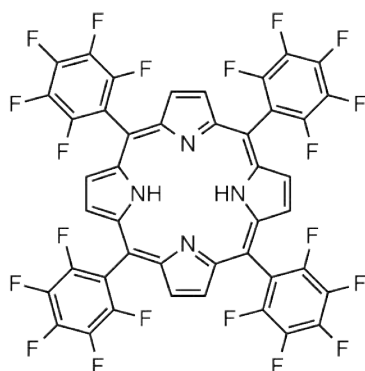
H2TFPP isobacteriochlorin



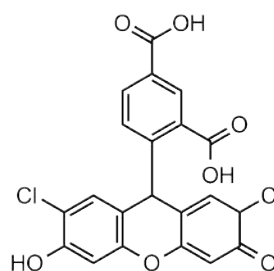
H2TFPPL



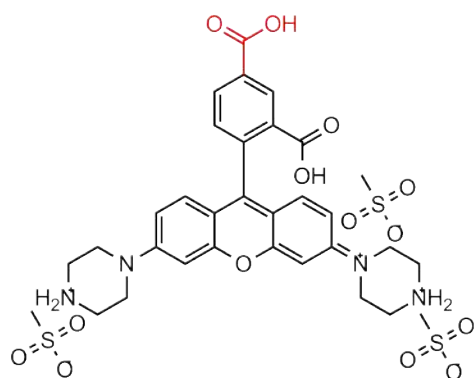
ZnNTBP



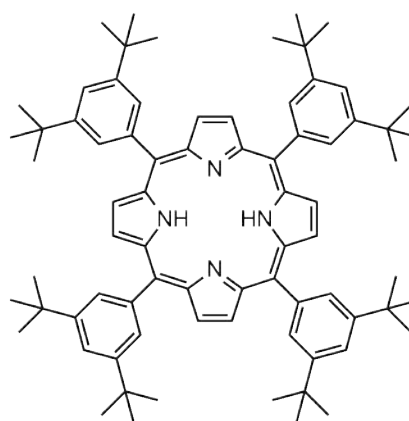
Meso-Tetra(pentafluorophenyl) porphyrin



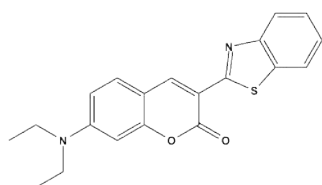
DiCl Fluorescein



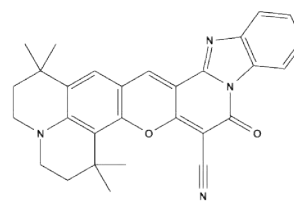
PET-Rhodamin 1 and 2 (red color)



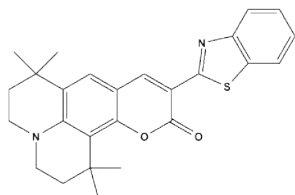
Meso-tetra-(3,5-di-t-butylphenyl) porphyrine



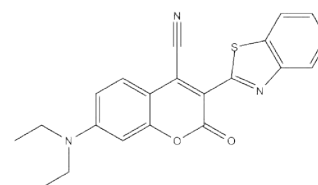
Coumarin 6



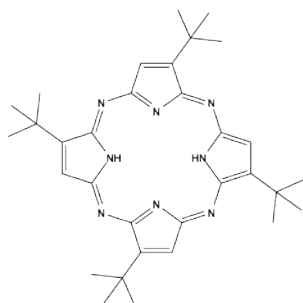
Coumarin X



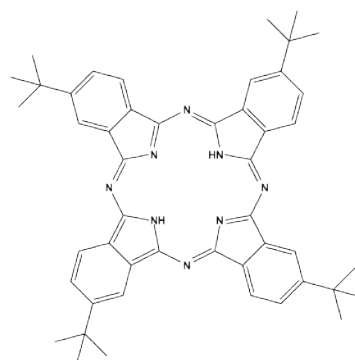
10-(benzo[d]thiazol-2-yl)-1,1,7,7-tetramethyl-2,3,6,7-tetrahydro-1H-pyrano[2,3-f]pyrido[3,2,1-ij]quinolin-11(5H)-one (C545T)



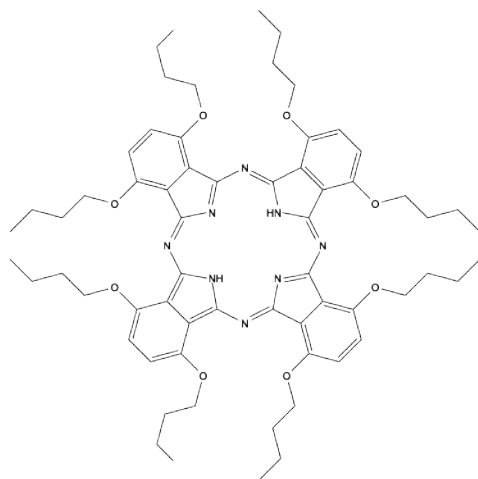
Macrolex Fluorescence Red



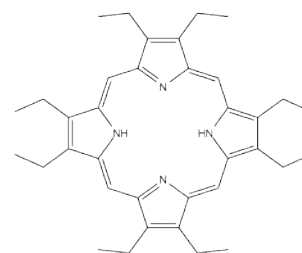
2,7,12,17-Tetra-tert-butyl-5,10,15,20 tetraaza,21H,23H, porphyrine



2,9,16,23-Tetra-tert-butyl-29H,31H-phthalocyanine



1,4,8,11,15,18,22,25-octabutoxy -29H,31H-phthalocyanine



Octaethylporphyrin

Examples of the assumed mechanisms for the reaction with ammonia for most dyes are presented in the figures below (Figure 4.42/ Figure 4.43). The reason for the choice of dyes for ammonia sensors is described in section 2.5.3.

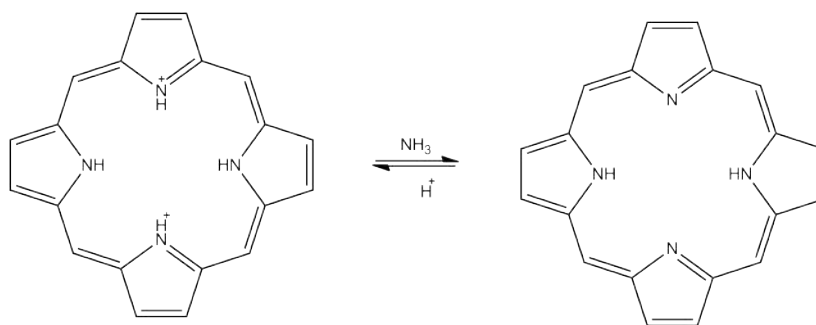


**Figure 4.42:** Reaction of a porphyrin with ammonia (same mechanism for ZnNTBP, but only partial deprotonation, while the Zn is still coordinated)

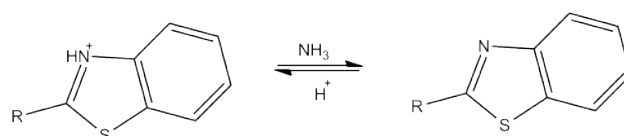


**Figure 4.43:** Reaction of coumarin and similar dyes with ammonia

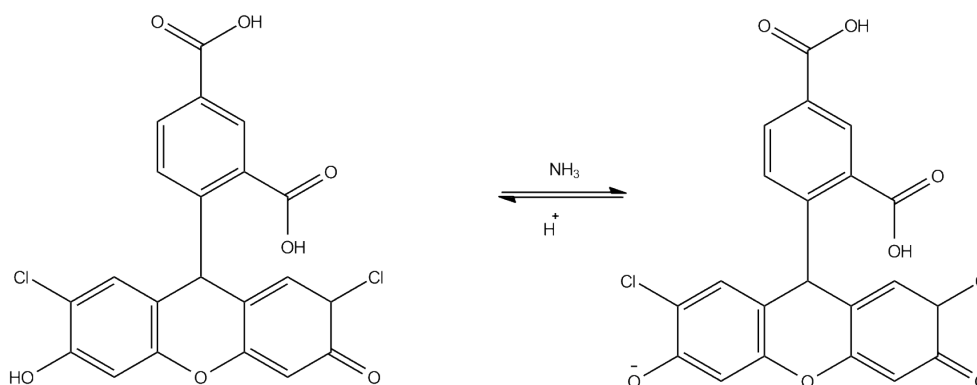


**Figure 4.44:** Reaction of DiCl Fluorescein with ammonia

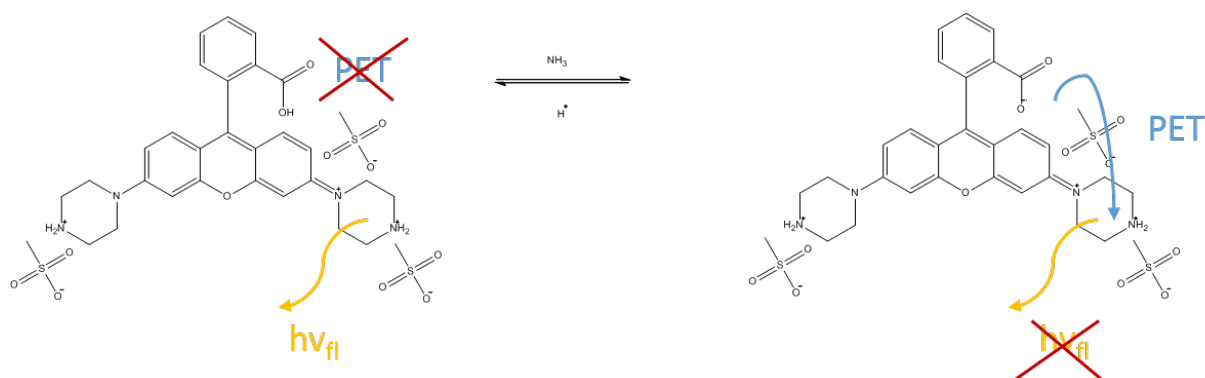


**Figure 4.45:** PET effect in rhodamin dyes

Sensors were prepared using cellulose acetate propionate as a matrix. Detection of reaction to ammonia was done via observation of color changes and absorption measurements.

Obtained results are listed in Table 4.2. All tests showed that none of the dyes was suitable as an ammonia sensor, since either no reaction to ammonia was visible or regeneration of the sensor was impossible.

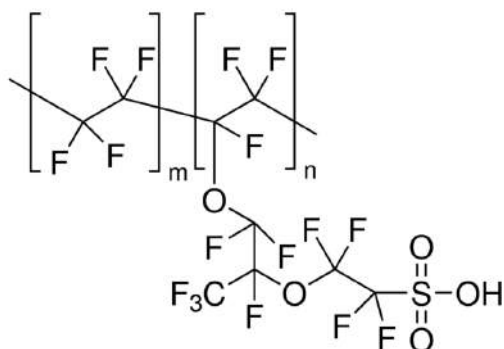


Table 4.2: Results for 1<sup>st</sup> dye screening in cellulose acetate propionate

Name	Reaction to NH <sub>3</sub>	Color before NH <sub>3</sub>	Color after NH <sub>3</sub>	Regeneration	MSA conc. [mg]
Octaethylporphyrin	yes	pink $\lambda_{\max} = 405$	brown $\lambda_{\max} = 400$	no	4,8
meso-Tetra(pentafluorophenyl) porphyrine	yes	yellow/greenish $\lambda_{\max} = 430$	brown $\lambda_{\max} = 410$	no	5,6
2,7,12,17-Tetra-tert-butyl-5,10,15,20 tetraaza,21H,23H, porphyrine	yes	blue/purple $\lambda_{\max} = 630$	blue/purple $\lambda_{\max} = 620$	no	5,6
meso-tetra-(3,5-di- <i>t</i> -butyl-phenyl) porphyrine	yes	yellow $\lambda_{\max} = 420$	yellow/brown $\lambda_{\max} = 450$	partially	4,8
2,9,16,23-Tetra-tert-butyl-29H,31H-phthalocyanine	yes	blue $\lambda_{\max} = 615$	blue $\lambda_{\max} = 600$	partially	4,8
1,4,8,11,15,18,22,25-octabutoxy-29H,31H-phthalocyanine		A precipitate is formed when an acid is added			
ZnNTBP	yes	green $\lambda_{\max} = 460$	green $\lambda_{\max} = 445$	partially	4,8
H <sub>2</sub> TFPPL	no	brown $\lambda_{\max} = 410$	-	-	4,8
H <sub>2</sub> TFPP chlorin	yes	yellow/green $\lambda_{\max} = 405$	light brown $\lambda_{\max} = 420$	no	5,6
H <sub>2</sub> TFPP bacterochlorin	yes	green $\lambda_{\max} = 380$	pink $\lambda_{\max} = 420$	no	5,6

### 4.2.3 Investigation of potential suitability of different dyes for ammonia sensors 2

Sensor preparation with a solid Nafion 117® membrane



**Figure 4.46:** Nafion 117® membrane used in its ion form for sensor preparation

In the second screening 19 dyes were tested as possible ammonia sensors.

A solid Nafion® membrane was used as a matrix (175  $\mu\text{m}$ ). The dye was incorporated by depositing parts of the Nafion® membrane into dye solutions. The amount of dye in solution strongly influenced the concentration in the matrix.



**Figure 4.47:** Preliminary test samples in Nafion 117® membrane

Nafion® was chosen as a matrix material because it was in its ionic form and therefore a kind of solid acid. This facilitates sensor preparation, because no addition of an extra acid is needed and the acid cannot leach out of the matrix. Another advantage is that leaching of the dye is significantly diminished.

All obtained results can be found in Table 4.3. Detection of responses to ammonia was done by observing changes in color or fluorescence, no acceptable spectra could be taken because the coloring of the samples was too intensive.

Only a few of the dyes fulfilled important criteria such as reaction with ammonia and regeneration.

Table 4.3: Results for first tests of the dye screening in Nafion 117® membrane

Name	Reaction to NH <sub>3</sub>	Color before NH <sub>3</sub>	Color after NH <sub>3</sub>	Regeneration	Solvent
Octaethylporphyrin	no	red	red	-	THF
ZnNTBP	no	green	green	-	EtOH
H <sub>2</sub> TFPPL	yes	yellow/brown	red	no	EtOH
Meso-Tetra(pentafluorophenyl) porphyrin	no	green	green	-	EtOH
H <sub>2</sub> TFPP chlorin	yes	purple/blue	green	no	EtOH
H <sub>2</sub> TFPP	yes	blue	red	yes	EtOH
isobacterochlorin					
2,7,12,17-Tetra-tert-butyl-5,10,15,20 tetraaza,21H,23H, porphyrine	yes	blue	blue/purple	no	EtOH
Meso-tetra-(3,5-di- <i>t</i> -butyl-phenyl) porphyrin	yes	green	purple	yes	THF
2,9,16,23-Tetra-tert-butyl-29H,31H-phthalocyanin	no	blue	blue	-	THF
Amino-dye	no	No changes in fluorescence			
DiCl-dye	no	No changes in fluorescence			
Coumarin 6	no	red/orange	red/orange	-	EtOH
Fluorescence red	yes	blue	red/orange	no	EtOH
C545T	no	red	red	-	EtOH
1,4,8,11,15,18,22,25-octabutoxy -29H,31H-phthalocyanine	yes	greenish-blue	light green	yes	THF
PET-Rhodamin 1	yes	fluorescence	no fluorescence	yes	EtOH
PET-Rhodamin 2	yes	fluorescence	no fluorescence	yes	EtOH
DiCl- Fluoresceine	yes	yellow	red	no	EtOH
Coumarin X	yes	fluorescence	no fluorescence	no	EtOH

These five dyes showed promising criteria, such as response to ammonia and regenerability and were therefore investigated further:

- PET-Rhodamin 1
- PET-Rhodamin 2
- Meso-tetra-(3,5-di-t-butyl-phenyl) porphyrin
- H<sub>2</sub>TFPP isobacterochlorin
- Octabutoxyphthalocyanine

Upon further inspection H<sub>2</sub>TFPP isobacterochlorin and octabutoxyphthalocyanin showed no regeneration after exposure to gaseous ammonia.

The rhodamin dyes (which were very similar) showed less fluorescence when exposed to ammonia, due to the PET effect (Figure 4.45), whereas the meso-tetra-(3,5-di-t-butyl-phenyl) porphyrine showed an increase in fluorescence, attributed to a shift in emission spectra. All three dyes could be regenerated after exposure to ammonia. The corresponding Fluorimeter measurements can be seen in Figure 4.48 - Figure 4.50.

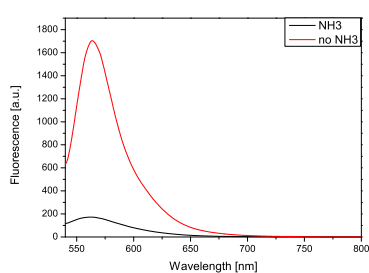


**Figure 4.48:** PET Rhodamin 2 dye

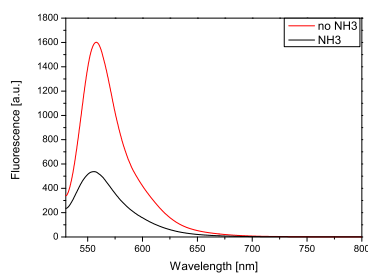


**Figure 4.49:** PET Rhodamin 1 dye

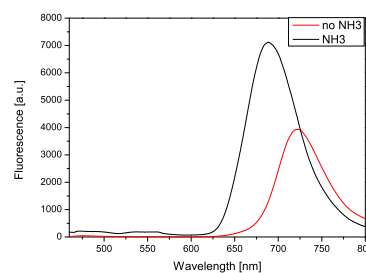


**Figure 4.50:** Meso-tetra-(3,5-di-t-butyl-phenyl) porphyrine dye

For sensor protection the sensors were dipped in a 20% solution of E4 silicone in cyclohexane and were dried overnight.

Characterization of the sensors was done on the Lock-In. For this the sensors were attached to small glass vials in order to overcome the problem of signal changes caused by movements. Addition of ammonia throughout the measurements was done by a syringe adding a 1+9 ammonia/water solution (2,5% ammonia), 1  $\mu$ l corresponding to 500 ppm ammonia gas. Measurements were very slow, due to the thickness of the sensors (175  $\mu$ m), which caused slow diffusion of the analyte to the dye. One cycle took about 5 hours and regeneration was done overnight with 100% N<sub>2</sub>.

PET rhodamin 1 and 2 are very similar and show almost the same behavior, therefore PET rhodamin 2 was not tested thoroughly.

The porphyrine dye showed interesting results. During the first two cycles steps could not really be detected but after regeneration, for every addition steps could be found. Another interesting problem was that now addition of ammonia seems to decrease the intensity, whereas preliminary measurements showed an increase in intensity when exposed to ammonia, it was first assumed, that this could be due to a change in LED but a decrease in intensity was also observed later when the same LED was used in a thinner Nafion 117 film (section 4.2.3). It is assumed that the sensor was already destroyed by ammonia and therefore showed inexplicable behavior.

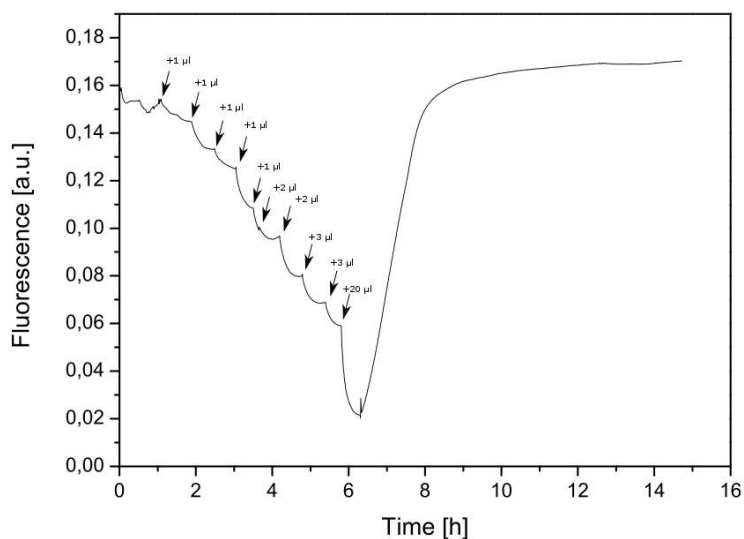


**Figure 4.51:** Response of ammonia sensor based on PET rhodamin 1 in Nafion 117® membrane with 470 nm LED

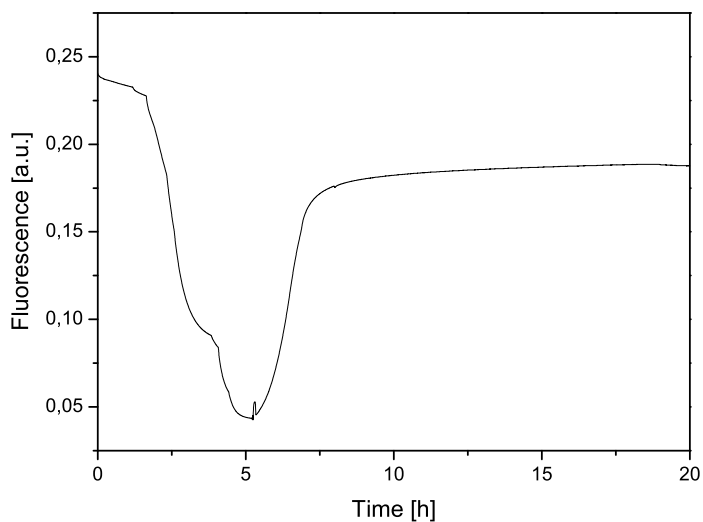


**Figure 4.52:** Response of ammonia sensor based on the porphyrine dye, with regeneration, in Nafion 117® membrane with 450 nm LED

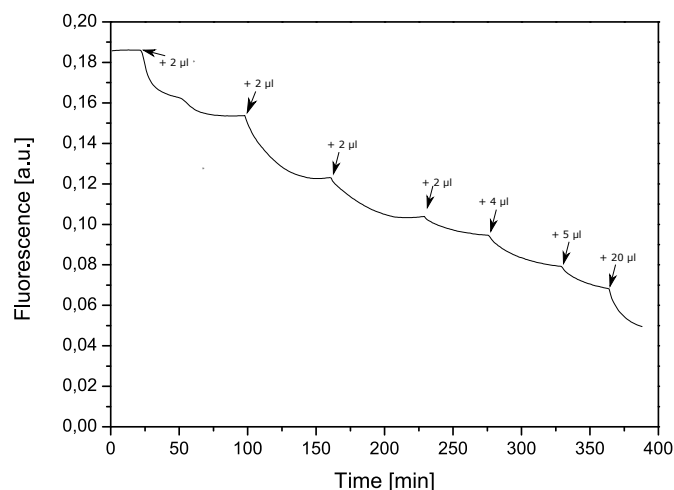


**Figure 4.53:** Response of ammonia sensor based on the porphyrine dye in Nafion 117® membrane with 450 nm LED

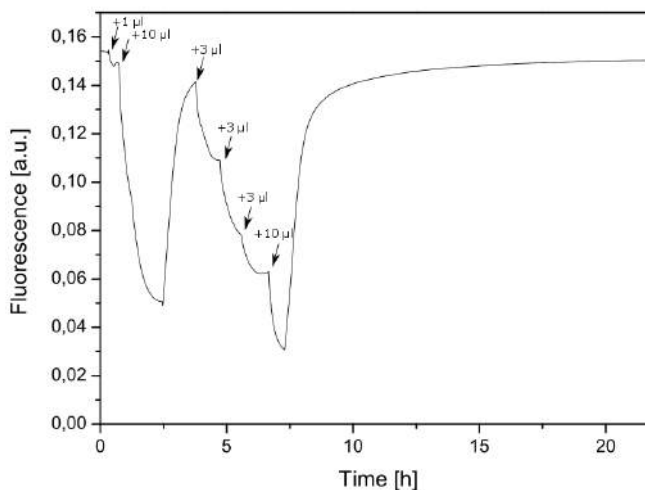


**Figure 4.54:** Response of ammonia sensor based on PET rhodamin 2 in Nafion 117® membrane with 470 nm LED

#### Ammonia sensors based on thin Nafion 117® films

Response times were rather long, but results proved to be quite promising, therefore a thinner sensor was prepared using a liquid Nafion® solution (1-4  $\mu\text{m}$ ). A PTFE membrane was added to increase signal intensity and for protection.

Defined steps can be observed for every addition of the ammonia solution. At the end of each cycle concentrations had to be strongly increased.

Response times were much faster when using the thinner film (1-4  $\mu\text{m}$  compared to 175  $\mu\text{m}$ ). One cycle including regeneration with  $\text{N}_2$  took about 1 hour, which is a major improvement to earlier measurements. A sensor containing PET rhodamin 1 was prepared and measured as explained before. Even though precise adjustment of ammonia concentrations was not possible, results are rather reproducible and good reversibility is observed.

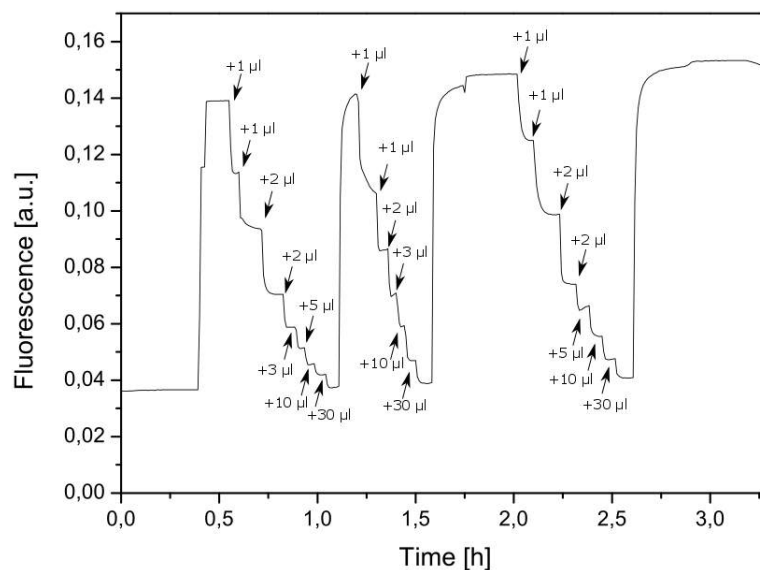


**Figure 4.55:** Response curve of rhodamin 1 in thin Nafion® measured in the gas phase

Exact measurements are not possible in the gas phase, therefore tests in the liquid phase with defined ammonia concentrations (concentrations can be found in Table 3.2) were done in a flow cell. The set-up can be seen in section 3.1.

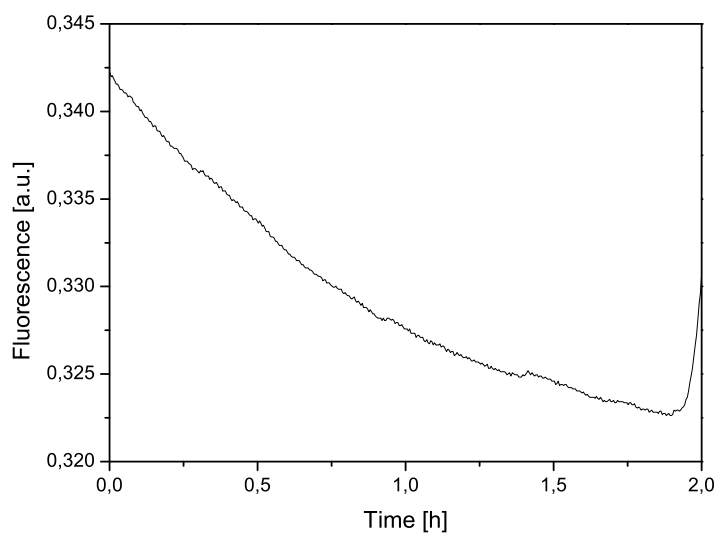


**Figure 4.56:** Test of rhodamin 1 in Nafion® in ammonium chloride buffer solutions; Flow cell set-up

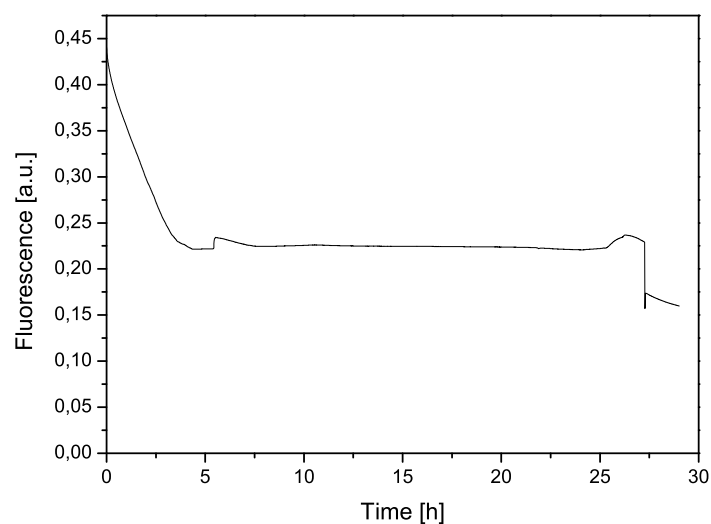


**Figure 4.57:** Test of rhodamin 1 in Nafion® in ammonium chloride buffer solutions; Fix set-up

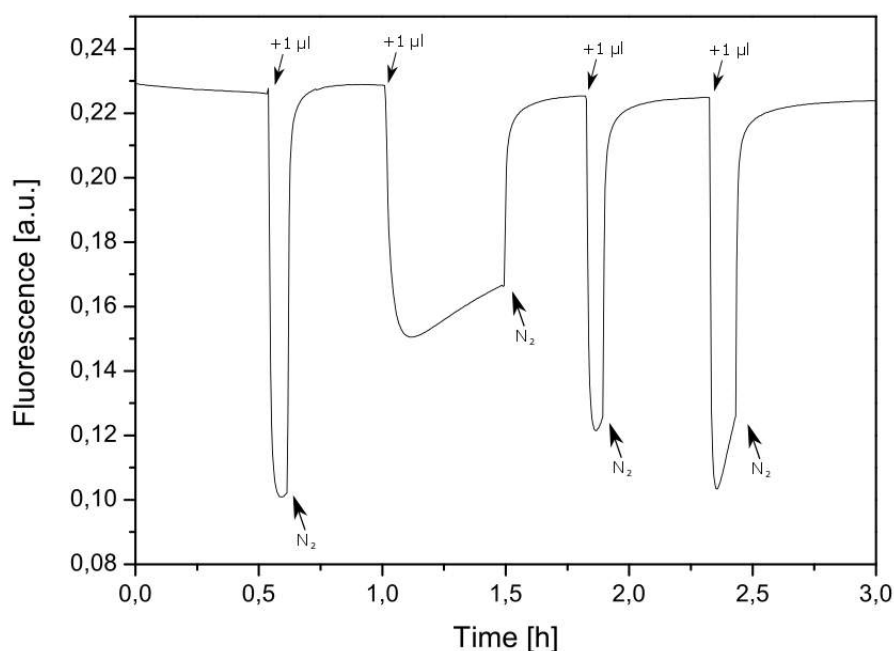


Figure 4.56 shows that no response to ammonia could be achieved in a flow cell set up even when changing concentrations from  $1 \mu\text{g}/\text{l}$  to  $1000 \mu\text{g}/\text{l}$ . It was assumed that this could be due to the use of silicone tubes that might take in most of the analyte.

This resulted in a change of set-up. The sensor was directly dipped into the solutions containing ammonium chloride and buffer. Changes in ammonia concentration were done frequently but no response could be detected even at high concentrations (Figure 4.57).

These results could be explained by swelling of the sensor due to the contact with water.

Whether humidity was the problem, was tested by gas phase measurements in a  $\text{H}_2\text{O}$  saturated environment. For this test always  $1\mu\text{l}$  1+9 ammonia/water solution was added (corresponding to 500 ppm gaseous ammonia), when the signal was stable, the flask was flooded with  $\text{N}_2$  saturated with  $\text{H}_2\text{O}$  vapor. This was done several times to assure reproducibility.



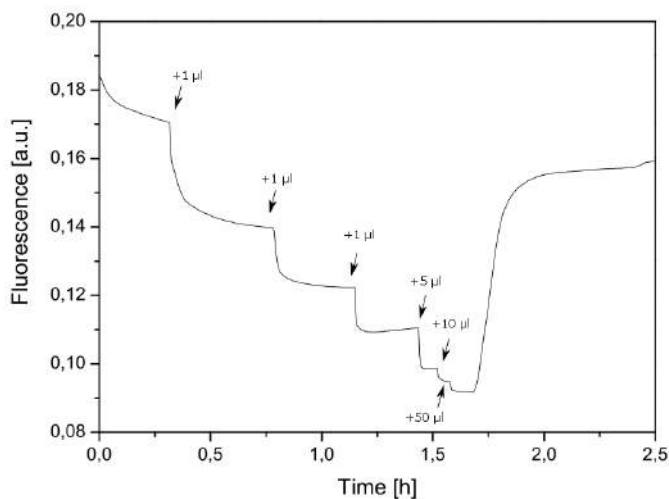
**Figure 4.58:** Test of Rhodamin in thin Nafion® with  $\text{H}_2\text{O}$  saturated environment

Figure 4.58 shows that humidity does not affect sensor response. This implies, that other sources must influence measurements in solution. Possibly other ions in solution interfere with the sensor and therefore change the signal.

Sensitivity of the sensor was not as high as hoped. It seems likely that by using Nafion® , the thin film sensor was more acidic than most sensors prepared so far [15]. It was hoped

that neutralizing the acidic groups by ion exchange with TOACl could lead to an increase in sensitivity.

Thin films were prepared containing between 2 and 9 mg of TOACl in MeOH. The 9 mg TOACl sensor was non-transparent probably due to precipitation of the Nafion® caused by the high basic content. The other two films were transparent, showed almost no change in sensitivity, but a decrease in dynamic range was detected (Figure 4.61). Also regeneration was less efficient and response times increased (Figure 4.59/Figure 4.60).



**Figure 4.59:** Response of the rhodamine 1 dye in Nafion with 26 w% TOACl to gaseous ammonia

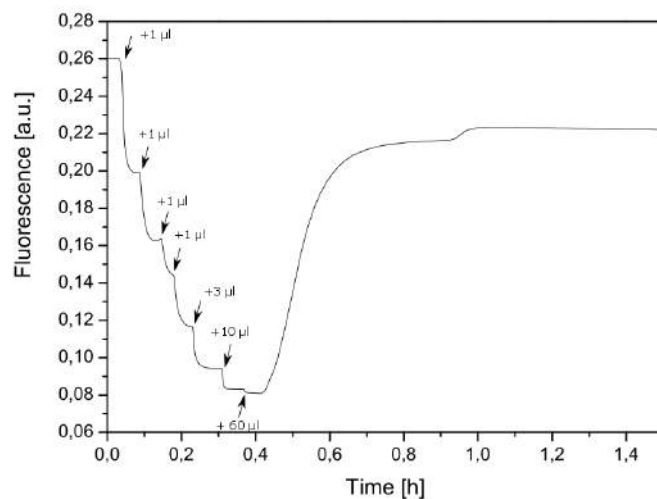


**Figure 4.60:** Response of the rhodamine 1 dye in Nafion with 8 w% TOACl to gaseous ammonia

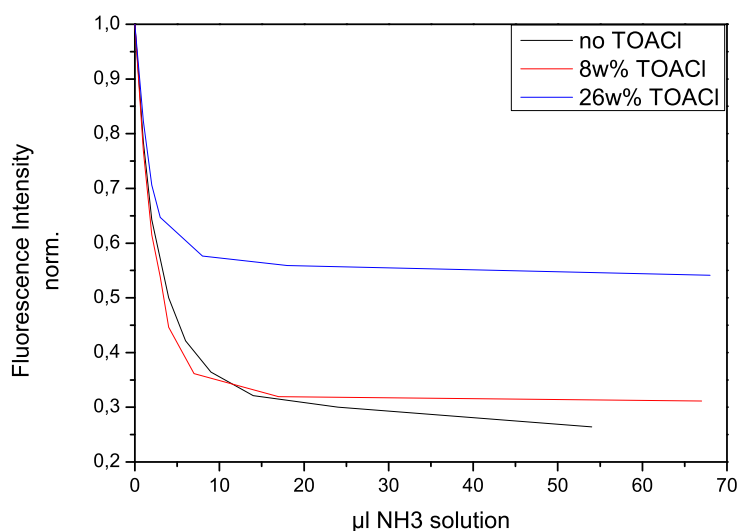


**Figure 4.61:** Comparison of thin Nafion® films with and without TOACl

The final tests were done with the porphyrin in a thinner Nafion® membrane.

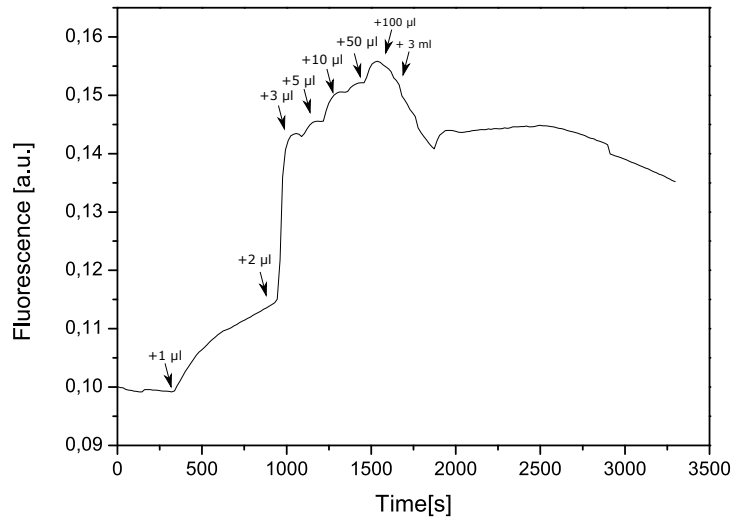


**Figure 4.62:** Response of the porphyrin dye in thin Nafion® to gaseous ammonia

Here, additions were made with a 1 + 99 ammonia/water solution. At first it seemed very promising, since the sensor responded to low concentrations of ammonia (0,25% solution, 1 µl, 50 ppm) but after a few additions of ammonia all the sudden the signal started to decrease. Even upon further addition of higher concentrated ammonia solutions, the signal kept decreasing. This can be explained by irreversible damage to the sensor caused by exposure to ammonia. This is in agreement with the results obtained earlier concluding that this dye is not suitable for the application as an ammonia sensor.



---

## 5 Conclusion and Outlook

In this thesis aza-BODIPY dyes were tested as CO<sub>2</sub> and ammonia sensors.

The prepared CO<sub>2</sub> sensors did not show the expected sensitivity. They responded to much higher CO<sub>2</sub> concentrations than hoped initially. Another problem was reproducibility of sensor fabrication which makes them unsuitable for the application as CO<sub>2</sub> sensors. Possibly sensor preparation is susceptible to environmental changes, causing a change in sensing abilities.

The use of aza-BODIPY dyes as ammonia sensors seemed quite promising at first, but extensive characterization showed unsatisfying results. None of the tested dyes was suitable for the application as an ammonia sensor.

This led to a new concept, testing several commercially available and home-made dyes as possible ammonia sensors. Cellulose acetate propionate and Nafion® were used as matrix materials. In Nafion® several dyes exhibited promising properties. Using Nafion as a matrix has a few advantages such as no need for additional acid, and eliminating leaching of the dye and acid.

Eventually, it was found that only the rhodamine dyes used in this thesis are suitable candidates for ammonia sensors. They show fast and detectable responses to ammonia, insensitivity to humidity and sufficient regeneration.

Nevertheless, the current sensors only showed responses at relatively high concentrations in the gas phase and virtually no response in water. Thus, optimization of the current sensors is required.

---

## 6 References

- (1) Schutting, S.; Borisov, S. M.; Klimant, I. Diketo-Pyrrolo-Pyrrole Dyes as New Colorimetric and Fluorescent pH Indicators for Optical Carbon Dioxide Sensors. *Anal. Chem.* **2013**, *85*, 3271–3279.
- (2) Von Bueltingsloewen, C.; McEvoy, A. K.; McDonagh, C.; MacCraith, B. D.; Klimant, I.; Krause, C.; Wolfbeis, O. S. Sol-gel Based optical carbon dioxide sensor employing dual luminophore referencing for application in food packaging technology. *Analyst* **2002**, *127*, 1478–1483.
- (3) McMurray, H. N. Novel Thin Optical Film Sensors for the Detection of Carbon Dioxide. *J. Mater. Chem.* **1992**, *2*, 401–406.
- (4) Burke, C. S.; Markey, A.; Nooney, R. I.; Byrne, P.; McDonagh, C. Development of an optical sensor probe for the detection of dissolved carbon dioxide. *Sensors and Actuators, B: Chemical* **2006**, *119*, 288–294.
- (5) Liu, Y.; Tang, Y.; Barashkov, N. N.; Irgibaeva, I. S.; Lam, J. W. Y.; Hu, R.; Birimzhanova, D.; Yu, Y.; Tang, B. Z. Fluorescent Chemosensor for Detection and Quantitation of Carbon Dioxide Gas. *Journal of American Chemical Society Communications* **2010**, *132*, 13951–13953.
- (6) Schutting, S.; Jokic, T.; Strobl, M.; Borisov, S. M.; de Beer, D.; Klimant, I. NIR optical carbon dioxide sensors based on highly photostable dihydroxy-aza-BODIPY dyes. *J. Mater. Chem.* **2015**, *3*, 5474–5483.
- (7) Nakamura, N.; Amao, Y. Optical sensor for carbon dioxide combining colorimetric change of a pH indicator and a reference luminescent dye. *Anal. Bioanal. Chem.* **2003**, *376*, 642–646.
- (8) Ali, R.; Lang, T.; Saleh, S. M.; Meier, R. J.; Wolfbeis, O. S. Optical Sensing Scheme for Carbon Dioxide Using a Solvatochromic Probe. *Analytical Chemistry* **2011**, *83*, 2846–2851.
- (9) Mills, A.; Chang, Q. Fluorescent Plastic Thin-film Sensor for Carbon Dioxide. *Analyst* **1993**, *118*, 839–843.
- (10) Mills, A.; Chang, Q.; McMurray, N. Equilibrium studies on colorimetric plastic film sensors for carbon dioxide. *Anal. Chem.* **1992**, *64*, 1383–1389.

- 
- (11) Jokic, T. New pH and CO<sub>2</sub> sensitive materials based on BF<sub>2</sub>-chelated aza-dipyromethenes., Ph.D. Thesis, Technical University of Graz, 2015.
  - (12) Timmer, B.; Olthuis, W.; van den Berg, A. Ammonia sensors and their applications - a review. *Sensors and Actuators, B: Chemical* **2005**, *107*, 666–677.
  - (13) Abel, T.; Ungerboeck, B.; Klimant, I.; Mayr, T. Fast responsive optical trace level ammonia sensor for environmental monitoring. *Chemistry Central Journal* **2012**, *6*, 1–9.
  - (14) Muthukumar, P.; John, S. A. Optochemical ammonia gas sensing properties of meso-substituted porphyrin derivatives immobilized Nafion film on glass slide. *Sensors and Actuators, B: Chemical* **2012**, *174*, 74–80.
  - (15) Waich, K.; Mayr, T.; Klimant, I. Fluorescence sensors for trace monitoring of dissolved ammonia. *Talanta* **2008**, *77*, 66–72.
  - (16) Waich, K.; Borisov, S.; Mayr, T.; Klimant, I. Dual lifetime referenced trace ammonia sensors. *Sensors and Actuators, B: Chemical* **2009**, *139*, 132–138.
  - (17) Hulanicki, A.; Glab, S.; Ingman, F. Chemical sensors Definitions and Classification. *Pure Appl. Chem.* **1991**, *63*, 1247–1250.
  - (18) McDonagh, C.; Burke, C. S.; MacCraith, B. D. Optical Chemical Sensors. *Chem. Rev.* **2008**, *108*, 400–422.
  - (19) Kalcher, K.; Mayr, T. Lecture on Chemosensors., 2014.
  - (20) Klimant, I. Lecture Chemo-und Biosensorik., 2014.
  - (21) Valeur, B., *Molecular Fluorescence Principles and Applications*; Wiley-VCH: 2001.
  - (22) Lakowicz, J. R., *Principles of Fluorescence Spectroscopy*; Springer: 2006.
  - (23) Quaranta, M.; Borisov, S. M.; Klimant, I. Indicators for optical oxygen sensors. *Bioanalytical Reviews* **2012**, *4*, 115–157.
  - (24) Strobl, M. Covalent coupling of fluorescent pH indicators in a polymeric matrix., MA thesis, Technical University Graz, 2013.
  - (25) Boens, N.; Leen, V.; Dehaen, W. Fluorescent indicators based on BODIPY. *Chem. Soc. Rev.* **2012**, *41*, 1130–1172.
  - (26) Stich, M. I. J.; Fischer, L. H.; Wolfbeis, O. S. Multiple fluorescent chemical sensing and imaging. *Chemical Society Reviews* **2010**, *39*, 3102–3114.
  - (27) <http://institutoecoacao.blogspot.co.at/2014/01/novo-gadget-mede-niveis-de-poluicao-em.html>.
  - (28) <http://www.intlsensor.com/pdf/infrared.pdf>.
  - (29) <https://en.wikipedia.org/wiki/Infrared-gas-analyzer>.
  - (30) [http://www.derangedphysiology.com/php/Arterial-blood-gases/Principles-of-pCO<sub>2</sub>-measurement-with-the-Severinghaus-electrode.php](http://www.derangedphysiology.com/php/Arterial-blood-gases/Principles-of-pCO2-measurement-with-the-Severinghaus-electrode.php).

- (31) Mills, A.; Lepre, A.; Wild, L. Effect of plasticizer-polymer compatibility on the response characteristics of optical thin CO<sub>2</sub> and O<sub>2</sub> sensing films. *Analytica Chimica Acta* **1998**, *362*, 193–202.
- (32) Gruber, P. Comparison and optimization of matrix materials for CO<sub>2</sub> sensors., MA thesis, Technical University of Graz, 2014.
- (33) Wolfbeis, O. S. Materials for fluorescence-based optical chemical sensors. *Journal of Materials Chemistry* **2005**, *15*, 2657–2669.
- (34) <https://en.wikipedia.org/wiki/Thymol-blue>.
- (35) <https://en.wikipedia.org/wiki/Phenol-red>.
- (36) <http://www.wiredchemist.com/chemistry/data/acid-base-indicators>.
- (37) <http://dictionary.reference.com/browse/cresol+red>.
- (38) <https://sites.google.com/site/chempendix/indicators>.
- (39) <https://de.wikipedia.org/wiki/Neutralrot>.
- (40) <https://www.thermofisher.com/order/catalog/product/H348>.
- (41) Schutting, S.; Klimant, I.; de Beer, D.; Borisov, S. M. New highly fluorescent pH indicator for ratiometric RGB imaging of pCO<sub>2</sub>. *Methods and Applications in Fluorescence* **2014**, *2*, 024001.
- (42) Borisov, S. M.; Gatterer, K.; Klimant, I. Red light-excitable dual lifetime referenced optical pH sensors with intrinsic temperature compensation. *Analyst* **2010**, *135*, 1711–1717.
- (43) Borisov, S. M.; Klimant, I. A versatile approach for ratiometric time-resolved read-out of colorimetric chemosensors using broadband phosphors as secondary emitters. *Anal. Chim. Acta* **2013**, *787*, 219–225.
- (44) Su, X.; Cunningham, M. F.; Jessop, P. G. Use of a switchable hydrophobic associative polymer to create an aqueous solution of CO<sub>2</sub>-switchable viscosity. *Polymer Chemistry* **2014**, *5*, 940–944.
- (45) Liu, Y.; Tang, Y.; Barashkov, N. N.; S., I.; Irgibaeva; Lam, J. W.; Hu, R.; Birimzhanova, D.; Yu, Y.; Tang, B. Z. Fluorescent Chemosensor for Detection and Quantitation of Carbon Dioxide Gas. *Journal of American Chemical Society Communications* **2010**, *132*, 13951–13953.
- (46) Waich, K.; Mayer, T.; Klimant, I. Microsensors for Detection of ammonia at ppb-concentration levels. *Measurement Science and Technology* **2007**, *18*, 3195–3201.
- (47) Preininger, C.; Mohr, G. J. Fluorosensors for ammonia using rhodamines immobilized in plasplastic poly(vinyl chloride) and in sol-gel; a comparative study. *Anal. Chim. Acta* **1997**, *342*, 207–213.



- 
- (48) Morales-Bahnik, A.; Czolk, R.; Ache, H. An optochemical ammonia sensor based on immobilized metalloporphyrins. *Sensors and Actuators, B: Chemical* **1994**, *18-19*, 493–496.
- (49) Trinkel, M.; Trettnak, W.; Reiningger, F.; Benes, R.; O’Leary, P.; Wolfbeis, O. S. Study of the performance of an optochemical sensor for ammonia. *Anal. Chim. Acta* **1996**, *320*, 235–243.
- (50) <http://www.fluorophores.tugraz.at>.
- (51) Jokic, T.; Borisov, S. M.; Saf, R.; Nielsen, D. A.; Kuhl, M.; Klimant, I. Highly Photostable Near-Infrared Fluorescent pH Indicators and Sensors Based on BF<sub>2</sub>-Chelated Tetraarylazadipyrromethene Dyes. *Anal. Chem.* **2012**, *84*, 6723–6730.
- (52) Chen, W.; Joly, A. G.; Malm, J.-O.; Bovin, J.-O.; Wang, S. Full-color Emission and Temperature Dependence of the Luminescence in Poly-P-phenylene ethynylene- ZnS/Mn<sup>2+</sup> Composite Particles. *J. Phys. Chem.* **2003**, *107*, 6544–6551.



---

## 7 List of Figures

2.1	Exemplary homogenous response time [19] . . . . .	5
2.2	Order of energies of orbital transitions [21] . . . . .	7
2.3	Orbital transition using formaldehyde as an example [21] . . . . .	7
2.4	Different types of luminescence [21] . . . . .	8
2.5	Jablonski Diagram[23] . . . . .	8
2.6	Stern-Volmer plot for dynamic quenching [24] . . . . .	11
2.7	Illustration of possible static quenching processes [21] . . . . .	12
2.8	Stern-Volmer plot for static quenching [24] . . . . .	12
2.9	Stern-Volmer plot showing simultaneous quenching [24] . . . . .	13
2.10	Examples for electron donors and acceptors for PET [21] . . . . .	13
2.11	Scheme for PET [22] . . . . .	14
2.12	Schematic of a spectrofluorometer [21] . . . . .	15
2.13	Schematic drawing of time resolved measurements [21] . . . . .	16
2.14	Principle of dual lifetime referencing measurement [26] . . . . .	17
2.15	Infrared CO <sub>2</sub> detector [27] . . . . .	18
2.16	Schematic drawing of the Severinghaus electrode and a reference electrode [30]	19
2.17	Structure of Ethyl cellulose . . . . .	21
2.18	Structures of thymol blue, phenol red, cresol red, m-cresol purple in different protonated states . . . . .	23
2.19	Structure of neutral red in neutral and protonated state . . . . .	23
2.20	Structure of brilliant yellow in neutral and deprotonated state . . . . .	23
2.21	Structure of m-nitrophenol in neutral and deprotonated state . . . . .	24
2.22	Structure of dihydroxy-aza-BODIPY dye in neutral and deprotonated states . .	24
2.23	Structure of HPTS in neutral and deprotonated state . . . . .	24
2.24	Structure of diketo-pyrrolo-pyrrole dyes in neutral and deprotonated state . . .	25
2.25	The polymer changes its viscosity upon exposure to CO <sub>2</sub> [44] . . . . .	27
2.26	Structures of the polymers [44] . . . . .	27
2.27	Reaction of a secondary amine with CO <sub>2</sub> to form a carbamate [5] . . . . .	28
2.28	Structure of 1,1,2,3,4,5-Hexaphenylsilole (HPS) . . . . .	28
2.29	Nile red . . . . .	28

---

2.30	Reversible reaction of the amidine with CO <sub>2</sub> . . . . .	29
2.31	Reaction of porphyrin dyes with ammonia . . . . .	33
2.32	Mechanism for protonation and deprotonation of bromophenol blue (R = -H) and bromocresol green (R = -CH <sub>3</sub> ) . . . . .	33
3.1	Measurement set up including the home made plastic cap . . . . .	36
3.2	Flow cell set up . . . . .	36
3.3	Reaction scheme for 1-(4-hydroxy-3-methoxyphenyl)-3-phenylprop-2-en-1-one .	38
3.4	Reaction scheme for chalcones . . . . .	39
3.5	Reaction scheme for 4-(2-((5-(4-hydroxy-3-methoxyphenyl)-3-phenyl-1H-pyrrol- 2-yl)imino)-3-phenyl-2H-pyrrol-5-yl)-2-methoxyphenol . . . . .	40
3.6	Reaction scheme for the synthesis of the BF <sub>2</sub> -chelate . . . . .	41
3.7	Sulfonation reaction of BF <sub>2</sub> -complex . . . . .	42
3.8	Amino-dye used for ammonia sensor preparation . . . . .	45
3.9	DiCl-dye used for ammonia sensor preparation . . . . .	45
4.1	Structures of DiMeOH (A) aza-BODIPY dye and DiOH (B) aza-BODIPY dye in protonated and deprotonated forms . . . . .	52
4.2	pH dependence of absorption in EtOH/aq. buffer solution (1:1) IS = 150 (DiMeOH)	53
4.3	Corresponding calibration curve of DiMeOH . . . . .	53
4.4	pH dependence of absorption in EtOH/aq. buffer solution (1:1) IS = 150 (DiOH)	53
4.5	Corresponding calibration curve of DiOH . . . . .	53
4.6	Thin film with EC and DMSO/Toluene/EtOH; 1/4/5 . . . . .	54
4.7	Absorption changes of the DiOH dye in 1-butanol . . . . .	56
4.8	Absorption changes of the DiMeOH dye in 1-butanol . . . . .	56
4.9	Emission spectra of DiOH dye in 1-butanol . . . . .	56
4.10	Emission spectra of DiMeOH dye in 1-butanol . . . . .	56
4.11	Absorption changes of DiOH dye in TEG . . . . .	57
4.12	Emission spectra of DiOH dye in TEG . . . . .	57
4.13	Schematic drawing of a sensor containing TEG and Hyflon as a matrix . . . . .	58
4.14	DiMeOH in TEG/Hyflon shows only minimal changes when exposed to CO <sub>2</sub> .	59
4.15	Preliminary test showed acceptable sensitivity for DiOH in TEG/Hyflon . . . . .	59
4.16	Emission spectra of DiOH dye in TEG/Hyflon; Fluorolog . . . . .	60
4.17	Gas cycles at 15°C for DiOH in TEG/Hyflon; steps are kPa CO <sub>2</sub> . . . . .	60
4.18	Gas cycles at 25°C for DiOH in TEG/Hyflon; steps are kPa CO <sub>2</sub> . . . . .	60
4.19	Gas cycles at 35°C for DiOH in TEG/Hyflon; steps are kPa CO <sub>2</sub> . . . . .	60
4.20	Normalized intensities for DiOH dye in TEG/Hyflon at different temperatures .	61

---

4.21 DiOH in TEG/Hyflon that did not show acceptable CO <sub>2</sub> response . . . . .	61
4.22 DiOH in TEG/Hyflon that showed acceptable CO <sub>2</sub> response . . . . .	61
4.23 DiOH in EC including tributylphosphate as a plasticizer . . . . .	62
4.24 Sample number 5 after preparation . . . . .	63
4.25 Sample number 5 after 1 month ideal storage . . . . .	63
4.26 Sample number 5 after 1 month storage in the laboratory . . . . .	64
4.27 Sample number 7 after 1 month storage in the laboratory . . . . .	64
4.28 Sample number 14 after sensor preparation . . . . .	64
4.29 Sample number 14 after 1 month storage in the laboratory . . . . .	64
4.30 Amino-dye . . . . .	66
4.31 DiCl-dye . . . . .	66
4.32 Reaction of amino dye with ammonia . . . . .	66
4.33 Reaction of DiCl dye with ammonia . . . . .	66
4.34 Measurement of the DiCl sensor in the gas phase . . . . .	67
4.35 DiCl sensor A liquid phase measurements 2 <sup>nd</sup> cycle steps are in $\mu\text{g}/\text{l}$ . . . . .	68
4.36 DiCl sensors A and C liquid phase measurements 1 <sup>st</sup> cycle steps are in $\mu\text{g}/\text{l}$ . . . . .	68
4.37 DiCl sensors A and C liquid phase measurements 2 <sup>nd</sup> cycle steps are in $\mu\text{g}/\text{l}$ . . . . .	68
4.38 DiCl sensors A and C liquid phase measurements 3 <sup>rd</sup> cycle steps are in $\mu\text{g}/\text{l}$ . . . . .	68
4.39 DiCl sensors A,B,D,E measured together after 2 weeks of storage . . . . .	69
4.40 Test of the DiCl sensor in the gas phase . . . . .	70
4.41 Measurement of DiCl sensor in the flow cell with buffers . . . . .	70
4.42 Reaction of a porphyrin with ammonia (same mechanism for ZnNTBP, but only partial deprotonation, while the Zn is still coordinated) . . . . .	73
4.43 Reaction of coumarin and similar dyes with ammonia . . . . .	73
4.44 Reaction of DiCl Fluoresceine with ammonia . . . . .	73
4.45 PET effect in rhodamin dyes . . . . .	73
4.46 Nafion 117®membrane used in its ion form for sensor preparation . . . . .	76
4.47 Preliminary test samples in Nafion 117®membrane . . . . .	76
4.48 PET Rhodamin 2 dye . . . . .	79
4.49 PET Rhodamin 1 dye . . . . .	79
4.50 Meso-tetra-(3,5-di-t-butyl-phenyl) porphyrine dye . . . . .	79
4.51 Response of ammonia sensor based on PET rhodamin 1 in Nafion 117®membrane with 470 nm LED . . . . .	80

---

4.52	Response of ammonia sensor based on the porphyrine dye ,with regeneration, in Nafion 117®membrane with 450 nm LED . . . . .	80
4.53	Response of ammonia sensor based on the porphyrine dye in Nafion 117®membrane with 450 nm LED . . . . .	81
4.54	Response of ammonia sensor based on PET rhodamin 2 in Nafion 117®membrane with 470 nm LED . . . . .	81
4.55	Response curve of rhodamin 1 in thin Nafion®measured in the gas phase . . . . .	82
4.56	Test of rhodamin 1 in Nafion®in ammonium chloride buffer solutions; Flow cell set-up . . . . .	82
4.57	Test of rhodamin 1 in Nafion®in ammonium chloride buffer solutions; Fix set-up	82
4.58	Test of Rhodamin in thin Nafion®with H <sub>2</sub> O saturated environment . . . . .	83
4.59	Response of the rhodamine 1 dye in Nafion with 26 w% TOACl to gaseous ammonia	84
4.60	Response of the rhodamine 1 dye in Nafion with 8 w% TOACl to gaseous ammonia	84
4.61	Comparison of thin Nafion®films with and without TOACl . . . . .	84
4.62	Response of the porphyrin dye in thin Nafion®to gaseous ammonia . . . . .	85
9.1	<sup>1</sup> H NMR of the DiMeOH Ligand in DMSO-d <sub>6</sub> . . . . .	101
9.2	<sup>1</sup> H NMR of the DiMeOH complex without sulfonate in DMSO-d <sub>6</sub> . . . . .	102
9.3	<sup>1</sup> H NMR of the DiOH complex without sulfonate in DMSO-d <sub>6</sub> . . . . .	102
9.4	NMR of the DiOH-BF <sub>2</sub> sulfonate complex in DMSO-d <sub>6</sub> . . . . .	103
9.5	NMR of the DiMeOH-BF <sub>2</sub> sulfonate complex in DMSO-d <sub>6</sub> . . . . .	103
9.6	Absorption spectra for DiOH dye in Toluene . . . . .	105
9.7	Absorption spectra for DiOH dye in THF . . . . .	105
9.8	Absorption spectra for DiOH dye in EtOH . . . . .	106
9.9	Absorption spectra for DiOH dye in isobutanol . . . . .	106

---

## 8 List of Tables

3.1	Compositions for preliminary ammonia sensor tests . . . . .	46
3.2	Concentrations of prepared ammonia solutions . . . . .	47
4.1	Matrix and solvents used for primary test . . . . .	55
4.2	Results for 1 <sup>st</sup> dye screening in cellulose acetate proprionate . . . . .	75
4.3	Results for first tests of the dye screening in Nafion 117®membrane . . . . .	78
9.1	List of Chemicals . . . . .	98
9.2	Abbreviations . . . . .	100

---

## 9 Appendix

### 9.1 List of Chemicals

**Table 9.1:** List of Chemicals

<b>Chemical</b>	<b>Supplier</b>	<b>CAS Number</b>
Ammonium chlorid	ROTH	12125-02-9
KOH	Sigma-Aldrich	1310-58-3
Ethyl cellulose	Sigma-Aldrich	9004-57-3
Natriumhydrogen phosphate	Sigma-Aldrich	7558-79-4
Tri-sodium phosphate	Riedel-deHoeb	7601-54-9
TiO <sub>2</sub>	Kemira	13463-67-7
Cellulose acetate proprionate	Acros Organics	9004-39-1
Polystyrene	Acros Organics	9003-53-6
Cellulose acetate butyrate	Acros Organics	9004-36-8
Hydromed D1-D7	Cardio Tech International Inc.	
Ammonia solution 25 %	Merck	1336-21-6
HCl	VWR	7647-01-0
DMSO	Roth	67-68-5
Natriumsulfat	ROTH	7757-82-6
Propane sultone	TCI Europe	1120-71-4
4-Hydroxy acetophenone	TCI Europe	99-93-4
4-Hydroxy 3-methoxy acetophenone	TCI Europe	498-02-2
NaOH	ROTH	1310-73-2
4-Dodecylbenzolsulfonsäure	Sigma-Aldrich	27176-87-0
Dichloromethane	VWR	75-09-2
Tetrahydrofuran	VWR	109-99-9
Acetone	VWR	67-64-1
Ethanol	VWR	64-17-5
Methanol	VWR	67-56-1
Ethylacetate	VWR	141-78-6



---

1-Butanol	Aber	75-36-3
Benzaldehyde	Aber	100-52-7
DMSO D6	Euriso-top	67-68-5
CHES	Roth	103-47-9
MOPS	Roth	1132-61-2
MES	Roth	4432-31-9
CAPS	Roth	1135-40-6
Sodium chloride	Fluka	7647-14-5
Sodium sulphate	Roth	7757-82-6
Acetic acid	ROTH	64-19-7
Methansulfonsäure	ABCR	75-75-2
Borontrifluoride	TCI Europe	7637-07-2
DMF	ROTH	68-12-2
Tetraethyleneglycol	Sigma-Aldrich	112-60-7
Nitromethan	Sigma-Aldrich	75-52-5
Natriumhydrid	Sigma-Aldrich	7646-69-7
Nafion 117 Membran	Ion Power	31175-20-9
Nafion 117 Solution 5,46%	Scientific Polymer Products	31175-20-9
N,N Diisopropylethylamine	TCI Europe	7087-68-5

## 9.2 Abbreviations

**Table 9.2:** Abbreviations

BODIPY	Difluoroboron dipyrromethene
DiOH	4-(5-((5-(4-hydroxyphenyl)-3-phenyl-2H-pyrrol-2-ylidene)amino)-4-phenyl-1H-pyrrol-2-yl)-2-methoxyphenol- BF <sub>2</sub> complex
DiMeOH	4-(2-((5-(4-hydroxy-3-methoxyphenyl)-3-phenyl-1H-pyrrol-2-yl)imino)-3-phenyl-2H-pyrrol-5-yl)-2methoxyphenol - BF <sub>2</sub> complex
DMF	Dimethylformamide
DMSO	Dimethylsulfoxide
EtOH	Ethanol
EC	Ethyl cellulose
TOAOH	Tetraoctylammoniumhydroxide
THF	Tetrahydrofuran
TEG	Tetraethyleneglycol
Amino-dye	7-(4-butoxyphenyl)-3-(4-((4-(dimethylamino)benzyl)carbamoyl)phenyl)-5,5-difluoro-1,9-diphenyl-5,9a-dihydro-1H-dipyrrolo[1,2-c:2',1'-f][1,3,5,2]triazaborinin-6-ium-5-uide
DiCl-dye	7-(3,5)-dichloro-4-hydroxyphenyl)-3-(4-(dodecylcarbamoyl)phenyl)-5,5-difluoro-1,9-diphenyl-5,9a-dihydro-1H-dipyrrolo[1,2-c:2',1'-f][1,3,5,2]triazaborinin-6-ium-5-uide
PTFE	Polytetrafluoroethylene
PET	Polyethylene terephthalate
TOACl	Tetraoctylammoniumchloride
MSA	Methanesulfonic acid
DCM	Dichloromethane
DBSA	Dodecylbenzene sulfonic acid
TAC	Total ammonia compounds
TMS	Tetra methyl silyl

## 9.3 Carbon dioxide sensors

### 9.3.1 NMR Spectra

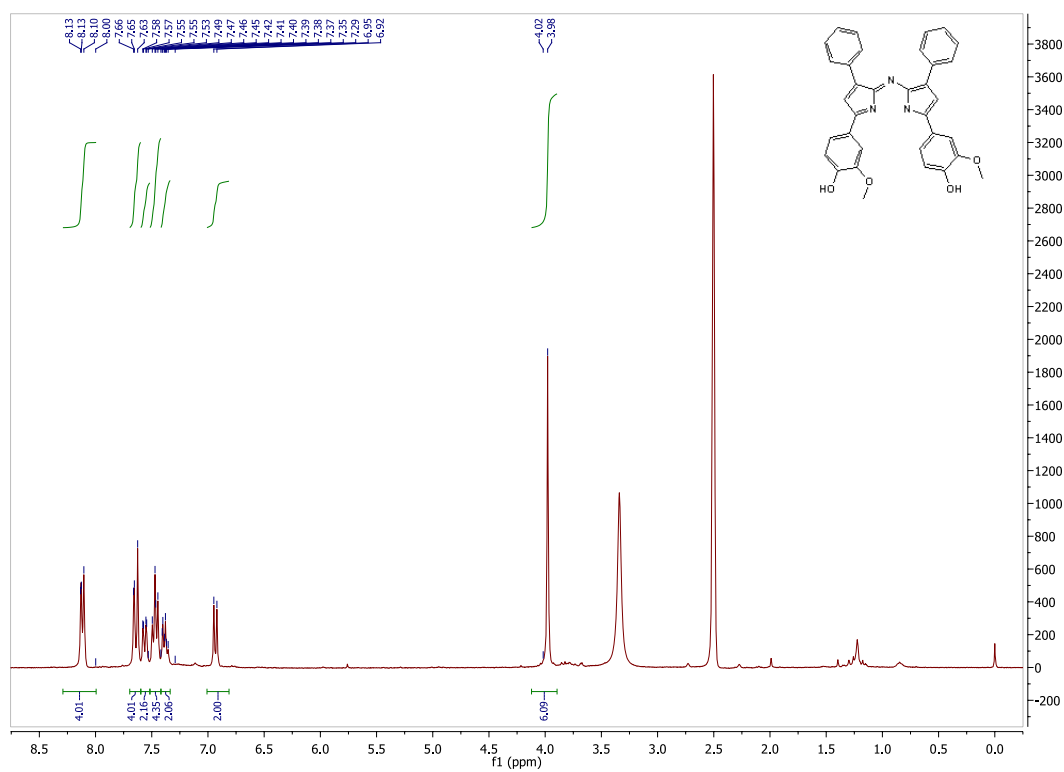


**Figure 9.1:**  $^1\text{H}$  NMR of the DiMeOH Ligand in  $\text{DMSO-d}_6$

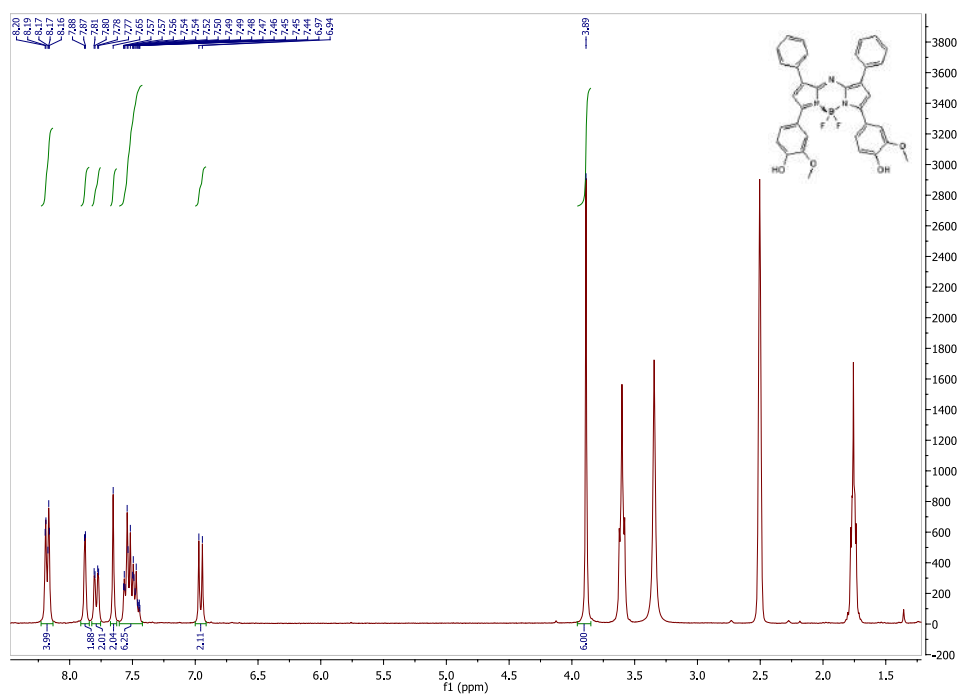


Figure 9.2:  $^1\text{H}$  NMR of the DiMeOH complex without sulfonate in DMSO-d<sub>6</sub>

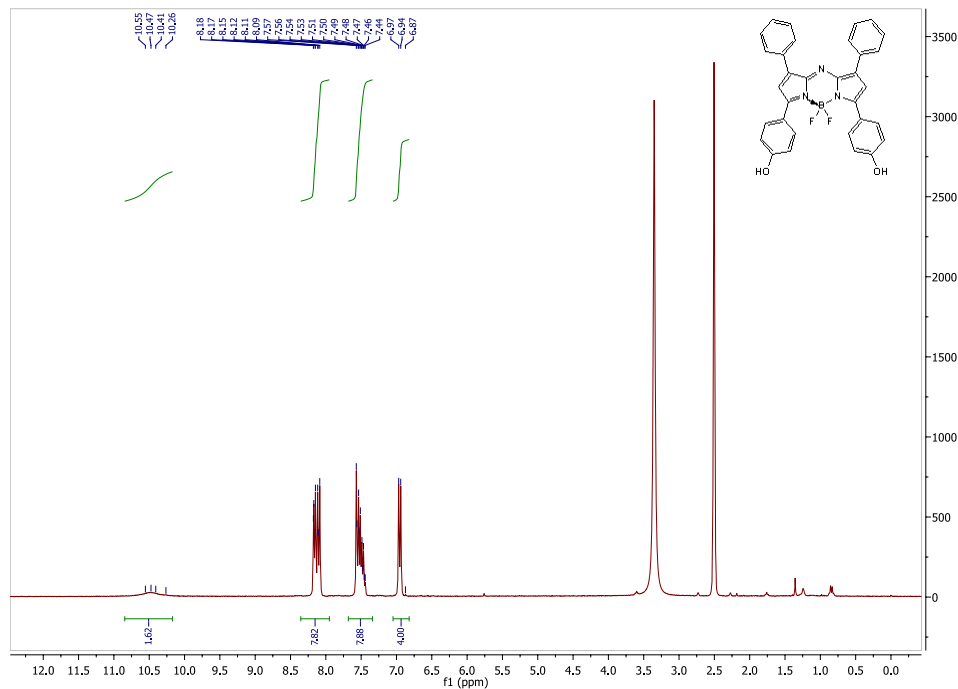
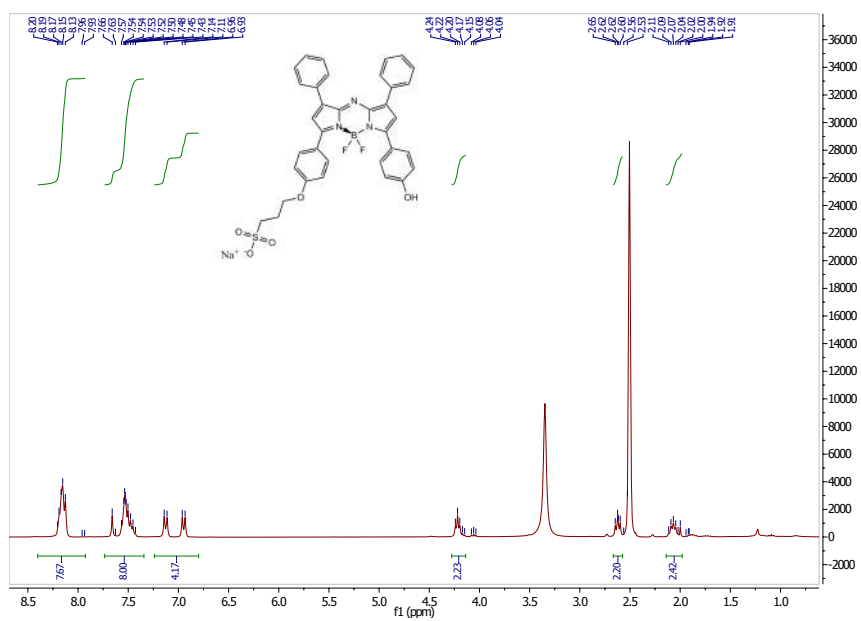
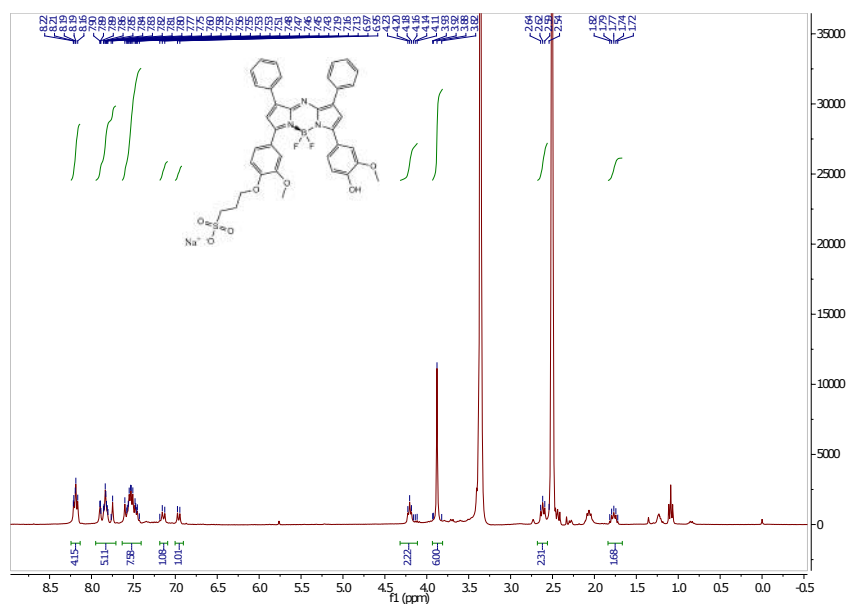


Figure 9.3:  $^1\text{H}$  NMR of the DiOH complex without sulfonate in DMSO-d<sub>6</sub>



**Figure 9.4:** NMR of the DiOH-BF<sub>2</sub> sulfonate complex in DMSO-d<sub>6</sub>



**Figure 9.5:** NMR of the DiMeOH-BF<sub>2</sub> sulfonate complex in DMSO-d<sub>6</sub>



## 9.3.2 Extracted dyes in solution

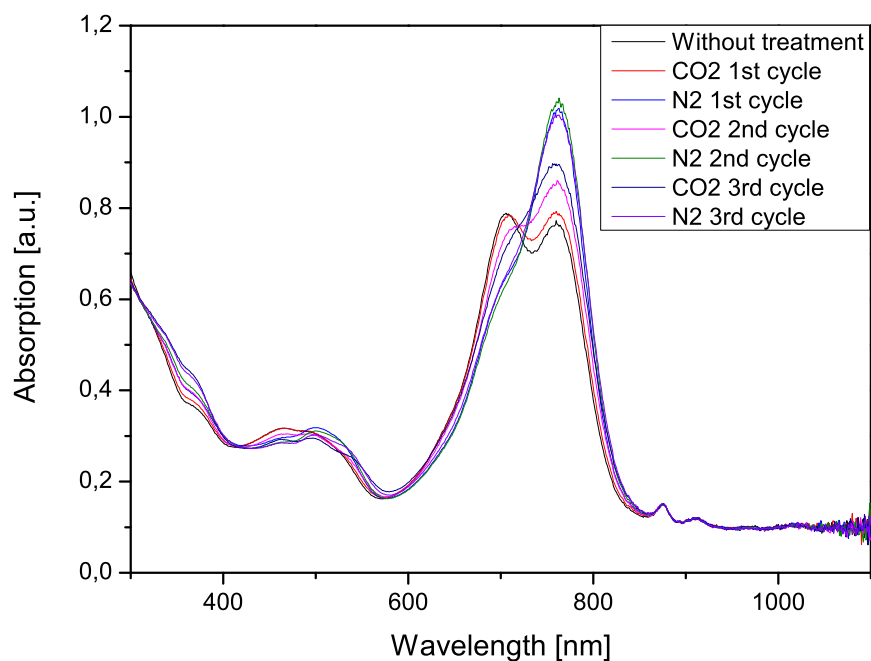


**Figure 9.6:** Absorption spectra for DiOH dye in Toluene

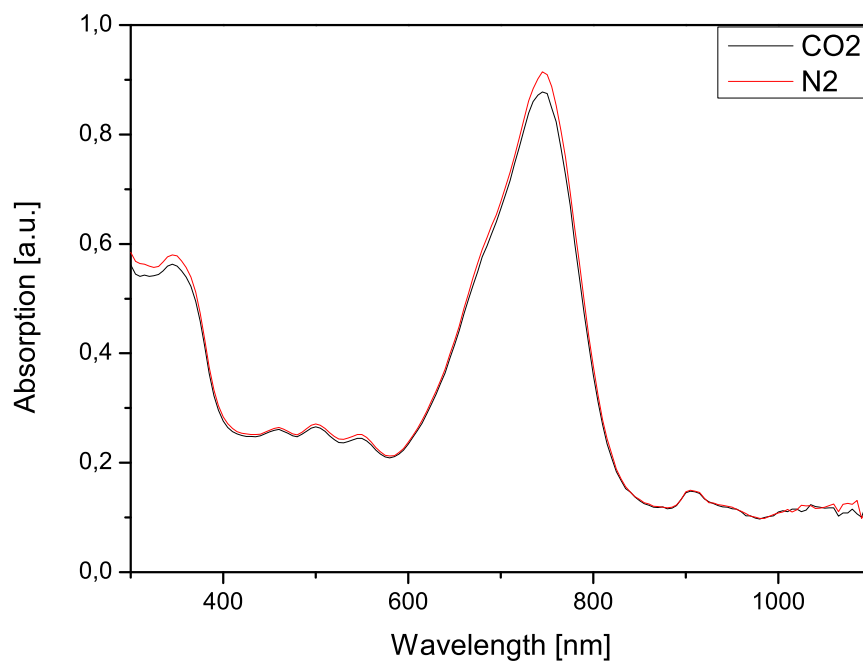


**Figure 9.7:** Absorption spectra for DiOH dye in THF

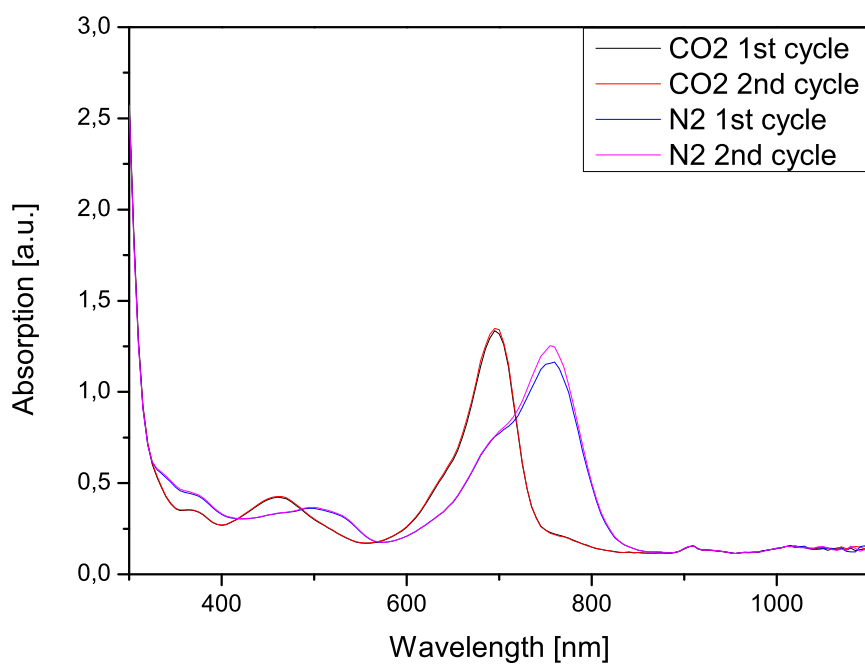


**Figure 9.8:** Absorption spectra for DiOH dye in EtOH

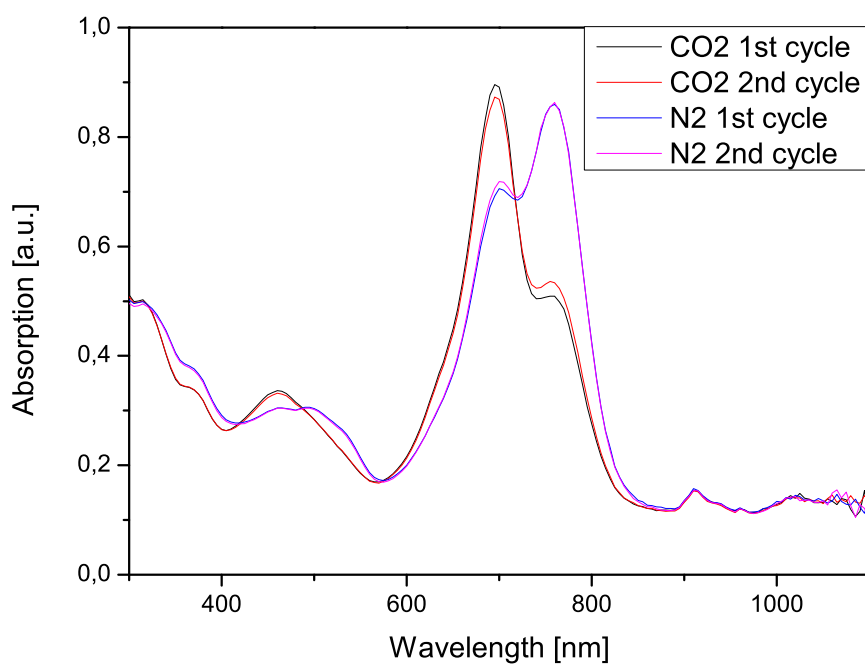


**Figure 9.9:** Absorption spectra for DiOH dye in isobutanol